C-type Lectin Receptors: from Immunomodulatory Carbohydrate Ligands to a Role in Murine Colitis

Inaugural-Dissertation

To obtain the academic degree

Doctor rerum naturalium (Dr. rer. nat.)

submitted to the Department of Biology, Chemistry, and Pharmacy

of Freie Universität Berlin

by

Magdalena Karin Matilda Eriksson

2013

The presented work was performed at the Max Planck Institute of Colloids and Interfaces in the Department of Biomolecular Systems between June 2009 and June 2013, under the supervision of Professor Dr. Peter Seeberger and Dr. Bernd Lepenies.

Reviewers: **Professor Dr. Peter Seeberger**

Professor Dr. Christian Freund

Date of defence: 31.10.2013

Acknowledgements

I would like to express my deepest gratitude to Professor Dr. Peter Seeberger for giving me the opportunity to perform my thesis in his department and for his support throughout the thesis. Moreover, I am grateful to Professor Dr. Christian Freund for taking the time to review my thesis.
Foremost, I would like to express my great appreciation to Dr. Bernd Lepenies for excellent and enthusiastic supervision, interesting scientific discussions as well as for valuable and constructive suggestions throughout my time as a PhD student.

I also wish to thank Professor Dr. Achim Gruber and Dr. Dorthe von Smolinsky at the Department of Veterinary Medicine at the Free University in Berlin for histological analysis of the colon tissue. Furthermore, I would like to sincerely thank the department members Dr. Mark Schlegel for sugar synthesis and Dr. Anish Chakkumkal and Felix Bröcker for providing the DSAP linker. Moreover, I am grateful to Dr. Daniel Kolarich and Kathirvel Alagesan for their assistance in the proteomic analysis and Sebastian Goetze for assistance in printing initial glycan array slides. I am also thankful to Dr. Kerry Gilmore for his valuable comments on the thesis.

I also want to thank the former and present glycoimmunology members Maha Maglinao for valuable support (mentally as well as practically) throughout the thesis, Timo Johannssen for the production of the SIGNR3-hFc fusion protein and for staining of the gut microbiota, Julia Hütter and Dr. Sandra Miltsch for highly appreciated advices and discussions about the thesis, Dr. Markus Irgang for general support, Stephanie Zimmermann for motivating me to go to post-lab sport, Uwe Vogel for technical support and Susanne for her assistance in the animal house. I also want to thank current and former members of the Department of Biomolecular Systems for general methodological support (especially Bopanna Monnanda, Eva Settels, Uwe Möginger and Kathrin Stavenhagen) and the pleasant working atmosphere and enjoyable breaks.

I want to show my gratitude to Stiftelsen Markussens Studiefond for motivating me to continue research. I also want to thank my friends for their encouragement, particularly Maja for valuable comments on the introduction of my thesis and Anke for statistical advices. Especially, thanks to my parents, sisters and brothers for their mental support (nu har ni mig snart i Sverige!). Finally and foremost, thanks to my dear Hannes for his endless support and encouragement throughout the thesis.

Abbreviations

A	adenine
AEC	3-Amino-9-ethylcarbazole
AMV	avian myoblastosis virus
APC	antigen presenting cells
bp	base pairs
BSA	bovine serum albumine
C	cytosine
CBA	cytometric bead array
CHO	chinese hamster ovary
cDNA	complementary DNA
CID	collision-induced dissociation
CLR	C-type lectins
CRD	carbohydrate recognition domain
CTLD	C-type lectin domains
CD	Crohn's disease
CTL	cytolytic T cell
CpG	deoxy-cytidylate-phosphate-deoxy-guanylate
CLIP	class II associated I_i peptide
CBA	cytometric bead array
DAMP	danger-associated molecular patterns
Da	Dalton
DC	dendritic cells
DCIR	dendritic cell immunoreceptor
DD	double digestion
DNA	deoxyribonucleic acid
dNTP	deoxynucleoside triphosphates
DSAP	disuccinimido adipate
DSS	dextran sodium sulfate
ERK	extracellular signal-regulated kinase
EtBr	ethidium bromide
ETD	electron-transfer dissociation

ELISA	enzyme-linked immunosorbent assay
ELISpot	enzyme linked immunosorbet spot
FACS	fluorescence-activated cell sorting
FCS	fetal calf serum
Fc	crystallizable fragment of IgG
FcγR	Fc gamma receptor
G	guanine
Gal	galactose
GalNAc	N-acetylgalactosamine
GALT	gut associated lymph tissue
Glc	glucose
GlcNAc	N-acetylglucosamine
hIgG	human immunoglobulin G
H&E	hematoxylin and eosin
HRP	horseradish peroxidase
IBD	inflammatory bowel disease
IgG	immunoglobulin
IL	interleukin
I_i	invariant chain
i.v.	intravenous
i.p.	intraperitoneal
ICAM	intercellular adhesion molecule
Lac	lactose
LC-MS	liquid chromatography-mass spectrometry
LPS	lipopolysaccharide
LTA	lipoteichoic acid
LTA4H	leukotrieneA4 hydrolase
LTB4	leukotriene B4
MHC	major histocompatibility complex
MFI	mean fluorescence intensity
MACS	magnetic-activated cell sorting

MALDI-TOF-MS	matrix-assisted laser desorption/ionization time-of-flight mass spectrometry
MGL	macrophage galactose-like lectin
MBL	mannan binding lecting
MCL	macrophage C-type lectin
MICL	myeloid inhibitory C-type lectin
MR	mannose receptor
MLN	mesenteric lymph node
M cells	microfold cells
NHS	N-hydroxysuccinimide
NLR	NOD-like receptor
NOD2	nucleotide oligomerization domain 2
NFkB	nuclear factor kB
OVA	ovalbumin
RNA	ribonucleic acid
SLP-76	Src-homology leucocyte protein 76
SPF	special pathogen free
TAP	transporter associated with antigen processing
TCR	T cell receptor
TLR	toll like receptors
TNBS	trinitrobenzenesulfonic acid
PMBC	peripheral blood monoculear cell
pNPP	p-Nitrophenyl-phosphate
PLCγ2	phospholipase C gamma 2
PE	phycoerythrin
PCR	polymerase chain reaction
PVDF	polyvinylidenfluoride
RIG-I	retinoid acid- inducible gene-1
RT	room temperature
PRR	pattern recognition receptor
PFA	paraformaldehyde
SDS-PAGE	sodium dodecyl sulfate polyacrylamide gel electrophoreses

SSEA	stage specific embryonic antigen
T	thymine
TBE	Tris/Borate/EDTA
TNF	Tumor necrosis factor
THAP	2',4',6'-trihydroxyacetophenone monohydrate
TLR	toll like receptor
Treg	regulatory T cells
U	uracil
UC	ulcerative colitis

Amino acids

Ala (A)	Alanine
Arg (R)	Arginine
Asn (N)	Asparagine
Asp (D)	Aspartic acid
Cys (C)	Cysteine
Glu (E)	Glutamic acid
Gln (Q)	Glutamine
Gly (G)	Glycine
His (H)	Histidine
Ile (I)	Isoleucine
Leu (L)	Leucine
Lys (K)	Lysine
Met (M)	Methionine
Phe (F)	Phenylalanine
Pro (P)	Proline
Ser (S)	Serine
Thr (T)	Threonine
Tyr (Y)	Tyrosine
Trp (W)	Tryptophan
Val (V)	Valine

Contents

1 INTRODUCTION

1.1 The immune system

The immune system is a complex system of specialized tissues, cells and molecules involved in protecting our body from invading microbes, toxins, other foreign substances and tumors. Invasion of a microbe (from here on called pathogen) activates different parts of the immune system. The innate immunity is a general defense against intruding pathogens and is activated immediately upon pathogen encounter. In contrast, the adaptive immunity is more specific and takes more time to be fully activated. However, a memory is induced to combat repeated infections. There is communication between the cell systems via soluble molecules and specialized cells. A tightly regulated immune response is of importance for the body homeostasis; a too weak immune defense can result in overwhelming pathogen infection, whereas an exaggerated immune response can cause immune pathology. Normally, immune cells are able to distinguish between self-antigens and non-self, and fight the pathogens without destroying the own body (Abbas, 2003; Delves and Roitt, 2000).

1.2 Innate immunity

Innate immunity is the first line of defense against pathogens and cells of the innate immunity are responsible for preventing the invasion of pathogens as well as killing and incapacitating them. If needed they are also able to direct and activate an adaptive immune response. The first line of innate immune defense that pathogens encounter is the epithelial surfaces of the skin or the gut. These surfaces function as physical barriers preventing the adherence of the pathogen and as chemical barriers that secrete antimicrobial enzymes and peptides (Hooper et al., 2012). If microbes manage to cross these barriers they are confronted by innate immune cells, for example macrophages, that recognize and phagocytose different types of pathogens. This leads to an inflammation and recruitment of other innate immune cells such as neutrophils. In addition, plasma proteins such as cytokines, acute phase proteins and complement factors are accumulated, the latter being a system of plasma proteins that interact with pathogens and opsonize them so

that phagocytic cells can recognize and endocytose them. Innate immune cells, such as neutrophils and macrophages, aim at removing common pathogens. However, when the infection is not fully controlled by innate immunity, the adaptive immune response is required. The innate immune cells are involved in initiating an adaptive immune response mainly via specialized antigen presenting cells (APCs). An adaptive immune response is not fully activated until four to seven days after infection and therefore innate immunity is crucial to control infection during this first period (Abbas, 2003).

1.2.1 Antigen presenting cells (APCs)

APCs are cells that can take up antigens from the surroundings and present them to T cells, thereby inducing either tolerance or immunity. The main APCs are dendritic cells (DCs), macrophages and B cells, although certain tissue cells such as endothelial and epithelial cells are also capable of antigen presentation (Abbas, 2003). The most potent and efficient APCs are the DCs. The main functions of DCs are to sample antigens from their surroundings and to initiate and direct adaptive immunity. DCs are generated in the bone marrow and are present in most body tissues. They have high endocytic capacity and continuously bind and sample self- and non-self-antigens (Banchereau and Steinman, 1998). Under steady-state conditions, semi-mature DCs continuously migrate to lymph nodes to present self-antigens to T cells, thereby actively inducing T cell tolerance towards harmless self antigens (Lutz, 2012). Upon pathogen recognition, DCs undergo maturation. This leads to upregulation of chemokine receptors, MHC-II molecules and co-stimulatory molecules (Banchereau and Steinman, 1998). Mature DCs show enhanced migration towards lymph nodes where they present the processed antigens to naïve T cells. This presentation on MHC-II molecules together with expression of co-stimulatory molecules activates T cells and adaptive immunity is induced (Dooms and Abbas, 2006). DCs are not only activated by the direct interaction with pathogens, but also by inflammation-related tissue factors such as cytokines, chemokines, eicosanoids and heat-shock proteins, expressed by surrounding cells due to pathogen invasion. These factors are called danger signals and are important messengers that amplify or fine-tune the pathogen-specific response (Takeuchi and Akira, 2010).

1.2.2 Pattern recognition receptors (PRRs)

The expression of pattern recognition receptors (PRRs) enables APCs to sense the presence of microbes. PRRs recognize conserved microbial structures called pathogen associated molecular patterns (PAMPs) (Medzhitov, 2001). PRRs also recognize molecules released from damaged or dead cells called danger-associated molecular patterns (DAMPs) (Takeuchi and Akira, 2010). Upon activation, the majority of the PRRs induce inflammatory responses, such as the production of cytokines, chemokines and antimicrobial proteins. Some PRRs are also directly involved in the endocytosis of the pathogen (Takeuchi and Akira, 2010). The main groups of PPRs are Toll-like receptors (TLRs), NOD-like receptors (NLRs), C-type lectin receptors (CLRs) and retinoid acid-inducible gene-1 (RIG-I) receptors (Chen et al., 2009; Hardison and Brown, 2012; Medzhitov, 2001; Takeuchi and Akira, 2010). Genetic defects in certain PRRs lead to improper signaling and have been shown to influence the pathogenesis of inflammatory diseases (Chen et al., 2009; Ogura et al., 2001). The most studied PRRs are the TLRs, which recognize extracellular antigens and antigens in the endolysosome. TLRs are expressed by both innate immune cells and resident tissue cells such as epithelial cells (Medzhitov, 2001). The TLRs bind to various structures on the pathogen such as the bacterial cell wall components lipopolysaccharides (LPS) and lipoteichoic acids (LTA). Activation of TLRs induces antimicrobial responses such as the production of nitrogen oxygen synthase and antimicrobial peptides. In addition, TLR engagement also up-regulates host defense genes coding for pro-inflammatory cytokines and co-stimulatory molecules. The majority of the TLRs share certain signal pathway mediators including the adaptor proteins MyD88 and TRAF6, and activation of a TLR induces the activation of nuclear factor kB (NFkB) and p38 MAPK. TLR engagement normally results in the maturation of the DC and induction of certain cytokines to direct the differentiation of T helper (Th) effector cells (Medzhitov, 2001).

1.3 Adaptive immunity

Some days after pathogen encounter, the more specific immune cell system called adaptive immunity sets in, which combats the infection parallel to the innate immune response. This system consists of B and T lymphocytes (called B and T cells) each with specific antigen receptors. Both lymphocyte subsets are generated in the bone marrow, but for further differentiation and selection B cells remain in the bone marrow, whereas T cells migrate to the thymus (Lemischka et al., 1986). During the differentiation and clonal selection, millions of different variants of antigen receptors are produced due to gene recombination. Lymphocytes with receptors that recognize self-molecules are deleted in the early cell development. In this way, a highly diverse mature lymphocyte repertoire is obtained. Each single lymphocyte expresses a receptor with unique antigen specificity. When the receptor is engaged by an antigen with high affinity, the lymphocyte is activated and divides into effector cells bearing the same receptor. A subset of activated lymphocytes differentiates into memory cells that are able to respond rapidly upon encounter with the priming antigen (Abbas, 2003).

The adaptive immune system can be divided in humoral and cellular immunity. Humoral immunity is mediated by antibodies produced by B cells. Upon activation induced by antigen-binding, and most often with T cell assistance, B cells differentiate into plasma cells that produce antigen-specific antibodies (Burnet, 1976). Antibodies can prevent microbes from infecting cells along with binding to microbes to target them for phagocytosis, a process called opsonization. Humoral immunity is the main defense mechanism against extracellular microbes. Cellular immunity, targeting predominantly intracellular microbes, is mediated by $CD8^+$ T and $CD4^+$ T cells (Abbas, 2003). These T cells are discussed in more detail in the following sections.

1.3.1 Antigen presentation

DCs present antigens to T cells on major histocompatibility complex (MHC) molecules. Antigens associated with the MHC molecules on the cell surface are recognized by the T cell receptor (TCR) of the T cell. Depending on the origin of the antigen, they are presented on MHC class-I or MHC class-II molecules which are recognized by $CD8^+$ T or $CD4^+$cells, respectively (Abbas, 2003). The process of peptide presentation by MHC-II molecules starts with the recognition and endocytosis of microbial antigens by immature DCs. Internalized proteins are localized in endosomes and lysosomes with an acidic pH and digested into peptides by proteolytic enzymes.

MHC class-II molecules are synthesized in the ER and transported to endosomes with a protein called invariant chain (I_i) bound to the peptide binding cleft. The I_i is degraded in the endosome by proteolytic enzymes into a peptide called class II associated I_i peptide (CLIP). This peptide is then removed by the chaperone HLA-DM (Kropshofer et al., 1996) and peptides from the antigens are loaded onto the peptide binding cleft. The MHC class-II/peptide complexes are transported to the cell membrane for recognition by the TCR expressed by $CD4^+$ T cells. Depending on which other signals and molecules are expressed by the DC, $CD4^+$ T cells differentiate into effector T cells (O'Shea and Paul, 2010). Peptides presented on MHC class-I molecules are cytosolic proteins, such as endogenously synthesized proteins or viral antigens, that are ubiquitinated followed by proteolytic degradation in the proteasome. The peptides are then transported into the lumen of the endoplasmic reticulum via the transporter associated with antigen processing (TAP), loaded on newly produced MHC-I molecules and presented on the cell surface. These MHC class-I molecules are recognized by $CD8^+$ T cells that can develop into cytolytic T cells (CTLs) that kill infected cells (Abbas, 2003). CTLs induce apoptosis of target cells by secreting the granule proteins perforin and granzymes that form pores in the membrane of target cells and induce caspase activation (Abbas, 2003). Activated CTLs also express the Fas ligand, which engages Fas on the surface of target cells inducing apoptosis. Phagocytosed antigens can also enter the proteosomal pathway and can be presented by MHC class-I molecules in a process called cross-presentation (Abbas, 2003; Burgdorf et al., 2007).

1.3.2 DC polarization of $CD4^+$ T cells

$CD4^+$ T cells recognize peptides presented by MHC-II molecules and can develop into effector T cells including Th1, Th2, Th17 cells or induced regulatory T cells (Tregs) (O'Shea and Paul, 2010). Three signals from the DC are important for the differentiation of $CD4^+$ T cells (Figure 1.1). As mentioned above, the recognition of the peptide presented by the MHC-II molecule by the TCR (signal 1) along with binding of the co-stimulatory molecules CD80 or CD86 (signal 2) by CD28 is necessary to induce T cell activation (Joffre et al., 2009; Kapsenberg, 2003; Monks et al., 1998). Activation of APCs by PAMPs normally leads to up-regulation of co-stimulatory molecules. If no co-stimulation is present, the T cell becomes anergic. If both signal 1 and 2 are present, local cytokines and factors (signal 3) influence the $CD4^+$ T cell to differentiate into specific effectors cells. The factors that DCs produce depend on how the DC was activated.

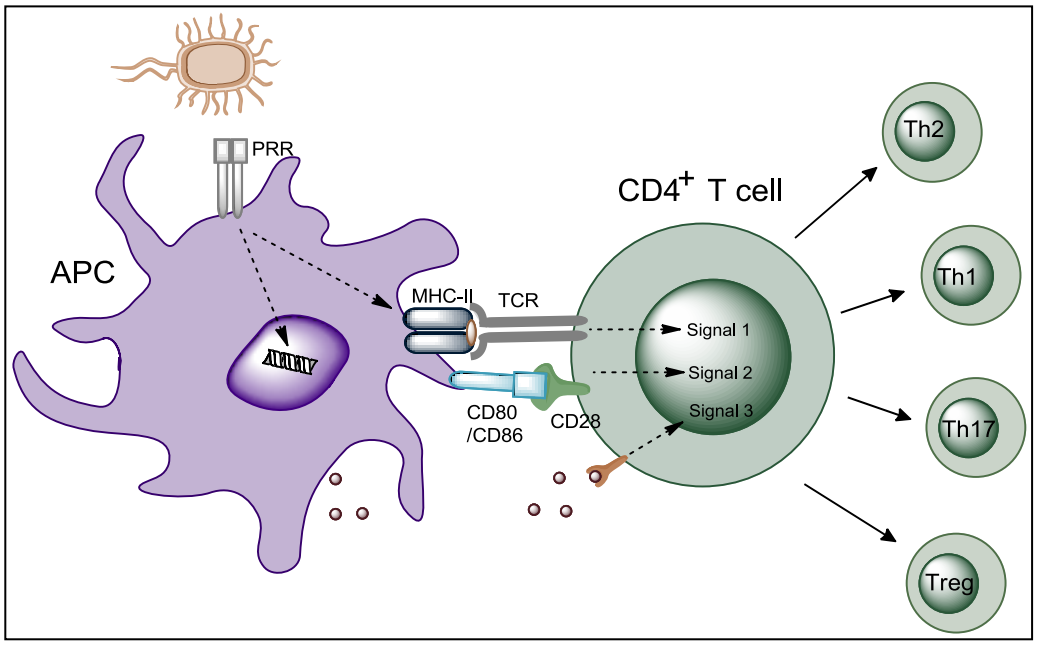

Figure 1.1 Simplified scheme of DC-T cell interactions.

DCs sense the presence of pathogens or danger signals via pattern recognition receptors (PRRs). PRR engagement can lead to the activation of signal pathways as well as uptake, protein degradation and antigen presentation by MHC-II molecules. T cells are activated by binding of the T cell receptor (TCR) to the MHC-II/peptide complex (signal 1) and costimulatory molecules (CD80/CD86 to CD28) (signal 2). Signal 3 directs T cells to develop into different effector T cell lineages.

Activation of a DC results in DC maturation and the expression of mediators that will promote Th1, Th2, Th17 or Treg development. Factors that, together with signal 1 and 2, promote Th1 cell development are IL-12, IL-23, IL-27, type 1 IFNs and cell-surface expressed intercellular adhesion molecule 1 (ICAM1) (O'Shea and Paul, 2010). Th1 cells are mainly involved in cell-mediated immunity against intracellular pathogens. This includes the production of IFN-γ and TNF-α and the stimulation of macrophages and CTLs. DC-derived factors favoring Th2 cell polarization are monocytic chemotactic protein 1 (MCP1) and OX40 ligand (OX40L). Th2 mainly promotes humoral immunity and stimulates B cell proliferation along with antibody production by IL-4, IL-5 and IL-13 secretion (Kapsenberg, 2003; O'Shea and Paul, 2010). The cytokine IL-6 seems to have a central polarizing role for $CD4^+$ T cell differentiation into Th17 cells. Th17 cells are involved in the anti-fungal immunity at mucosal surfaces (Hardison and Brown, 2012). In addition, $CD4^+$ T cells can develop into Tregs with the help of IL-10 and transforming-growth factor-β (TGF-β). Tregs are important to avoid an excessive chronic T cell response and to regulate Th1 or Th2 activity. However, Tregs can also have a detrimental effect

for the host, by providing a beneficial environment for the pathogen. This Treg-mediated suppression occurs in a non-antigen specific manner through the production of regulatory cytokines, in a process called bystander suppression (Belkaid, 2007; Vignali et al., 2008).

1.4 C-type lectin receptors (CLRs)

One family of PRRs that are expressed by APCs and involved in pathogen recognition and capture is the C-type lectin receptor (CLR) superfamily. CLRs belong to a large superfamily of proteins containing one or more C-type lectin domains (CTLDs) (Drickamer, 1999; Zelensky and Gready, 2005). A subclass of these CTLD-containing proteins involved in innate immunity is the CLRs expressed by myeloid cells. These CLRs are transmembrane proteins that recognize mainly carbohydrate motifs present on pathogens and self-antigens. However, certain CLRs can also recognize protein ligands exposed by apoptotic or necrotic cells as well as oxidized lipids (Ahrens et al., 2012; Hoshikawa et al., 1998; Mizuochi et al., 1998; Zhang et al., 2012). Activation of a CLR can induce signal transduction and gene transcription, promote endocytosis and alter the potential of DCs to direct T cell responses (Brown, 2006; Burgdorf et al., 2007). CLRs contain one or more extracellular carbohydrate recognition domains (CRDs), of which some contain Ca^{2+} binding sites, giving name to the "*C*" in C-type lectin receptors. Certain amino acids in the CRD determine the carbohydrate specificity of the CLR. It has been reported that CLRs expressing the amino acid motif EPN (Glu-Pro-Asn) in the CRD are specific to mannose-based ligands, whereas galactose-specific CLRs often express the amino acid motif QPD (Gln-Pro-Asp) (Sancho and Reis e Sousa, 2012). The ligand specificity and the immunological signaling of CLRs vary between different CLRs. For example, certain CLRs bind mainly to pathogens, such as the recognition of fungi by dectin-1 which initiates pro-inflammatory signaling. However, other CLRs bind to self-ligands, such as Clec9a binding to filamentous actin (F-actin) exposed in necrotic cells thus inducing cross presentation (Ahrens et al., 2012; Zelensky and Gready, 2005; Zhang et al., 2012). An overview of the main properties of the CLRs relevant for this thesis is presented in Table 1.1.

Table 1.1 Murine CLRs analyzed in this thesis.

CLR	Expressed by	Ligands	Signaling	Functions	References
MGL1	DCs, macrophages	Lewis X, Lewis A Tn-antigen, α-GalNAc, terminal Gal, apoptotic bodies, gut commensals *(Streptococcus spp. Lactobacillus spp.)*	n.d.	Removal of apoptotic cells in embryogenesis, involvement in inflammation and IL-10 production	(Saba et al., 2009; Sato et al., 1992; Singh et al., 2009; Tsuiji et al., 2002)
Clec9a /DNGR1	$CD8^+$ DCs $CD103^+$ $CD11b^-$ DCs	F-actin and necrotic cells	hemITAM, Syk	Cross-presentation	(Ahrens et al., 2012; Sancho et al., 2009; Zhang et al., 2012)
SIGNR3 /CD209d	$CD11b^+$ DCs, macrophages and monocytes	Zymosan, high mannose, fucose, *M.tuberculosis*	hemITAM, Syk, Raf, MEK, ERK	Involved in the host defense against *M.tuberculosis*	(Galustian et al., 2004; Nagaoka et al., 2010; Park et al., 2001; Takahara et al., 2004; Tanne et al., 2009)

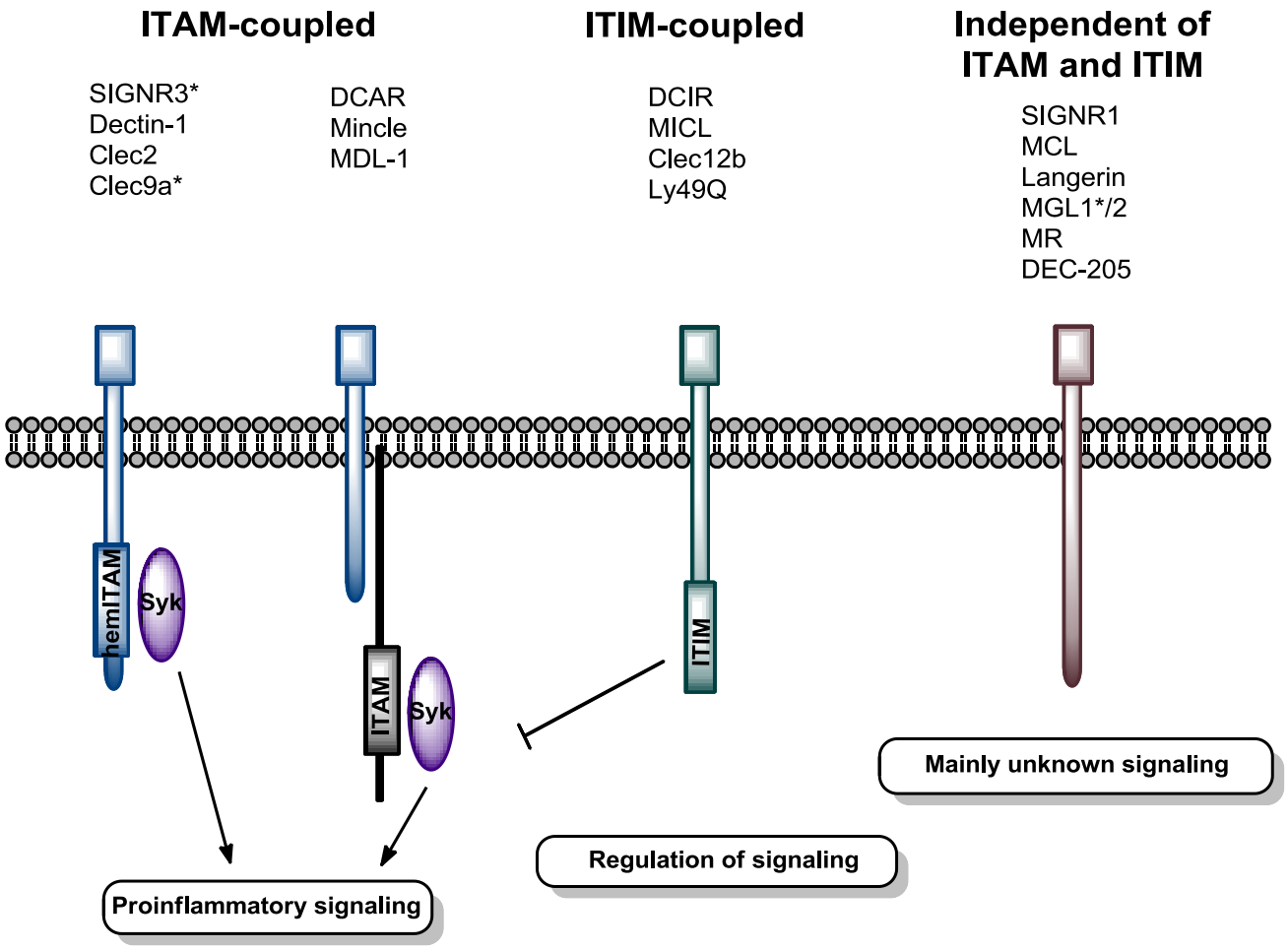

Figure 1.2 Subgroups of myeloid CLRs

Subgroups of some murine myeloid C-type lectin receptors dependent on the intracellular signaling motif. ITAM: immunoreceptor tyrosine based activating motif; ITIM, immunoreceptor tyrosine based inhibitory motif. *CLRs relevant for this thesis.

The CTLD superfamily and myeloid CLRs are categorized into subclasses depending on their structure and Ca^{2+}-dependency (Table 1.2). However, there are major differences in the signaling within these groups. Therefore, an additional categorization according to common signaling motifs divides the myeloid CLRs into the immunoreceptor tyrosine based activating motif (ITAM)-coupled, the immunoreceptor tyrosine based inhibitory motif (ITIM)-coupled or ITAM/ITIM-independent CLRs (Figure 1.2) (Sancho and Reis e Sousa, 2012). ITAM-coupled CLRs either have one intracellular single tyrosine-based motif called hemITAM or are coupled with adaptors (FcRγ or DAP12) bearing one or more ITAMs. Upon receptor activation, the

ITAMs are phosphorylated and generate a docking site for the SH2 domains of Syk. This leads to a conformational change of Syk, followed by autophosphorylation. Active Syk binds to motifs in downstream signaling pathways such as PI3K, SLP-65 or PLCγ, resulting in pro-inflammatory signals (Mocsai et al., 2010). In contrast, CLRs containing an intracellular ITIM recruit phosphatases such as SHP-1 and SHP-2, negatively regulate previously activated kinase-dependent signaling. These CLRs can inhibit signals from ITAM-coupled CLRs (Richard et al., 2006). The last subgroup are CLRs signaling without a known ITAM or ITIM motif (Figure 1.2) (Sancho and Reis e Sousa, 2012).

Table 1.2 CLRs expressed by murine myeloid cells are members of the subfamilies II, V and VI of the CTLD superfamily

Group	transmembrane	CRD	Calcium dependency?	Examples of murine members
II	type II	Single	Ca^{2+} binding sites present	SIGNR1, SIGNR3, DCAR1, DCAR2, Dectin-2, MCL, Mincle, Langerin, MGL1/2
V	type II	Single	Ca^{2+} independent binding	MICL, Clec2, Clec9a, Dectin-1, LOX1, Clec12b, Clec1a
VI	Type I	8-10	Ca^{2+} dependent binding	MR, DEC-205

1.4.1 Targeting of CLRs

Since DCs are crucial in initiating adaptive immunity, there is a large degree of therapeutic interest in modulating the function of DCs. Examples of desired applications are the induction of tolerance to an antigen to prevent autoimmune diseases, or targeted vaccine delivery. DC modulation can be achieved by the use of antibodies that induce DC maturation or by directing antigens to DCs (Caminschi et al., 2009; van Kooyk et al., 2013). The myeloid CLRs are selectively expressed on various DC subtypes and are potential targets to modulate DC functions

specifically. By conjugating an antigen to an antibody against the CLR DEC-205, it was possible to enhance $CD4^+$ and $CD8^+$ T cell-mediated immunity both *in vitro* and *in vivo* (Bonifaz et al., 2002; Bonifaz et al., 2004). Similarly, studies in mice and non-human primates show that directing a malaria parasite antigen to DEC-205 leads to increased antibody titers and specific T cell responses (Boscardin et al., 2006; Tewari et al., 2010). Several of these targeting studies use CLR-specific antibodies. However, there is a risk of inducing unspecific immune responses against the antibody due to binding of Fc receptors and complement activation. In addition, a humoral response against the antibodies can be induced (DeNardo et al., 2003; Khazaeli et al., 1994). Moreover, antibodies are large proteins that can hinder tissue penetration and can bind unspecifically (Hagemeyer et al., 2009).

Another strategy is to target CLRs by their natural carbohydrate ligands. This has the advantage that carbohydrates are small and might not induce unspecific immune responses (Unger et al., 2012). In addition, carbohydrates are rapidly degradable and the ligand presentation can be defined (Grunstein et al., 2011). By encapsulating an antigen in a particle covered with carbohydrates, the actual pathogen can be mimicked (Adams et al., 2004). Although targeting by antibodies has shown to induce stronger immune responses (Cruz et al., 2012), carbohydrate delivery can lead to a more specific targeted delivery (Unger et al., 2012), which is useful for the fine tuning of immune responses. By conjugating carbohydrates to an antigen, the initiated T cell response can be polarized (Adams et al., 2008). Targeting of Dectin-1 by antigen-loaded particles covered with β-glucan led to a stronger antifungal response, including increased frequencies of Th1 and Th17 cells, compared to antigen administration together with an adjuvant (Huang et al., 2010). Similarly, by coating antigen filled nanoparticles with DC-SIGN ligands, antigen presentation was enhanced along with an increase of $CD4^+$ and $CD8^+$ T cell proliferation (Unger et al., 2012). In addition, using the Mincle-ligands TDM and TDB as adjuvants together with a recombinant *Mycobacterium tuberculosis* subunit vaccine induced robust Th1 and Th17 responses and protection after challenge with *M. tuberculosis* (Khader et al., 2007; Schoenen et al., 2010; Werninghaus et al., 2009). Thus, there is a high potential of targeting CLRs by using carbohydrate ligands (Lepenies et al., 2013). However, the effects of different CLR-ligands need to be further characterized.

1.4.2 MGL and MGL1/2

The human macrophage galactose-like lectin (MGL) is expressed by DCs and macrophages and recognize terminal GalNAc and GalNAc-Ser/Thr (Tn-antigens) (Higashi et al., 2002; Suzuki et al., 1996; van Vliet et al., 2005). MGL recognizes antigens on tumor-associated mucin and on effector T cells and is involved in homeostasis of the adaptive immunity (van Vliet et al., 2008). There are two murine homologues of MGL, MGL1 and MGL2 (Sato et al., 1992; Tsuiji et al., 2002), which are expressed by the same cell types as the human receptor (van Vliet et al., 2006b) and have different carbohydrate specificity: MGL2 binds to GalNAc, whereas MGL1 binds strongly to Lewis X and to Lewis A, but also weakly to GalNAc (Sato et al., 1992; Singh et al., 2009; Tsuiji et al., 2002; van Vliet et al., 2008). MGL1 is involved in immune regulation (Saba et al., 2009), recognition of tumors (Ichii et al., 1997, 2000), and removal of apoptotic cells during embryogenesis (Mizuochi et al., 1998; Yuita et al., 2005). The signaling pathways involved, however, have yet to be elucidated.

1.4.3 Clec9a

Clec9a, also called DGNR-1, is an endocytic CLR expressed by $CD8\alpha^+$ DCs that signals via hemITAM and Syk (Caminschi et al., 2008; Hovius et al., 2008; Sancho et al., 2009). Clec9a interacts with ligands exposed by dead cells (Caminschi et al., 2008; Hovius et al., 2008; Sancho et al., 2009) and is involved in promoting the processing and cross-presentation of dead cell-associated antigens (Zelenay et al., 2012). Recently, filamentous actin was identified as a ligand of Clec9a (Ahrens et al., 2012; Zhang et al., 2012). Targeting antigens to Clec9a has been shown to stimulate T cell responses and to induce strong antibody responses in the absence of adjuvants (Caminschi et al., 2008; Joffre et al., 2010; Lahoud et al., 2011). Thus, Clec9a is an interesting target for delivery of antigens to DCs.

1.4.4 SIGNR3

SIGNR3 (CD209d) is one of eight murine homologues of the human DC-SIGN molecule (Park et al., 2001; Powlesland et al., 2006). Although they all share structural homology with the human DC-SIGN, the specific sugar ligand binding and endocytic capability differs between the homologues. Like the human receptor, SIGNR3 recognizes terminal fucose, galactose or

N-acetylgalactosamine residues. In addition, SIGNR3 is the only mouse homologue showing endocytic activity, including ligand release under acidic conditions (Powlesland et al., 2006). Thus, SIGNR3 is suggested to be the most relevant murine homologue for functional analysis of the human DC-SIGN molecule (Powlesland et al., 2006; Takahara et al., 2004; Tanne et al., 2009). In addition to sharing common ligands with DC-SIGN, SIGNR3 also binds to certain Lewis antigens, high mannose glycans (Galustian et al., 2004) and mycobacterial surface glycans (Tanne et al., 2009) (Table 1.1). To date, the role of DC-SIGN and SIGNR3 in innate immunity is not yet clear. SIGNR3-deficient ($SIGNR3^{-/-}$) mice are more sensitive to infection with *M. tuberculosis* than wild-type mice, indicating the involvement of SIGNR3 in early pulmonary resistance to this bacterium (Tanne et al., 2009). SIGNR3 signaling involves an intracellular hem-ITAM, activation of Syk, Raf-1 kinase and extracellular signal regulated kinase (ERK). This leads to the activation of NF-ƙB and induction of TNF-α and IL-6 expression (Tanne et al., 2009; Tanne and Neyrolles, 2010). A regulatory role of SIGNR3 in macrophages upon recognition of *Leishmania infantum* was recently described (Lefevre et al., 2013). SIGNR3 was suggested to negatively regulate the production of the enzyme leukotrieneA4 hydrolase (LTA4H), which is crucial for the leukotriene B4 (LTB4) synthesis and caspase-1-dependent activation of IL-1β (Lefevre et al., 2013). Additional phenotypic analysis of $SIGNR3^{-/-}$ mice revealed an increase of $IgG^{+}IGM^{+}$ B cells in spleen along with more adipocytes present in the bone marrow (Orr et al., 2012). The biological effect of these observations still needs to be clarified.

1.5 Intestinal immunity

The complex mixture of microbes that inhabit the lower intestine is called the gut microbiota and consists of 100 trillion (10^{14}) microbes (Hooper et al., 2012; Ley et al., 2006). The gut microbiota consists of mainly bacteria, but also other microbes such as viruses and fungi (Iliev et al., 2012; Ott et al., 2008; Reyes et al., 2010). To raise a proper immune response to harmful antigens on the one hand, but to maintain tolerance to food and commensals on the other hand, the intestinal immunity is well organized (Carvalho et al., 2012). First of all, the number of microbiota coming in contact with immune cells is limited, a process called stratification (Figure 1.3) (Hooper et al., 2012). The microbiota is separated from the intestinal epithelial cells by a network of the glycoprotein mucin that forms a mucus layer. This layer can be divided into two parts, one loosely packed where some bacteria reside, and one densely packed layer which is normally impermeable to bacteria (Carvalho et al., 2012; Johansson et al., 2011). Further ways of hindering microbiota to cross the mucosal barrier are production of antibacterial factors, such as lysozyme and secretory phospholipase A_2, by intestinal epithelial cells and Paneth cells. These mediators hydrolyze the gram-negative cell wall component lipopolysaccharide (LPS) thereby killing these bacteria. Other antibacterial factors produced are α-defensins, which are small (2-3 kDa) secreted pore-forming peptides, and RegIIIγ that binds to the peptidoglycan in gram-positive bacteria resulting in bacterial lysis (Hooper et al., 2012). The mucus also contains secretory IgA that forms complexes with the bacteria and thereby inhibits their translocation across the epithelial layer (Macpherson and Uhr, 2004).

In addition to the stratification described above, an unwanted immune response is avoided by limiting the exposure of infiltrating microbes to the gut-associated lymphoid tissue (GALT), a process called compartmentalization (Figure 1.3) (Hooper et al., 2012). APCs are the first immune cells to come into contact with the microbiota. They sense bacterial antigens via PRRs which are important to keep the balance between tolerance and immune activation against commensals (Chen and Nunez, 2009; Hardison and Brown, 2012; Rakoff-Nahoum et al., 2004). The recognition of microbial antigens by TLRs has been well investigated. For example, LPS or flagellin binding to TLR4 and TLR5 followed by activation of MyD88 leads to the production of antimicrobial proteins, such as RegIIIγ, by epithelial cells (Hooper et al., 2012; Mukherjee et al., 2009).

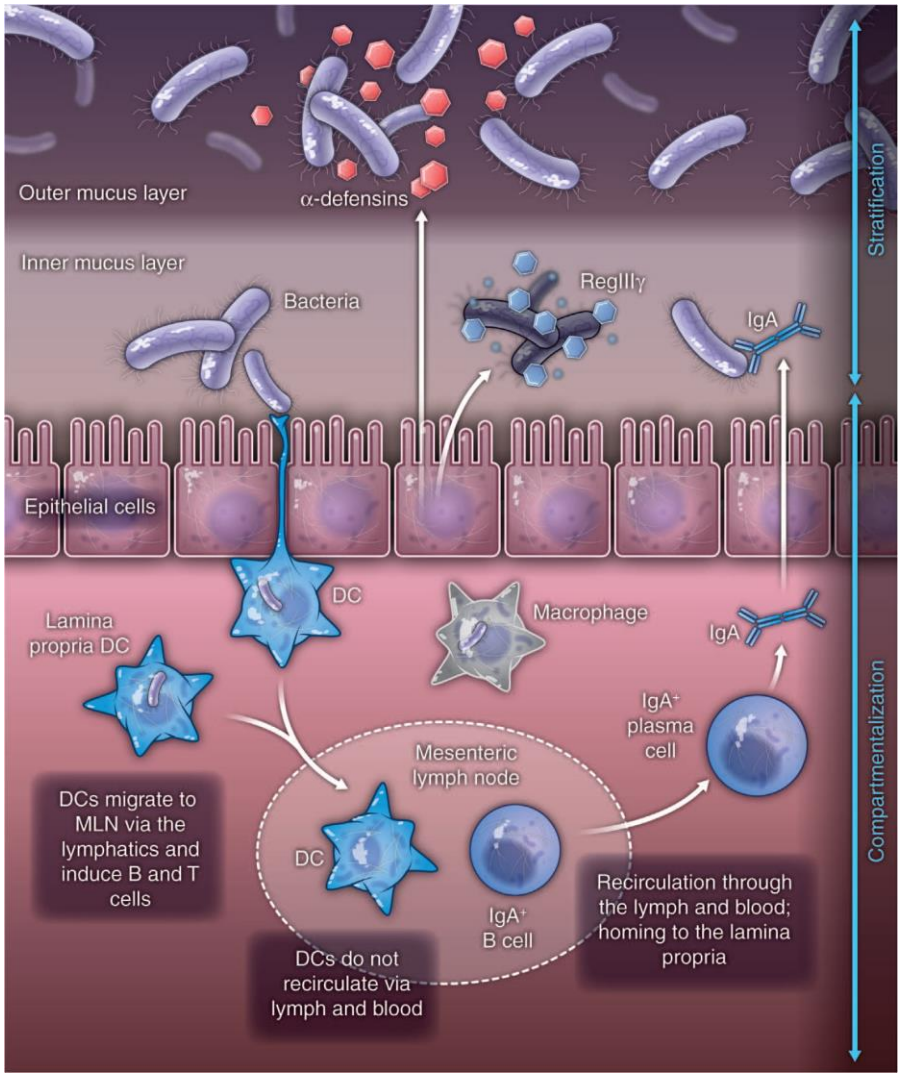

Figure 1.3 Control of microbiota by the intestinal immunity

The host controls the invasion of microbiota by stratification and compartmentalization. Figure from Hooper et al., 2012.

Normally, there is no immune response against food antigens or commensal bacteria. This phenomenon is called oral tolerance and depends on the antigen dose along with the cell type that encounters the antigen. Administration of a single high dose of antigen or repeated exposure of low doses can lead to antigen uptake by epithelial cells and peptide presentation by MHC-II molecules that are recognized by T cells through their TCRs. However, since epithelial cells lack the expression of co-stimulatory molecules necessary for T cell activation, these T cells go into anergy. In addition, low-dose tolerance is mediated by Treg secreting immunosuppressive cytokines (Mayer and Shao, 2004; Mowat, 2003). High doses of antigens can also lead to the

upregulation of the Fas-ligand by APCs. As a result, Fas-dependent caspase activation occurs in potentially autoreactive T cells and tolerance is induced (Chen et al., 1995). However, the intestinal immune system can come into contact with microbiota or invading pathogens in different ways and can also meditate inflammatory immune responses. DCs can sample gut antigens by extending dendrites between the epithelial cells. Antigen-loaded DCs migrate through the draining lymphatic to the mesenteric lymph node (MLN) where they interact with T cells (Mowat, 2003). Whole bacteria that manage to cross the mucosal and epithelial barrier are either phagocytosed by lamina propria macrophages or engulfed by DCs and transported to the MLNs. These DCs stimulate IgA production by B cells (Macpherson and Uhr, 2004). In addition, antigens can diffuse through the epithelial cells where they are either recognized by DCs or passively transported to peripheral lymph nodes (Mowat, 2003). Another route of entry for antigens is through microfold cells (M cells). These are specialized epithelial cells that take up certain antigens by endocytosis or phagocytosis. M cells release antigens to the underlying lymphoid structure called Peyer's patches and APCs, such as DCs, take up the antigen. Antigen-loaded DCs either interact with the local T and B cells in Peyer's patches or follow the draining lymphatic to the MLNs (Hooper et al., 2012). When a T cell is primed by a DC, it normally differentiates into an effector T cell in the MLN before migrating to the lamina propria via the blood stream where it may mediate a local immune response. The main lymphocytes in the intestinal lamina propria are IgA-producing B cells and effector $CD4^+$ T cells, of which some might be Tregs. In contrast, $CD8^+$ T cells mainly migrate to the intestinal epithelium (Hooper et al., 2012).

1.5.1 Inflammatory bowel disease

Inflammatory bowel disease (IBD) is a condition of acute and chronic inflammation in the gastrointestinal tract, and can be divided into ulcerative colitis (UC) and Crohn's disease (CD). The main symptoms of IBD are diarrhea, abdominal cramps and nausea. In addition, IBD patients have an increased risk of developing colon carcinoma (Bouma and Strober, 2003). Although both forms share several clinical features, UC is mainly limited to the mucosal lining of the colon and rectum, whereas CD inflammation occurs throughout the whole intestinal wall and may affect the entire gastrointestinal tract. The prevalence of IBD is 10-200 cases per 100.000 individuals in Europe and North America and there has been an increase in the incidence of CD during the last

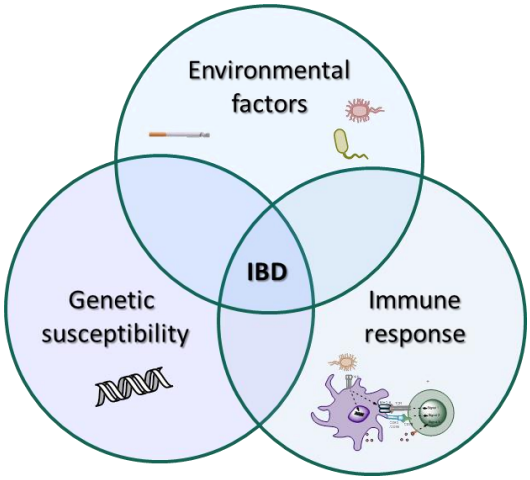

Figure 1.4 Multifactorial model of IBD

An interplay between several different factors such as genetic susceptibility, environmental factors such as smoking and gut microbes, and the immune system influences the pathogenesis of IBD.

few decades, especially in the western world (Loftus, 2004; Sartor, 2006). The etiology of IBD is poorly understood. Epidemiological and genetic studies in patients and IBD-related animal models suggest that a combination of genetic susceptibility, environmental factors, and an altered immune response contribute to IBD initiation and pathology (Sartor, 2006; Wirtz et al., 2007). One important environmental factor that plays a major role for pathogenesis is the interaction of commensal bacteria with intestinal immune cells, such as dendritic cells (Ng, 2011). Other environmental factors such as cigarette smoking and appendectomy are potential risk factors for CD, but not for UC (Figure 1.4) (Bouma and Strober, 2003; Sartor, 2006).

The treatment of IBD is individualized and most often consists of one or more anti-inflammatory agents, such as aminosalicylates or corticosteroids, first to treat the acute disease and then the remission phase (Engel and Neurath, 2010). TNF-α was shown to be a central immune mediator in intestinal inflammation (Apostolaki et al., 2010; Neurath et al., 1997) and administration of TNF-α-neutralizing antibodies is an approved medical therapy for IBD patients not responding to other anti-inflammatory agents (Engel and Neurath, 2010). However, all medicaments used today only treat the symptoms of IBD and not the IBD cause, and there are problems with side effects as well as with limited drug efficacy (Engel and Neurath, 2010).

1.5.2 Pathogenesis of IBD

The immunological mechanisms behind UC and CD are not fully understood. One important mechanism of the pathogenesis is the uncontrolled reactivity of $CD4^+$ T cells towards the microbiota or other self-antigens. The uncontrolled effector T cell activity is either a result of excessive effector T cell responses or deficient Treg functions (Powrie et al., 1993). Intestinal

inflammation is believed to be rather Th1-mediated in CD and Th2-mediated in UC (Bouma and Strober, 2003). The interactions of microbiota and intestinal innate immune cells, such as DCs, are critical factors for the subsequent mucosal $CD4^+$ T cell response (Engel and Neurath, 2010) (Ng et al., 2011). In the last decade, there has been increasing evidence of the crucial involvement of PRRs in the pathogenesis of IBD (Chen and Nunez, 2009; Iliev et al., 2012; Ogura et al., 2001; Rakoff-Nahoum et al., 2004; Rubino et al., 2012b). The expression of certain PRRs, such as TLRs, is up-regulated by intestinal DCs in IBD patients (Hart et al., 2005). In addition, a correlation of TLR4 expression by colon tissue from CD patients and disease severity has been reported, although the total expression of TLR4 did not differ between CD patients and healthy controls (Ng et al., 2011).

The most studied PRR involved in IBD is the Nucleotide oligomerization domain 2 (NOD2) (Chen and Nunez, 2009; Ogura et al., 2001; Rubino et al., 2012b). NOD2 is an intracellular PRR recognizing the bacterial cell wall antigen muramyl dipeptide, which activates the canonical NF-κB signal pathway resulting in the production of proinflammatory cytokines (Chen and Nunez, 2009; Inohara et al., 2001). In addition, NOD2 is involved in inducing a tolerogenic environment by up-regulation of IL-10 expression and proliferation of Tregs (Macho Fernandez et al., 2011). Three variants of the human NOD2 gene are correlated with an increased risk of CD development (Rubino et al., 2012a). $NOD2^{-/-}$ mice are more susceptible to colitis (Watanabe et al., 2006) and the administration of NOD2 ligands ameliorates colitis (Macho Fernandez et al., 2011). These studies demonstrate the importance of PRRs and their interaction with microbial ligands in the pathogenesis of IBD.

1.5.3 Models of murine colitis

Genome wide associated screens of IBD patients have revealed several susceptibility genes. However, a polymorphism in a susceptibility gene does not necessary lead to disease, thus it is difficult to analyze the exact mechanisms behind IBD in humans. To further elucidate the pathogenesis and to develop efficient treatments, appropriate animal models are needed. In these models, different genetic variants and/or environmental factors affecting the pathogenesis can be analyzed. There are numerous mouse models used to analyze IBD. However, due to the heterogeneous mechanisms behind the diseases, there is no “gold standard” animal model for CD or UC (Engel and Neurath, 2010; Wirtz et al., 2007). The choice of an appropriate IBD animal

model depends on the pathological mechanism to be investigated. Combinations of different animal studies along with IBD patient analyses are needed to clarify the mechanisms of innate and adaptive immunity in IBD. One way to analyze either T cell or innate mechanisms is chemically induce colitis by administrating either dextran sodium sulfate (DSS), trinitrobenzenesulfonic acid (TNBS) or oxazolone.

1.5.3.1 DSS-model of murine colitis

Mice and rats that are fed drinking water containing the polymer DSS for four to seven days develop an acute colitis, characterized by bloody diarrhea, ulceration and granulocyte infiltration (Wirtz et al., 2007). Since mice lacking functional B and T lymphocytes also develop this inflammation, adaptive immunity does not seem to play a major role the pathogenesis, at least not in the acute phase (Dieleman et al., 1994). Therefore, the DSS-induced colitis is a suitable model to analyze the role of innate immune mediators in intestinal inflammation (Wirtz et al., 2007). In this model of colitis, inflammation is induced due to the toxicity of DSS that disrupts the two mucosal layers protecting the epithelium due to the toxicity of DSS. Normally, bacteria reside only in the outer mucosal layer, whereas the inner layer is dense and impermeable for commensals. When DSS is added, bacteria infiltrate the inner mucosal layer and reach the epithelium where they are recognized by local immune cells, initiating an inflammatory response against the normally harmless bacteria (Johansson et al., 2011; Johansson et al., 2010). As such, this model is not only useful for analyzing innate immunological mechanisms in IBD, but also helps elucidate the interaction of commensal bacteria and intestinal mucosal immune cells.

1.5.4 CLRs in intestinal inflammation

Recent reports demonstrate a role for CLRs in gut inflammation and to date, four CLRs have been reported to be involved in murine colitis (Iliev et al., 2012; Müller et al., 2010; Saba et al., 2009; Saunders et al., 2010). The role of Dectin-1 in murine colitis was recently reported and debated (Heinsbroek et al., 2012; Iliev et al., 2012). Dectin-$1^{-/-}$ mice exhibit more pronounced colitis symptoms than wild-type mice upon colitis induction. In addition, the proportion of opportunistic pathogenic fungi, mainly *C. tropicalis*, is increased in the microbiota during DSS-induced colitis. Interestingly, this increase was more pronounced in dectin-$1^{-/-}$ mice than in wild-type mice and DCs lacking dectin-1 are less capable of killing *C. tropicalis in vitro*. During

colitis, fungi invaded colonic tissue in Dectin-1$^{-/-}$ mice, whereas these populations remained in the colon lumen in wild-type mice. Consistently, a polymorphism in the Dectin-1 gene (CLEC7A) has been found to be associated with medically refractory UC patients, indicating that there is a relation between this haplotype and severity of the disease (Iliev et al., 2012).

Another CLR that also has a protective role in murine colitis is the mannan binding lectin (MBL). Upon colitis induction, MBL$^{-/-}$ mice exhibit more severe colitis symptoms accompanied by higher antifungal antibody serum titers than wild-type mice. Circulating MBL is suggested to limit microbial invasion over the intestinal epithelium, thus preventing excessive inflammation (Müller et al., 2010). In addition, the CLR mMGL1 has a protective role in DSS-induced colitis, demonstrated by more a severe inflammation in MGL1$^{-/-}$ mice during colitis (Saba et al., 2009). This receptor is expressed by colonic lamina propria macrophages and was suggested to induce IL-10 production in response to invading commensal bacteria, resulting in suppressed intestinal inflammation in mice during colitis (Saba et al., 2009). In contrast to aforementioned studies, mice lacking SIGNR1, one of the murine homologues of DC-SIGN, are less susceptible to chemically induced colitis (Saunders et al., 2010). Since macrophages from these mice produce less IL-1β and IL-18 upon LPS-stimulation, SIGNR1 is believed to recognize LPS and to be involved in meditating the intestinal inflammation in colitis (Saunders et al., 2010).

Taken together, there is increasing evidence of the involvement of microbiota-sensing CLRs in intestinal inflammation. Further analysis of CLR-microbiota interactions is needed to characterize the impact of these interactions.

2 AIMS

CLRs and their carbohydrate ligands are involved in several different inflammatory processes and there is a high potential of targeting CLRs by using carbohydrate ligands to modulate immune responses. However, the exact ligand binding and the impact of these interactions on the immune response are not known for the majority of the CLRs. The first aim of this PhD thesis was to establish a platform to facilitate the screening of CLR-ligand interactions and their impact *in vitro* and *in vivo*. For this purpose, one objective was to generate CLR-hFc fusion proteins that can be used for screening of natural or synthetic carbohydrate ligands using glycan array. The subsequent objective was to analyze the immune modulatory properties of the identified CLR ligands *in vitro* and *in vivo.* Experimental models using transgenic T cells were used for this purpose.

Based on increasing evidence of the involvement of microbiota-sensing CLRs in intestinal inflammation, the second aim of this thesis was to analyze the role of CLRs in murine colitis. For this purpose, screening for CLR ligands in gut microbiota with the use of CLR-hFc proteins was performed. One of the CLRs binding to gut microbiota was SIGNR3. To date, SIGNR3 is reported to be involved in the immune response to *M. tuberculosis* infection. However, the involvement of this receptor in intestinal inflammation is not known. To analyze the impact of the interaction of SIGNR3 and microbiota on intestinal inflammation, one objective within this thesis was to study the role of SIGNR3 in murine colitis. To this end, DSS-induced colitis was to be induced in SIGNR3-deficient mice and wild-type mice, followed by the detection of colitis symptoms and measurement of local cytokines.

3 MATERIAL AND METHODS

3.1 Materials

Mice

C57BL/6 wild type mice	Charles River, Sulzfeld, Germany Max Planck Institute of Infection Biology, Berlin, Germany
SIGNR3$^{-/-}$ mice C57BL/6-Cd209$^{dtm1.1Cfg}$/Mmucd 031934-UCD	NIH-sponsored Mutant Mouse Regional Resource Center (MMRRC) National System
OT-II transgenic mice/ C57BL/6-Tg(TcraTcrb)425Cbn/J	Max Planck Institute of Infection Biology, Berlin, Germany

Antibodies

Hamster anti-mouse CD11c, APC	BD Pharmingen, Heidelberg, Germany
Hamster anti-mouse CD11c, PE	BD Pharmingen, Heidelberg, Germany
Hamster anti-mouse CD11b, PE	BD Pharmingen, Heidelberg, Germany
Hamster anti-mouse CD80, FITC	BD Pharmingen, Heidelberg, Germany
Rat anti-mouse CD69, PerCP-Cy5.	eBioscience, Frankfurt, Germany
Rat anti-mouse CD19, FITC	BD Pharmingen, Heidelberg, Germany
Rat anti-mouse CD86, PE	BD Pharmingen, Heidelberg, Germany
Rat anti-mouse CD4-FITC	eBioscience, Frankfurt, Germany
Rat anti-mouse CD8, APC H7	BD Pharmingen, Heidelberg, Germany
Rat anti-mouse CD16/32	BD Pharmingen, Heidelberg, Germany
Rat anti-mouse IFN-γ (ELISpot capture)	BD Pharmingen, Heidelberg, Germany
Rat anti-mouse IFN-γ (ELISpot detection)	BD Pharmingen, Heidelberg, Germany
Rat anti-mouse IL-2 (ELISpot capture)	BD Pharmingen, Heidelberg, Germany
Rat anti-mouse IL-2 (ELISpot detection)	BD Pharmingen, Heidelberg, Germany
Rat anti-mouse IL-4 (ELISpot capture)	BD Pharmingen, Heidelberg, Germany
Rat anti-mouse IL-4 (ELISpot detection)	BD Pharmingen, Heidelberg, Germany
Goat-anti-mouse IgG (H+L), AP, AffiniPure	Jackson Immuneresearch, West Grove, USA
Goat-anti-mouse IgG_1, AP, AffiniPure	Jackson Immuneresearch, West Grove, USA

Goat-anti-mouse IgG_{2a}, AP, AffiniPure	Jackson Immuneresearch, West Grove, USA
Mouse anti-human IgG_1-AF488	Invitrogen, Carlsbad, CA, USA
Goat anti-human Fc antibodies, AP	Dianova, Hamburg, Germany
Goat-anti-human Fc, PE	Dianova, Hamburg, Germany
Goat-anti-human Fc, HRP	Dianova, Hamburg, Germany
Rabbit anti-*Candida Albicans* antibody, FITC	Meridian Life Science Inc., Memphis, USA

Vectors

pDRIVE, (including *E.coli* DH5α competent cells)	Qiagen, Hilden, Germany
pFUSE-hIgG1-Fc2	Invivogen, Toulouse, France
pUNO-SIGNR3	Invivogen, Toulouse, France
pCDNA3.1	Life technologies, Darmstadt, Germany

Molecular biology reagents

*Ecor*I, *Ecor*V, *Bgl*II, *Nco*I, *Not*I	NEB, Frankfurt am Main, Germany
Buffers 1,2,3 and 4	NEB, Frankfurt am Main, Germany
dNTPs (10 mM)	NEB, Frankfurt am Main, Germany
Ligation buffer (10x)	NEB, Frankfurt am Main, Germany
Nucleobond Xtra Midi kit	Macherey nagel, Düren, Germany
Marker, 100 bp, 1kbp	NEB, Frankfurt am Main, Germany
Qiaprep Mini kit	Qiagen, Hilden, Germany
QIAEXII kit	Qiagen, Hilden, Germany
Proteinase K	Sigma-Aldrich, St. Louis, USA
Ribolock RNase inhibitor	Thermo Scientific, Rockford, USA
Oligo(dT)18-Primer	Thermo Scientific, Rockford, USA
Taq buffer (10 x)	NEB, Frankfurt am Main, Germany
Taq polymerase	NEB, Frankfurt am Main, Germany
T4 ligase	NEB, Frankfurt am Main, Germany
TRI Reagent Solution RNA Isolation kit	Life technologies, Darmstadt, Germany

Cell culture material

BD Cytofix/Cytoperm™ Fixation/Permeabilization Kit	BD Pharmingen, Heidelberg, Germany
Cell culture dishes (10 cm, 6-well, 24-well)	Corning, New York, USA
FreeStyle MAX CHO expression system	Life technologies, Darmstadt, Germany
Cell culture 96-well plates (flat, round and v shaped wells)	Greiner, Frickenhausen, Germany
Combitips, 2,5 ml	Eppendorf, Wesseling-Berzdorf, Germany
CELLine CL350 bioreactors	Integra Biosciences, Fernwald, Germany
CHO cells	(Puck et al., 1958)
Cell strainer (40 µM)	BD Pharmingen, Heidelberg, Germany
CD11c microbead kit	Miltenyi Biotec, Bergisch Gladbach, Germany
Coverslips	Menzel GmbH, Braunschweig, Germany
ECL Plus™ Western Blotting Detection Reagents	GE Healthcare, Uppsala, Sweden
FACS tubes	Sarstedt, Nuremberg, Germany
Falcon tubes (15 and 50 ml)	Corning, New York, USA
Lipofectamine Reagent	Life technologies, Darmstadt, Germany
Multiscreen HTS Filter plate (ELISpot)	Millipore corportation, Bedford, USA
Inject needle, 17G, 20G	B. Braun, Melsungen, Germany
Pasteur pipette, glass	Roth, Karlsruhe, Germany
Pan T Cell Isolation Kit II	Miltenyi Biotec, Bergisch Gladbach, Germany
Sterile filter (0.45 µM)	Roth, Karlsruhe, Germany
Serological plastic pipettes	Corning, New York, USA

Cell culture media

RPMI 1640	PAN Biotech, Aidenbach, Germany
IMDM	PAN Biotech, Aidenbach, Germany
Sodium pyruvate (100 mM)	PAN Biotech, Aidenbach, Germany
Glutamine, stable (200 mM)	PAN Biotech, Aidenbach, Germany
Penicillin (10,000 U/ml)/ Streptomycin (10 mg/ml)	PAN Biotech, Aidenbach, Germany
Fetal calf serum, South America 3302	PAN Biotech, Aidenbach, Germany

Biochemistry material

Amicon ultra centrifugation unit, 10 kDa	Merck, Darmstadt, Germany
BCA Protein Assay Kit	Thermo Scientific, Rockford, USA
Cytrometric bead array Flex sets for IFN-γ, IL-4, IL-6, IL-10, TNF-α, IL-12/IL-23 and IL-1β	BD Pharmingen, Heidelberg, Germany
ColorPlus™ Prestained Protein Marker, Broad Range	NEB, Frankfurt am Main, Germany
ELISA Kit, murine IL-2	PeproTech, Rocky Hill, NJ, USA
HiTrap Protein G HP, 1 ml	GE Healthcare, Uppsala, Sweden
hFc	Merck Millipore, Darmstadt, Germany
Haemoccult test	Beckman Coulter, Galway, Ireland
Micro BCA Protein Assay Kit	Thermo Scientific, Rockford, USA
Ovalbumin (OVA)	Hyglos, Bernried am Starnberger See, Germany
p-Nitrophenyl-phosphate (pNPP)	Thermo Scientific, Rockford, USA
PageRuler Plus Prestained Protein Ladder	Thermo Scientific, Rockford, USA
Protease-inhibitor X	Serva Electrophoresis, Heidelberg, Germany
Protease-inhibitor HP	Serva Electrophoresis, Heidelberg, Germany
Syringe filter, PVDF, 0.45 µm	Roth, Karlsuhe, Germany
SYTO®61 red fluorescent nucleic acid stain	Life technologies, Darmstadt, Germany
Tooth pick	Roth, Karlsuhe, Germany

Chemicals

ABTS	AppliChem, Darmstad, Germany
Avidin-HRP	BD Pharmingen, Heidelberg, Germany
BSA	Life technologies, Darmstadt, Germany
Coomassie blue R-250	Serva Electrophoresis, Heidelberg, Germany
DAPI	AppliChem, Darmstad, Germany
DMSO	Serva, Heidelberg, Germany
FITC	Fluka, Sigma-Aldrich, St. Louis, USA
Sodium dextran sulfate salt 35,000–50,000 kDa	MP Biomedicals, Illkirch, France
Triethylamine	Alfa Aesar, Karlsruhe, Germany

Zeocin	Invivogen, Toulouse, France
Zymosan	Imgenex, San Diego, USA
Additional chemicals were obtained from	Sigma-Aldrich, St. Louis, USA
	Roth, Karlsuhe, Germany
	Merck, Darmstadt, Germany

Instruments

AmaZon ETD ion trap	Bruker Daltoniks, Bremen, Germany
Agarose gel system	Biozym, Hamburg, Germany
Analytic balance	Mettler Toledo, Columbus, OH, USA
Autoclave, Laboclav	Steriltechnik AG, Detzel Schloss, Germany
Autoflex™ Speed mass spec trometer equipped with smartbeam™ II laser optics	Bruker Daltonics, Bremen, Germany
Biorad electrophoresis system	Biorad, Munich, Germany
Eppendorf centrifuge 5810R, 5417R	Eppendorf, Wesseling-Berzdorf, Germany
ELISA plate reader, Tecan Infinite M200	Tecan, Crailsheim, Germany
ELISPOT reader, Bioreader 5000	Biosys, Karben, Germany
FACSCanto II	BD Pharmingen, Heidelberg, Germany
Fujifilm LAS-4000	Fujifilm, Tokyo, Japan
Freezer	Liebherr, Ochsenhausen, Germany
Fluorecent scanner, glycan array, Genepix 4300A	Molecular Devices, Sunnyvale, USA
IKA T10 homogenizer	IKA-Werke GmbH & Co. Staufen, Germany
Incubator, cell culture, Binder C150	Binder, Tuttlingen, Germany
Incubator, bacteria culture	Memmert, Schwabach, Germany
Hoefer TE22 buffer tank	Hoefer, Inc, Holliston, USA
LSM 700 confoncal scanning microscope	Zeiss, Oberkochen, Germany
Magnet stirrer, Heidolph MR Hei-Tec	Heidolph, Schwabach
Microwave	Panasonic, Hamburg, Germany
Microarray printer, Scieflexarrayer	Scienion, Berlin, Germany
Multi-pipette, Multi-channel	Eppendorf, Wesseling-Berzdorf, Germany
Oven	Binder, Tuttlingen, Germany
Light microscopte, Hund Wilovert,	Wilovert, Buckinghamshire, UK

NanoQuant plate	Männedorf, Switzerland
Neubauer cell counter chamber	Marienfeld, Lauda Königshofen, Germany
pH meter	Mettler Toledo, Columbus, USA
ProteCol™ Capillary Column, SGE,	Ringwood, Vic, Australia,
Pipettes	Eppendorf, Wesseling-Berzdorf, Germany
Specrometer Ultrospec 63	GE Healthcare, Uppsala, Sweden
Shaker, bacteria incubation, Multitron,	Infors HT ,Basel, Switzerland
Shaker	Neolab, Heidelberg Germany
Thermomixer comfort	Eppendorf, Wesseling-Berzdorf, Germany
Thermal cycler C100	Biorad, Munich, Germany
Ultimate 3000 UHPLC system	Dionex, Thermo Scientific, Rockford, USA
Water bath	Memmert, Schwabach, Germany

Software

FCAP Array Analysis Software	BD Pharmingen, Heidelberg, Germany
FlowJo analysis software	Tree Star Inc., Ashland, USA
FlexControl 3.3 software	Bruker Daltonics, Bremen, Germany
Graph pad prism	La Jolla, USA
GenePixPro7	Molecular devices, Sunnyvale, USA
MASCOT 2.3	MatrixScience, UK
ProteinScape 3	Bruker Daltonics, Bremen, Germany
Tecan nucleic acid software	Tecan, Crailsheim, Germany
DNASTAR Lasergene 9 Core Suit	DNASTAR Inc., Madison, USA
Clone Manager	Sci-Ed Software, Cary, USA
Primer 3	(Rozen and Skaletsky, 2000)
SAS software version 9.3	SAS Institute Inc, Cary, US

Table 3.1 Primers used for PCRs. Primers were synthesized by Eurofins MWG Operon, Ebersberg, Germany

Target	Primer sequence (restriction site underlined)	Ta (°C)	Product length	Restriction site
β-actin				
Forward	5'-GTCGTACCACAGGCATTGTGATGG-3'	60	493 bp	
Reverse	5'-GCAATGCCTGGGTACATGGTGG-3'			
Mgl1				
Forward	5'-GATATCCCAGTTAAGGAGGGACCTAGGCA-3'	62	749 bp	*Ecor*V
Reverse	5'-CCATGGAGCTCTCCTTGGCCAGCTTCATC-3'			*Nco*I
Clec9a				
Forward	5'-GAATTCGGGCATCAAGTTCTTCCAGGTATCC-3'	62	641 bp	*Ecor*I
Reverse	5'-CCATGGTGCAGGATCCAAATGCCTTCTTC-3'			*Nco*I
SIGNR3				
Forward	5'-GAATTCCATGCAACTGAAGGCTGAAG-3'	62	451 bp	*Ecor*I
Reverse	5'-AGATCTTTTGGTGGTGCATGATGAGG-3'			*Bgl*II
SIGNR3 expression				
Forward	5'-CTCATGCAACTGAAGGCTGA-3'	60	466 bp	
Reverse	5'-GCAGAGGCTGAGATGAGGTC-3'			
SIGNR3 genotyping				
SD.378	5'-TCCCCCTTCTGCCCTTTTGG-3'	58	WT: 243 bp	
SD.375	5'-CCAATTCCCAGCTTCCACGG-3'		KO: 129 bp	
SD.200	5'-GTTTGGGGGAAATCCAGCTG-3'			
Clec12b expression				
Forward	5'-ACTTTCTCCTAGGATGTCTG-3'	62	620 bp	
Reverse	5'-GCATGGGTTTGCAATAGGTC-3'			
Sequencing in pDrive				
M13 Forward	5'-GTAAAACGACGGCCAGT-3'			
M13 Reverse	5'-AACAGCTATGACCATG-3'			

3.2 Medium and Buffers

Molecular Biology

Proteinase K lysis buffer	0.1 M Tris, 0.2 M NaCl, 5 mM EDTA, 0.4% SDS, pH 8.0
TBE buffer (10x)	0.89 M Tris base, 0.89 M boraric acid, 20 mM Na_2EDTA, pH 8.0
LB medium (agar)	10 g Tryptone, 5 g Yeast Extract, 10 g NaCl (+ 15 g Agar) in 1000 m l water
LB medium (agar) low salt	10 g Tryptone, 5 g Yeast Extract, 5 g NaCl (+ 15 g Agar) in 1000 ml water
SOC medium	20 g Tryptone, 5 g Yeast Extract, 2 ml 5 M NaCl, 2.5 ml 1 M KCl, 10 ml 1 M $MgCl_2$, 10 ml 1 M MgSO4, 20 ml 1 M Glucose in 1000 ml water

Cell Culture

Complete RPMI	10 % FCS, 2 mM L-glutamine, 5 mM Penicillin-Streptavidin,
Complete IMDM	10 % FCS, 2 mM L-glutamine, 5 mM Penicillin-Streptavidin, 50 µg/ml Gentamycin
Erythrocyte lysis buffer	4,5 ml 160 mM Ammonium Chloride, 0.5 ml 100 mM TRIS, pH 7.5
FACS/MACS buffer	1xPBS 0.5% BSA and 2 mM EDTA

Biochemistry

ABTS substrate buffer	0.4 mg/ml ABTS, 0,03% hydrogen peroxide, 0.1 M Citrate buffer, pH 4.0
Coomassie solution	0.5 % coomassie blue R-250, 50% methanol, 7 % acetic acid
Destaining solution	50% methanol, 7 % acetic acid
EDTA-buffer	50 mM HEPES 25 mM EDTA, pH 7.4
Electrophoresis running buffer	25 mM Tris, 192 mM Glycin, 0.1 % SDS, pH 8.3
ELISA wash Buffer	0.05 % Tween 20 in PBS
ELISA blocking buffer	0.5 % BSA in PBS
ELISA antibody diluent	1 % BSA, 0.05% Tween 20 in PBS
Elution buffer	0.1 M glycine-HCl, pH 2.7
Glycan array blocking solution	2% BSA in lectin binding buffer
Lectin binding buffer	50 mM HEPES, 5 mM $MgCl_2$, 5 mM $CaCl_2$, pH 7.4

Modified Greenberger lysis buffer	300 mM NaCl, 15 mM Tris, 2 mM MgCl2, 0.5% Triton X-100, Protease-inhibitor X and Protease-inhibitor HP
Neutralization buffer	1 M Tris-HCl, pH 9.0
pNPP substrate buffer	10 mM Diethanolamine, 0.5mM $MgCl_2$
Protein G binding buffer	20 mM sodium phosphate, pH 7.0
Sample buffer (4X)	40 % Glycerin, 0.25 M Tris HCl pH 6.8, 4 % SDS, 0.015% BPB, 100 mM DTT (freshly added)
Separating gel 12 %	3 ml 1.5M Tris-HCl pH 8.8, 7.2 ml 30% bisacrylamide, 7.5 ml water, 125 µl 10% APS, 12.5 µl TEMED
Sodium carbonate buffer	50 mM Na_2CO_3, 100 mM NaCl, pH 7.5
Stacking gel 4%	2.7 ml 0.5 M Tris-HCl pH 6.8, 1.3 ml 30% Bisacrylamide, 6 ml water, 70 µl 10% APS, 7 µl TEMED
TBS (10X)	100 mM Tris, 1.5 M NaCl pH 7.3
TBS-T	1xTBS, 0.1% Tween 20
Transfer/Blotting buffer	25 mM Tris, 192 mM Glycine, 100 mL methanol, 900 mL H_20
Quenching solution	100 mM Ethanolamine, 100 mM Di-sodiumhydrogenphosphate, pH 9.0

3.3 Methods

3.3.1 Molecular biology

3.3.1.1 RNA extraction

Total RNA extraction from mammalian cells can be performed by lysing the cells in guanidinium hydrochloride and phenol (Chomczynski and Sacchi, 1987). This procedure rapidly inhibits endogenous RNases and by addition of chloroform, the homogenate is separated into two phases and an interphase. The upper aqueous phase contains the RNA, whereas the proteins are in the organic phase and the DNA in the interphase. RNA is then precipitated with isopropanol, washed with ethanol and then solubilized. By using this method, total RNA was extracted from C57BL/6 mouse spleen cells or mammalian cell lines with the TRI Reagent Solution as described by the manufacturer. Precipitated RNA was washed in 75 % Ethanol before being dissolved in 250 µl RNase-free water.

3.3.1.2 Reverse transcription

To transcribe single stranded RNA into complementary DNA (cDNA), the reverse transcriptase from avian myoblastosis virus (AMV) can be used. This is a DNA polymerase that transcribes total RNA into cDNA with the help of an Oligo(dT) primer that binds in the poly (A) region of the messenger RNA (mRNA). First, 1 µg of total RNA diluted in 10 µL RNase-free water was heated to 65 °C for 5 minutes. A 10 µl reaction containing 5 mM $MgCl_2$, 1x reaction buffer, 1 mM dNTPs, 20 units of RNase inhibitor, 15 units of AMV Reverse Transcriptase and 500 ng Oligo(dT)15 primer was added to the RNA. The reaction was incubated at 42 °C for 45 minutes followed by inactivation at 95 °C for 5 minutes and then stored at 4 °C.

3.3.1.3 DNA extraction

To extract genomic DNA (gDNA) from wild-type and SIGNR3$^{-/-}$ mice, 0.3 to 0.5 cm of a mouse tail biopsy was incubated with proteinase K (0.2 mg/ml) in 500 µl lysis buffer at 56 °C overnight under shaking. Following centrifugation at 18000 g for 5 min, DNA present in the supernatant was precipitated with isopropanol followed by washing with 70 % ethanol. DNA was dissolved in water and 1 µl was used for the genotyping PCR.

3.3.1.3 Polymerase chain reaction (PCR)

The PCR method is used to amplify a specific DNA sequence starting from a single stranded DNA sequence. To do this, two specific oligonucleotide primers are designed for the target sequence. DNA is first denatured at 95 ºC. After cooling, primers bind specifically to the complementary DNA strands. In the presence of a thermostable DNA polymerase and the four deoxynucleoside triphosphates (dNTPs), the synthesis and elongation of DNA segments complementary to the initial DNA target is started. In the following cycle, the newly synthesized DNA strands will be denatured and act as template for further DNA synthesis. The target DNA will be exponentially amplified by cycles of denaturation, primer annealing, and elongation. Amplification of the extracellular regions of three different murine CLRs was performed by PCR with specific primers and restriction site sequences (table 3.1). The PCR reaction mixture is presented in table 3.2. The optimal annealing temperature of each primer pair was identified using a temperature gradient PCR. The PCR program in table 3.3 was used to amplify each of the CLRs extracellular regions as well as for the expression analysis of SIGNR3. Primer design was performed with the software Primer 3. DNA analysis and calculations of molecular weights were performed with DNASTAR. For genotyping of the SIGNR3 gene, the same PCR conditions as described above were used, with the exception of that the three primers SD.378, SD.375 and SD.200 (table 3.1) were added in a concentration of 0.4 µM.

Table 3.2 PCR reaction mixture

Reagents	**Final conc.**
cDNA template	50-500 ng
Forward primer	0.5 µM
Reverse primer	0.5 µM
dNTPs	200 µM
10x Taq buffer	2.5 µl
Taq polymerase	1 U
Autoclaved H_2O	ad 25 µl

Table 3.3 PCR cycle

PCR step	Temp	Time	
Initial denaturation	95 ºC	3 min	
Denaturation	95 ºC	30 sec	} × 35 cycles
Annealing	See table 3.1	30 sec	
Elongation	72 ºC	45 sec	
Final elongation	72 ºC	5 min	
Cooling	8 ºC	∞	

3.3.1.5 Agarose gel electrophoresis and gel purification of DNA fragments

DNA fragments can be separated by size using agarose gel electrophoresis. When loaded on an agarose gel under an electric field, the negatively charged DNA migrates towards the anode. Larger fragments migrate more slowly through the agarose pores than smaller fragments. Total RNA and DNA samples as well as PCR products were analyzed by agarose gel electrophoresis (100V, 45 min). The 1.5 % agarose gel was stained with the DNA intercalating agent ethidium bromide (EtBr, 2 µg/ml) in TBE buffer for 10 min before being visualized and photographed under UV-light. PCR products and linearized plasmids aimed to be used for cloning or stable transfection were cut out from the agarose gel with a clean scalpel. To remove agarose, ethidium bromide, primers and other PCR reagents that could possible interfere with the following experimental steps, DNA was purified from the gel with the QIAEXII kit as described by the manufacturer.

3.3.1.6 Cloning of PCR products into cloning vector

Purified PCR products were ligated into the cloning vector pDrive. The DNA Taq polymerase is non-proof reading and leaves an overhang of the nucleotide adenine (A) on each 3’ end of the PCR product. By using a linearized cloning vector with 5’ overhang of uracil (U) at each side, such PCR products ligate to the vector. The purified PCR products of the CLR extracellular regions were cloned into the cloning vector pDRIVE as described by the manufacturer.

3.3.1.7 Ligation of PCR products into the pFUSE-hIgG1-Fc2 vector

The pFUSE-hIgG1-Fc2 expression vector facilitates the production of secreted fusion proteins consisting of the target protein fused to the Fc part of the human IgG_1 ($hIgG_1$). The Fc region contains the CH2 and CH3 domains of the IgG heavy chain and the hinge region. The hinge region serves as a flexible spacer between the protein of interest and the hFc part. The two proteins fused are thus able to function independently. The secreted fusion protein will form dimers, due to sulfide bridges between cystein residues in the hinge region (Capon 1989, Hollenbaugh 2002). The IL-2 secretion sequence allows for protein secretion.

To insert the amplified CLR extracellular regions in frame with the coding sequence of the Fc part in the expression vector, the first six base pairs of the 5' end of each of the primers were designed to correlate to restriction sites present in the multiple cloning site of the vector. The cloning vector containing the target sequence was digested, followed by gel purification. The insert was ligated into the pFUSE-hIgG1-Fc2 vector by incubating the ligation reaction (table 3.4) at 16 °C overnight.

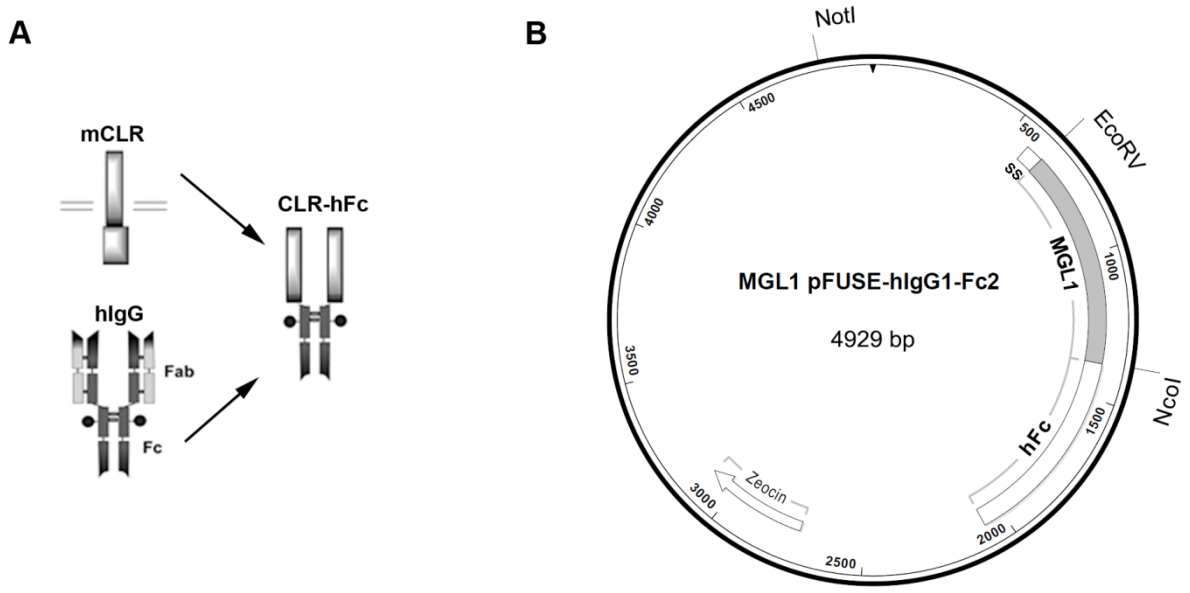

Figure 3.1 Fusion protein construction

A, Scheme of CLR-hFc fusion protein construction. *B*, pFUSE-hIgG1-Fc2 vector with the extracellular region of MGL1 inserted. This vector contains the IL-2 signal sequence (SS) for secretion and the zeocin resistance gene for selection.

Table 3.4 Ligation reaction

Reagents	Concentration
10x ligation buffer	2 µL
T4 ligase	1µL (400U)
pFUSE-hIgG1-Fc2 vector	80 ng
Insert	100 ng
Autoclaved H_20	ad 20 µL

3.3.1.8 Transformation into competent *E.coli* cells

Ligated insert and vectors were transformed into *E.coli* DH5α competent cells via the heat shock method. An aliquot of 50 µl competent cells were thawed on ice and 2 µl of the ligation reaction was added and incubated on ice for 30 min. The tube was then incubated at 42 ºC for 30 seconds before adding 250 µL of pre-warmed SOC medium followed by incubation at 37 ºC under 225 rpm shaking for 1h. The transformation solution (100 µl) was plated on agar plates containing selection antibiotics. Agar plates were incubated at 37 ºC overnight.

3.3.1.9 Colony PCR

To analyze whether the vector with the target construct was successfully transformed into the bacteria, single colonies were picked from the agar plate with a sterile toothpick. The sterile toothpick was shortly dipped in 50 µl of autoclaved water before being inoculated in 5 ml LB medium with antibiotics (for overnight cultures). After boiling the tube of water and bacteria at 95 ºC for 10 min, 1 µl was used for colony PCR. The PCR was performed as described above with the same primers as used for initial amplification of the target sequence.

3.3.1.10 Plasmid extraction

To extract plasmids from transformed *E.coli*, either a 5 ml inoculation (mini) or 100 ml culture (midi) was grown in LB media containing antibiotics. For bacteria transformed with the pDrive cloning vector, 100 µg/ml ampicillin was used and 50 µg/ml Zeocin in low salt LB medium was used for the pFUSE-hIgG1-Fc2-transformed bacteria. Overnight cultures were harvested by centrifugation at 4000 g, 4 ºC for 5 (miniprep) or 30 min (midiprep). Plasmid extraction was

performed by alkaline lysis of bacterial cells followed by adsorption of DNA onto silica. Miniprep was performed with the Qiaprep Mini kit and midiprep with the Nucleobond Xtra Midi kit following the manufacturer's recommendations. Extracted plasmids with inserts were sequenced with the primers in table 3.1 by the company Eurofins MWG Operon.

3.3.1.11 Measurement of nucleic acid concentration

Nucleic acid absorbs ultraviolet light and by measuring the optical density at 260 nm (OD_{260}) the concentration of nucleic acid in solutions can be determined. In addition, the purity of such solutions can be evaluated by the ratio of OD_{260}:OD_{280}. A ratio of 1.8 for RNA and 2.0 for DNA represents a pure preparation. The concentration of DNA and RNA were measured using the NanoQuant plate measured by the ELISA reader and analysis was performed with the Tecan nucleic acid software. After blanking each quartz spot with water, 2 µl of DNA or RNA solutions were used for measurement.

3.3.1.12 Digestion analysis

To perform analytic or preparative digestions, restriction enzymes corresponding to the inserted restriction site (table 3.1) were used. Shortly, 1-10 U restriction enzyme/µg plasmid were incubated in the total volume of 50 µl with the NEB buffer 1, 2, 3 or 4 at 37 ºC for 1h (analytic) or 4h (preparative). Before stable transfection, pFUSE-hIgG1-Fc2 was linearized with *Not*I.

3.3.2 Biochemistry

3.3.2.1 Purification of the CLR-hFc fusion proteins

Fusion proteins were purified from the supernatant of the bioreactors using protein G columns. Protein G is a type II Fc receptor expressed by Group G *streptococci*, which exhibits high affinity for the Fc region of human IgG at pH 7.0. Proteins expressing an Fc part bind to the protein G in the matrix of the column, thus are separated from other proteins. After washing with buffer, proteins are eluted by acidic pH.

To purify the CLR-hFc fusion proteins, the cell culture supernatants were first filtered through a 0.45 µM filter. A protein G column was equilibrated with binding buffer before the

supernatant was added to the column using a peristaltic pump (1 ml/min). Subsequently, the column was washed with 10 ml of binding buffer before eluting the fusion proteins with 10 ml glycin buffer (pH 2.7). The eluate was immediately neutralized with 100 µl of 1M Tris-HCl buffer (pH 9.0) per 1 ml eluted fraction. The protein G column was washed and stored in 20% ethanol. Proteins were concentrated and buffer change into PBS buffer was performed with the help of a 10 kDa Amicon ultra centrifugation unit, centrifuged repeatedly at 4000 g, 4 ºC for 10 min. Protein concentration was measured with the Micro BCA Protein Assay Kit, with bovine serum albumin (BSA) as standard. Preparation of IgG-depleted medium was performed by running FCS twice over a protein G column as described above.

3.3.2.2 Sodium dodecyl sulfate polyacrylamide gel electrophoreses (SDS-PAGE)

Proteins were separated by a sodium dodecyl sulfate polyacrylamide gel electrophoresis (SDS-PAGE). Gels were prepared by adding the freshly mixed reagents for a 12 % acrylamide separating gel in a gel casting chamber. Gels were polymerized for 30 min before the freshly prepared stacking gel was added. Samples were mixed with 4x sample buffer and heated at 95 ºC for 10 minutes before loading them in the slots of the acrylamide gel. The electrophoresis was run in running buffer until the front dye exited the gel (130 V, 1.5 h).

3.3.2.3 Coomassie staining

Coomassie is a triphenylmethane dye that binds strongly but non-covalently to amino acids and can be used to stain proteins separated by gel electrophoresis. Proteins separated on a SDS-PAGE gel were stained in coomassie solution for 30-60 min and thereafter washed in destaining solution until clear bands were observed.

3.3.2.4 Immunoblotting

Gels to be blotted were shortly washed in water and immersed in blotting buffer for 10 min. The blot sandwiches were packed, transferred into the Hoefer TE22 buffer tank and blotted (250 mA/gel) for 60 min. To prevent unspecific binding, the membranes were blocked overnight with 3% low fat milk solution in TBS-T. Membranes where then washed five times for five minutes each and were incubated with specific goat anti-human Fc antibodies (diluted 1:10 000 in TBS-T) at RT for 1 h. Membranes were again washed five times and developed using freshly

made ECL solution as described by the manufacturer. Detection was performed by a Luminescent Image Analyzer.

3.3.2.5 Preparation and labeling of gut microbiota

To analyze the interaction of CLR-hFc fusion proteins with commensal microbes, heat inactivated gut microbes were used. The microbiota content of C57BL/6 wild type mice colon was resuspended in PBS, filtered through a 40 µM Nylon Cell Strainer and diluted in PBS to an OD_{600} of 0.6. This was heat-inactivated at 65 ºC for 2 h under mild shaking. For binding analysis with CHO cells, 1 ml of gut microbes were labeled with FITC (5 mg/mL) in sodium carbonate buffer at 37 ºC for 30 min under shaking. After washing in PBS (supplemented with 0.25% BSA) five times, samples were resuspended in 100 µl PBS and directly used for binding studies.

To characterize the stool component recognized by SIGNR3, heat-inactivated stool microbes were labeled with SYTO61 red fluorescent nucleic acid stain at 2.5 µM in PBS at RT for 30 min and washed three times in PBS. Labeled microbiota suspension, representing 50 µl of the original unstained preparation (OD_{600} of 0.6), were blocked in PBS supplemented with 0.5 % BSA at 4 °C for 30 min. After centrifugation at 3000 g for 10 min, cells were incubated with 1 µg/ml CLR-hFc fusion protein in lectin buffer supplemented with 0.5 % BSA at 4°C for 1 h. After two washing steps, samples were incubated with PE-conjugated goat anti-hFc antibody. Commensal fungi were detected by staining the samples with FITC-conjugated rabbit anti-*Candida albicans* antibody at 4 °C, for 30 min in the dark. This antibody cross reacts with other yeasts as described by the manufacturer and has been used to stain indigenous fungi in murine gut microbiota (Iliev et al., 2012). Samples were washed three times and analyzed by flow cytometry.

3.3.2.6 Enzyme-linked immunosorbent assay (ELISA)

The concentration of IL-2 in the cell culture supernatants was analyzed by a sandwich ELISA. First, 50 µl of capture antibody (200 µg/ml) was coated on 96-well plates at 4 °C overnight. After incubating with blocking buffer for 2 h, 30 µl of supernatants or standards were incubated at RT for 2 h. After incubation with 50 µl of biotinylated specific detection antibody (100 µg/ml) for 2 h, 50 µl of avidin-HRP (1:1000) was added. Between each incubation step, wells were washed four times with ELISA wash buffer. The ELISA was developed by adding freshly prepared

ABTS substrate (final concentration of 1 mg/ml) in 0.1 M citrate buffer, pH 4.0 and hydrogen peroxide (1 µl/ml). Color development was measured spectrophotometrically at a wavelength of 405 nm, with a reference at 650 nm. The concentration of IL-2 in each supernatant was calculated from a standard curve (0-2000 pg/ml).

For analysis of the binding of CLR-hFc proteins to OVA-carbohydrate conjugates, OVA and OVA-carbohydrate conjugates (100 ng/well) were coated on a 96-well plate at 4°C overnight. After blocking as described above, 100 µl of fusion protein or hFc (20 µg/ml) were incubated in lectin binding buffer overnight. After incubation with alkaline phosphatase (AP)-conjugated goat anti-hFc (1:5000) at RT for 2 h, 100 µl of 1 mg/ml solution of p-Nitrophenyl-phosphate (pNPP) was added and incubated for 20 min before recording at the wavelength 405 nm. Washing between each step was performed as described above.

For analysis of antibody titers in sera from immunized mice, 2 µg OVA/well were coated on a 96-well plate at 4°C overnight. After blocking, different dilutions of sera were incubated for 2 h hours followed by incubation with the goat anti-mouse IgG (H+L) for 2 h (diluted 1:1000). To determine the IgG subtype of the antibodies in the sera, goat anti-mouse IgG_1 or IG_{2a} (both diluted 1:1000) were used. Washing steps and detection with the substrate pNPP was performed as described above.

To analyze the interaction of CLR-hFc proteins with commensal microbes, 50 µl of the preparation of heat inactivated gut microbes were coated on 96-well ELISA plates at RT overnight. After blocking with 1% BSA for 2 h, recombinant MGL1-hFc, Clec9a-hFc, SIGNR3-hFc or hFc were added at 10 µg/ml in either lectin binding buffer or 25 mM EDTA buffer at RT for 2 h. Washing steps were performed with either lectin binding buffer or EDTA buffer. Coated zymosan incubated with SIGNR3-hFc was used as a positive control. Detection steps were performed with the substrate pNPP as described above.

3.3.2.7 Colon homogenization

To analyze cytokines produced by the local intestinal immune cells, cytokine concentrations in the colon homogenates were measured. On day seven of DSS-treatment, mice were sacrificed and the whole colon was removed, flushed with PBS and stored at -80 ºC until use. Colon was homogenized in a modified Greenberger lysis buffer containing 1x protease-inhibitor X and HP cocktail using an IKA T10 homogenizer. Samples were incubated on ice for 1 h followed by

centrifugation at 12 000 rpm at 4 °C. Protein concentration was determined in the supernatant by the bicinchoninic assay using a Micro BCA Protein Assay Kit with BSA as standard (0-500 µg/ml). Aliquots of 2 mg/ml were frozen at -80 °C until further use.

3.3.2.8 Cytometric bead array

The cytometric bead array (CBA) is a method to analyze low concentrations of soluble proteins, such as cytokines, in a biological sample. Antibody-coupled beads are incubated with the samples and protein standards. Phycoerythrin (PE)-labeled detection antibodies are added and these bind to the antigen bound to the beads. Unbound antigens are washed away. During analysis with flow cytometry, each group of bead can be gated differently due to its specific fluorescence intensity. By measuring the intensity of PE and comparing it with protein standards, the concentration of the analyte can be determined. This method allows for quantification of several cytokines in the same tube.

The measurement of cytokines in the colon homogenate as well as in the supernatant of stimulated T cells was performed using CBA as described by the manufacturer. Briefly, provided standards and supernatants or colon homogenates (at a total protein concentration of 2 mg/ml) were incubated with a mixture of up to seven capture bead preparations in the wells of a 96-well round bottom plate for 1 h. Subsequently, PE-detection antibodies were added and after another hour of incubation, beads were washed and analyzed by flow cytometry. The following cytokines were measured: IFN-γ, IL-4, IL-6, IL-10, TNF-α, IL-12/IL-23, IL-17A and IL-1β. By plotting the protein standard curve (10-2000 pg/ml) the cytokine concentration was calculated using the FCAP Array Analysis software.

3.3.2.9 Glycan array

Glycan array is a method by which the interaction between carbohydrates and proteins can be analyzed. Functionalized carbohydrates are immobilized as small spots on glass slides, mimicking the natural presentation of carbohydrates on the cell surface. These are then incubated with either a fluorescently labeled protein or a lectin that afterwards can be detected by a fluorophore-labeled secondary antibody. Glycan array allows for efficient screening of multiple proteins with several carbohydrate ligands in parallel. An additional advantage of this method is

that only low amounts of sugar and protein are needed (Horlacher, Oberli et al. 2010; Lee, Hsu et al. 2011).

Synthetic carbohydrates were gathered from the library of synthetic glycans in the department and printed on epoxy glass slides as described below. A wide range of carbohydrates ranging from simple disaccharides to complex high mannose structures were used (Boonyarattanakalin et al., 2008; Bosse et al., 2002; Hanashima et al., 2007; Horlacher et al., 2010; Schlegel et al., 2011; Werz et al., 2007; Yin and Seeberger, 2010).

Amino- and thiol-functionalized carbohydrates, diluted in 50 mM sodium phosphate to the final concentrations of 1-1000 µM, were printed at approximately 1.2 nl per spot on epoxy-derivatized glass slides. Printing was performed using a piezoelectric microarray with an uncoated glass nozzle at 30 % humidity. For each glass slide, 16 replicate subarrays were printed, with each carbohydrate probe spotted in triplicates. Following printing, the slides were stored in a dark moisture chamber at RT for 24 h. Thereafter, slides were washed twice with distilled water, and centrifuged at 2000 rpm for 5 min. Unreacted amines and thiols on the glass slide were quenched by incubating the slides in 100 mM ethanolamine (quenching buffer) at 50 ºC for 1 h. After washing with distilled water, slides were dried and a 16-well grid was tightly attached to the slide. Each well was incubated with 100 µl blocking buffer for 1 h under mild shaking. Fusion proteins, diluted to 10 µg/ml in lectin buffer containing 0.01 % Tween, were added to each well and incubated at RT under mild shaking overnight. For detection, the Alexa488-anti-hFc antibody (diluted 1:500 in lectin buffer) was incubated in each well. Washing between incubation steps was performed in lectin buffer three times five minutes each, under mild shaking. Finally, the 16-well grid was removed and the slides were washed twice in 10 ml lectin buffer in a petri dish before washing with water. Slides were dried by centrifugation in a 50 ml Falcon tube at 1000 rpm for 5 min. Fluorescence was detected by scanning the samples with a microarray scanner. Analysis was performed with the software GenePixPro7.

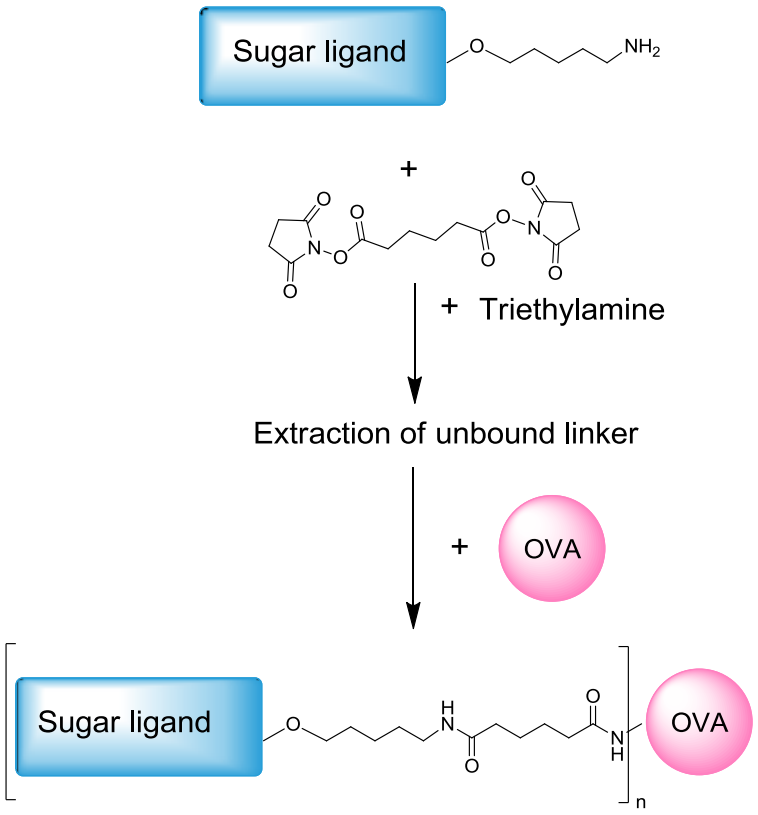

Figure 3.2 Scheme of conjugation of carbohydrate to OVA

3.3.2.10 OVA-sugar conjugation

Amino-functionalized Lewis X, 1,3-lactosamine and Gb5 were chemically synthesized by Dr. Mark Schlegel. Carbohydrates were conjugated with ovalbumin (OVA) with a disuccinimido adipate (DSAP) linker (synthesized by Felix Bröcker and Dr. Anish Chakkumkal). The DSAP linker contains an amine-reactive *N*-hydroxysuccinimide (NHS) ester at each end of a 6-carbon spacer arm. These NHS esters can react with primary amines at pH 7-9 to form stable amide bonds (Mattson et al., 1993). Thus, this linker can be used to conjugate a synthetic carbohydrate with an amine linker to primary amines in the side chain of lysine on the surface of a protein. The DSAP linker was dissolved in DMSO and activated by 10 µl triethylamine. Carbohydrates dissolved in DMSO were added dropwise and let to react under stirring for 1.5 h. Additional 250-500 µl phosphate buffer was added and unreacted linker was extracted by adding 10 ml of chloroform followed by centrifugation at 3000 g for 3 min. Bound carbohydrate-linker was

pipetted from the aqueous phase and this chloroform extraction was repeated two times. Carbohydrate-linker was incubated with OVA in 250-500 µl sodium phosphate buffer at pH 7.4 under stirring, overnight. Samples were concentrated in a 10 kDa Amicon centrifugation unit and dissolved in either water for MALDI analysis or sterile PBS and stored at -20 °C until further use.

3.3.2.11 MALDI-TOF-MS

To characterize the average amount of carbohydrate conjugated on each OVA molecule, matrix-assisted laser desorption/ionization time-of-flight mass spectrometry (MALDI-TOF-MS) analysis was performed. MALDI-TOF-MS analysis was performed on an Autoflex™ Speed mass spectrometer equipped with smartbeam™ II laser optics running at 1000 Hz. The instrument was controlled by FlexControl 3.3 software. The samples were prepared at a concentration of 1 mg/ml in water. Equal amounts of sample and the matrix 2',4',6'-trihydroxyacetophenone monohydrate (THAP; 50 nmol/µl in 50 % acetonitrile) were mixed and 1 µL was spotted onto a 384-spot MALDI target (600 µm polished steel) and allowed to dry at room temperature. Internal calibration was performed using a standard calibration mix. MS spectra were acquired in linear-positive ion within the mass range of *m/z* 25,000 to *m/z* 65,000. After analysis, acquired spectra were baseline corrected and smoothed using Gauss algorithm with m/z 0.2 widths and 1 cycle with the software Flex Analysis.

3.3.2.12 LC-MS/MS analysis

To further characterize the fusion proteins, peptide analysis by LC-ESI-MS was performed. CLR-hFc fusion protein were separated by SDS-PAGE and stained with coomassie solution. Bands of interest were cut out and tryptic digestion was performed as described previously (Kolarich et al., 2012) with minor modifications. Liquid chromatography-mass spectrometry (LC-MS) analysis was performed on an AmaZon ETD ion trap coupled to an Ultimate 3000 UHPLC system. Tryptic peptides were separated by reversed phase chromatography using a ProteCol™ Capillary Column. Peptide trapping and reversed phase separation was performed at a column temperature of 45 °C. After desalting the sample on the trap column, a gradient (appendix I) using an increasing concentration of solvent B (starting with 2 % of acetonitrile with 0.1% formic acid) was applied. The instrument was set up to perform electron-transfer dissociation (ETD) fragmentation as well as collision-induced dissociation (CID) on the selected precursors. An m/z

range from 400-1500 Da was used for data-dependent precursor scanning. The three most intense signals in every MS scan were selected for MS/MS experiments. The data was recorded in the "enhanced resolution mode". Data analysis was performed using ProteinScape 3 and MASCOT 2.3 using the following search parameters: Cysteine as carbamidomethyl was set as fixed modification, and deamidation (Asn/Gln) and oxidation (Met) were set as variable modifications. Up to two missed cleavages were allowed. Peptide tolerance (both MS and MS/MS) was set at ±0.2 Da. Data were searched against the SwissProt protein database with no restriction in taxonomy.

3.3.3 Cell biology

3.3.3.1 Cell culture

Chinese hamster ovary (CHO) cells were cultivated in complete RPMI medium at 37 °C in a humidified incubator with 5% CO_2 on 10 cm cell culture dishes. The cells were splitted every 3-4 days. This was performed by removing medium and washing cells with pre-warmed PBS followed by incubation with 5 ml PBS containing 0.05 % EDTA at 37 °C for 5 min. Cells were resuspended in medium and centrifuged at 300 g for 5 min. After resuspension in 5 ml fresh medium, 500 µl of cell suspension was diluted into a new cell culture dish with 10 ml medium.

3.3.3.2 Stable and transient transfection

Transient and stable transfection was performed with the Lipofectamine transfection reagent as described by the manufacturer. Briefly, 0.6 µg DNA and 2.5 µl transfection reagent were mixed in FCS-free RPMI medium and left to form DNA-liposome complexes at RT for 15 min. This solution was added dropwise on cells grown to 50-80% confluency in 24-well plates. For selection of stable clones, complete RPMI medium containing 250 µg/ml zeocin was added to the cells 48 h after transfection and cells were cultured for 10 days. Medium was replaced by fresh zeocin-containing medium every second day until the majority of cells (representing untransfected cells) died. To obtain single clones stably expressing the CLR-hFc fusion proteins, 100 µl of cell suspensions with the concentrations of 300, 30 or 3 cells/ml were seeded in 96-well plates. After 4-5 days of growth, wells where single clones were growing were marked. Monoclonal cells were analyzed by intracellular staining and expanded in 24-well plates. For

transient transfection, CHO cells were seeded on coverslips in 24-well plates and transfected as described above.

3.3.3.3 Intracellular staining

To analyze whether cells were successfully expressing the CLR-hFc fusion protein, intracellular staining of the human Fc part was performed with the BD Cytofix/Cytoperm™ Fixation/Permeabilization Kit. Cells were harvested and approximately 10^5 cells were centrifuged and resuspended in 250 µl Fixation/Permeabilization solution at 4°C for 20 min. This procedure permeabilizes the cell membrane, thus allowing for intracellular staining. After washing twice with BD Perm/Wash™ buffer, cells were resuspended in 50 µl staining solution containing PE-labeled goat anti-human IgG antibody (diluted 1:100) and incubated at 4°C in the dark for 30 min. Once again, cells were washed twice before resuspension in 250 µl PBS and measurement by flow cytometry.

3.3.3.4 Staining of cell surface markers

For analysis of cell surface markers, approximately 5 x 10^5 cells were stained with fluorochrome-conjugated antibodies (diluted 1:200) at 4 °C in the dark for 30 minutes. Certain hematopoetic cells such as macrophages, B cells and dendritic cells express the FcγRII/III. These receptors recognize epitopes present in the constant region of antibodies. To block this Fc-receptor mediated binding, splenic cells were pre-incubated with anti-CD16/32 (diluted 1:200) at 4°C for 20 min before staining of surface markers. Subsequently, cells were washed twice and measured by flow cytometry. All staining and washing steps were performed in FACS buffer.

3.3.3.5 Flow cytometry

Cells subjected to staining of cell surface markers and intracellular proteins were resuspended in 300-500 µl FACS buffer and measurement was performed using a FACS Canto II flow cytometer. Data were analyzed using FlowJo analysis software.

3.3.3.6 Production of CLR-hFc fusion proteins

Each stably transfected CHO cell line was cultivated in the inner compartment of a CELLine CL350 bioreactor according to the manufacturer's instructions. This bioreactor allows a high amount of cells to grow in a small volume of medium. A semipermeable 10 kDa membrane separates this inner compartment from the outer compartment with 100 ml of complete medium. Nutrients from both compartments reach the cells whereas proteins of the size > 10 kDa remain in the inner compartment.

For the production of MGL1-hFc and Clec9a-hFc, the inner compartment of a bioreactor contained 5 ml of complete RPMI medium depleted of bovine IgGs, whereas 100 ml of complete RPMI without FCS was added to the outer compartment. The bioreactors were incubated at 37 °C with 5 % CO_2. The supernatant was harvested weekly and an aliquot of the cells was diluted in fresh medium and returned into the bioreactor. Subsequently, the harvested medium was centrifuged at 300 g, 4 °C for 7 min. The cell-free supernatants containing the CLR-hFc fusion proteins were stored at -20 °C until protein purification.

For the production of SIGNR3-hFc, the FreeStyle™ CHO-S Cell system was used as described by the manufacturer. Shortly, 37.5 µg of the CLR-hFc vector were mixed with the FreeStyle™ MAX Transfection Reagent and incubated at 10 min to let DNA-lipid complexes form. This was then added to 3 x 10^7 FreeStyle™ CHO-S suspension cells in a volume of 30 ml in FreeStyle™ CHO Expression Medium. Three days after transfection, cell suspension was centrifuged at 200 g, 4 °C for 5 min. Medium was harvested and stored at -20 °C until protein purification.

3.3.3.7 Isolation of spleen cell subsets

To isolate spleen cells, spleens were removed from sacrificed mice and flushed with complete RPMI medium with a fine needle. The cell suspension was filtered through a 40 µM cell strainer to remove cell aggregates. After centrifugation at 300 g for 5 min, cell pellets were resuspended in 5 ml freshly prepared erythrocyte lysis buffer and incubated at RT for 3-5 min. Cells were washed in complete RPMI medium and centrifuged before resuspension in MACS buffer. $CD11c^+$ cells were isolated from C57BL/6 mice spleen and T cells from OT-II mice by magnetic-activated cell sorting (MACS) using CD11c microbeads and Pan T Cell Isolation Kit II, respectively. Before incubating with CD11c microbeads, cell surface FcγRII/III was blocked with

anti-CD16/32. Cells incubated with magnetic microbeads were loaded on a column placed in a magnetic field. Unbound cells were washed away with MACS buffer. $CD11c^+$ cells were eluted by removing the column from the magnetic field and flushing with buffer. To increase purity, $CD11c^+$ cell purification was repeated as described. To isolate T cells, non-target cells were magnetically labeled (with antibodies against CD11b, CD11c, CD19, CD45R, CD49b, CD105, MHC class II and Ter-119) and therefore trapped in the column whereas T cells were present in the flow through. Isolated cell subsets were subsequently centrifuged and resuspended in complete medium.

3.3.3.8 Isolation of mesenteric lymph node cells

For the isolation of mesenteric lymph node (MLN) cells, the lymph nodes in the mesentery along the colon and small intestine were removed. Tissue was homogenized between two sterile glass slides which were then washed with complete RPMI medium. Cells were filtered through a 40 µM cell strainer and washed in PBS twice before RNA extraction.

3.3.3.9 *In vitro* stimulation with OVA-carbohydrate conjugates

To analyze whether the different OVA-carbohydrate conjugates could modulate the activation of T cells *in vitro*, an OT-II cell-based assay was used. T cells from transgenic OT-II mice have a TCR specific for the $OVA_{323-339}$ peptide presented by MHC class-II $I\text{-}A^b$ molecules (Barnden et al., 1998; Robertson et al., 2000) and this model is often used to analyze specific $CD4^+$ T cell activation. Pulsing APCs with whole OVA protein leads to protein endocytosis and intracellular degradation. $OVA_{323-339}$ peptide is loaded on MHC-II molecules and presented to OT-II T cells. In this thesis, the OT-II cell model was used to analyze whether carbohydrate ligands of CLRs could modulate the uptake and processing of OVA by $CD11c^+$ cell, thereby affecting T cell activation.

MACS purified $CD11c^+$ DCs were seeded on a 96-well cell round bottom culture plate (2×10^4 cells/well) in complete IMDM medium. After 30 min, cells were pulsed with OVA and OVA-carbohydrate conjugates at a final concentration of 30 µg/ml. One hour later, 1×10^4 purified OT-II T cells were added to each well. Activation of $CD11c^+$ cells and T cells were analyzed by flow cytometry after 48 and 72 h. Cytokines in the supernatant were analyzed by ELISA or CBA.

3.3.3.10 Enzyme-linked immunosorbent spot (ELISpot) assay

To analyze the number of activated T cells in spleens from mice immunized with OVA-carbohydrate conjugates, ELISpot analysis was performed. ELISpot is a method where the number of cells producing a target molecule can be determined (Czerkinsky et al., 1983). Examples of target molecules are B-cell produced antibodies or cytokines produced by T cells. For analysis of cytokines, the respective capture antibody is coated on a polyvinylidenfluoride (PVDF) membrane on the bottom of the wells of a 96-well ELISpot plates. Cells are added and the produced cytokines are rapidly captured. These captured antigens can be detected by enzyme-conjugated antibody and by addition of the enzyme substrate one spot is detected for each cytokine-producing cell.

To determine the number of IL-2, IL-4 or IFN-γ secreting cells in spleens from mice immunized with OVA-carbohydrate conjugates, the PVDF membranes in 96-well ELISpot plates were pre-wet with 35 % ethanol for one minute. After washing three times with PBS, 50 µl of the capture antibody (5 µg/ml) were added and incubated at RT for 6 h. Subsequently, wells were washed twice with RPMI medium before blocking unspecific binding by adding 200 µl complete RPMI medium to each well at RT for 2 h. After decanting of the blocking medium, 100 µl of $OVA_{323-339}$ (50 µg/ml) or anti-mouse CD3/CD28 (10 µg/ml) were added to the wells. Subsequently, 4 x 10^5 splenic cells were added to each well and incubated at 37 °C for 18 h. All steps were performed under sterile conditions. The following day, wells were washed with PBS containing 0.05 % Tween, followed by addition of 50 µl of biotinylated antibodies (2 µg/ml in PBS with 10 % FCS) and incubation for 2 h. After washing with PBS containing 0.05 % Tween, 50 µl of avidin-HRP (diluted 1:1000 in PBS with 10 % FCS) were added and incubated at RT for 1 h. After washing four times with PBS containing 0.05 % Tween and two times with PBS, 100 µl of the substrate solution 3-Amino-9-ethylcarbazole (AEC) was added. The reaction was stopped by washing with deionized water. The plates were air dried overnight and the numbers of spots were detected using a Bioreader 5000.

3.3.3.11 Interaction studies of transiently transfected CHO cells and gut microbiota

To analyze the interaction of gut microbiota with SIGNR3-expressing cells, CHO cells seeded on coverslips were transiently transfected with either pUNO-SIGNR3 or pcDNA3.1 (mock vector).

After 24 h, cells were fixed in 400 µl of 4 % paraformaldehyde (PFA) at 4 ºC for 20 min before quenching with 400 µl of 100 mM glycine for 10 min. FITC-labeled bacteria (diluted 1:40) were incubated in 400 µl lectin binding buffer under mild shaking at 4 ºC for 2.5 h. Cell nuclei were stained with DAPI. Cells were washed twice in lectin binding buffer or 25 mM EDTA-buffer before microscopic analysis. Blinded analysis was performed with a LSM 700 confoncal scanning microscope.

3.3.4 Animal experiments

3.3.4.1 Animal conditions

Mice were housed under special pathogen free (SPF) conditions in the animal facility of the Federal Institute for Risk Assessment (BfR), Berlin, and were provided irradiated food and water *ad libitum*. Animal experiments were performed in strict accordance with the German regulations of the Society for Laboratory Animal Science (GV-SOLAS) and the European Health Law of the Federation of Laboratory Animal Science Associations (FELASA). All protocols were approved by the Landesamt für Gesundheit und Soziales (LAGeSo) Berlin. All efforts were made to minimize suffering.

3.3.4.2 Adoptive transfer

To analyze whether the different OVA-carbohydrate conjugates could modulate the immune response *in vivo*, immunization studies were performed. To induce a specific response with a low dose of antigen, adoptive transfer of OT-II cells into wild-type mice was performed one day before immunization. To analyze proliferation of the transferred cells, labeling with a fluorescent dye was performed before adoptive transfer. Splenic cells were obtained from 10-week old female OT-II transgenic mice, on C57BL/6 background, and the erythrocytes were lysed in lysis buffer as described above. The cells were then labeled with Cell Proliferation Dye eFluor® 670 according to the manufacturer's instructions. Briefly, 3 x 10^8 cells were washed with room tempered PBS before adding the eFluor 670 (final concentration of 5 µM) under vortexing. Cells were incubated in the dark at 37 °C for 10 min before labeling was stopped by addition of complete RPMI medium. After washing three times and counting of the cells, 1.5 x 10^7 labeled cells in 100 µl PBS were injected intravenously (i.v.) into female wild-type C57BL/6 mice. Each step of cell labeling was performed under sterile conditions. To analyze for successful cell

transfer, peripheral blood from the tail was taken 1 h after i.v. injection. Blood was taken into a heparinized syringe and centrifuged at 450 g, 4 ºC for 5 min. Subsequently, cells were resuspended in erythrocyte lysis buffer and incubated at RT for 7 min, before repeating centrifugation. The cells in the pellet were resuspended in FACS buffer, and the surface markers CD45 and CD4 were stained as described in section 3.3.3.4.

3.3.4.3 Immunization

One day after the adoptive transfer of OT-II transgenic spleen cells into wild-type C57BL/6 mice, pre-immunization sera were obtained from the recipient mice. These mice were then prime-immunized by intraperitoneal injection (i.p.) of PBS, 22 µg OVA, OVA-Alum (22 µg OVA; 1:1 mixture of OVA and Alum), 22 µg OVA-Lewis X, 22 µg OVA-1,3-lactosamine, or 22 µg OVA-Gb5 in the total volume of 200 µl. On day 21, boost immunization was performed using the same amounts of controls and OVA-carbohydrate conjugates. Sera were obtained on days 7, 13, 21, and 27 post-immunization.

3.3.4.4 Serum collection

For analysis of antibody titers in sera, blood was retrieved from the mouse tail vein. Blood was incubated at RT for 30 min, before centrifugation at 10000 rpm, RT for 10 min. Sera were pipetted into new Eppendorf tubes and stored at -80 ºC until further use.

3.3.4.5 Chemically induced colitis

Colitis can be induced in mice by adding DSS to the drinking water for seven consecutive days. DSS disrupts the mucosal surface in the colon thus immune cell get into contact with microbiota and a local inflammation is induced.

Before induction of colitis, 3% DSS (w/v) was dissolved in water and sterile filtered. Female SIGNR3-/- mice and the respective C57/BL6 wild-type control mice in the age of 8-11 weeks, were co-housed for 2-3 weeks before start of the experiment. To induce colitis, mice were fed 3% DSS (w/v) for eight days. The weight of the mice was analyzed daily and water bottles were regularly exchanged to bottles with fresh DSS or water. On day eight, mice were sacrificed and the colon length was measured. A disease activity index (DAI) was assigned to each mouse as previously described by others (Saunders, 2010, modified from Cooper, 1993). Shortly, a score

of 0-4 (table 3.5) was assigned to each mouse depending on stool consistency, presence of blood in feces and weight loss. Blood in feces was detected with Greegor's modified Guaiak test as described by the manufacturer.

3.3.4.6 Histology

Fresh whole colon of each mouse was prepared as Swiss roles in an embedding cassette and fixed with 4% buffered formalin. The following procedure and histologic analysis were performed by Dr. Dorthe von Smolinski. Samples were embedded in paraffin, sectioned at 4 µm thickness and stained with hematoxylin and eosin (H&E). Sections were evaluated histopathologically in a blinded manner. The Swiss roles were divided in three segments of identical length and each part was scored as described in table 3.6. Shortly, the degree of infiltration of inflammatory cells and mucosal erosion/ulceration was graded from none, mild, moderate to severe. Additionally, the percentage of altered tissue was calculated for each segment of identical length.

Table 3.5 Scoring for disease activity index

Score	Blood in feces	Stool consistency	Weight loss
0	No blood detected	Normal	0 %
1			1-3%
2	Blood detected	Loose stool	3-6%
3			6-9%
4	Gross blood detected	Diarrhea	>9%

Table 3.6 Scoring system for histological evaluation of intestinal lesions

Score	Infiltration of inflammatory cells	Mucosal erosion/ulceration
0	none	none
1	mild	mild
2	moderate	moderate
3	severe	severe

3.3.5 Statistical analysis

Significant differences between sample groups with normally distributed values were analyzed with two-tailed, unpaired student t-test. Level of significance was set to 5%. Normal distribution was examined with the Shapiro-Wilk test. If values were not normally distributed, the Mann-Whitney test was used. Generally, a null-hypothesis was designed and if the calculated p value was lower than 0.05, the null-hypothesis was rejected. If there was no variance of the different values in the control group of experiments, one sample t-test was performed. The experimental group values were compared with the value in the control group. Statistical analyses were performed using the Graph pad prism software. For analysis of the body weight, mixed linear model was used taking multiple measurements per mouse into account and the structure of these measurements are assumed to be autoregressive (indicating that each measurement depends on the measurement of the day before). In addition to the factor group, day was also a factor in the model. The mixed linear model was performed using SAS software version 9.3.

4 RESULTS

4.1 Thesis overview

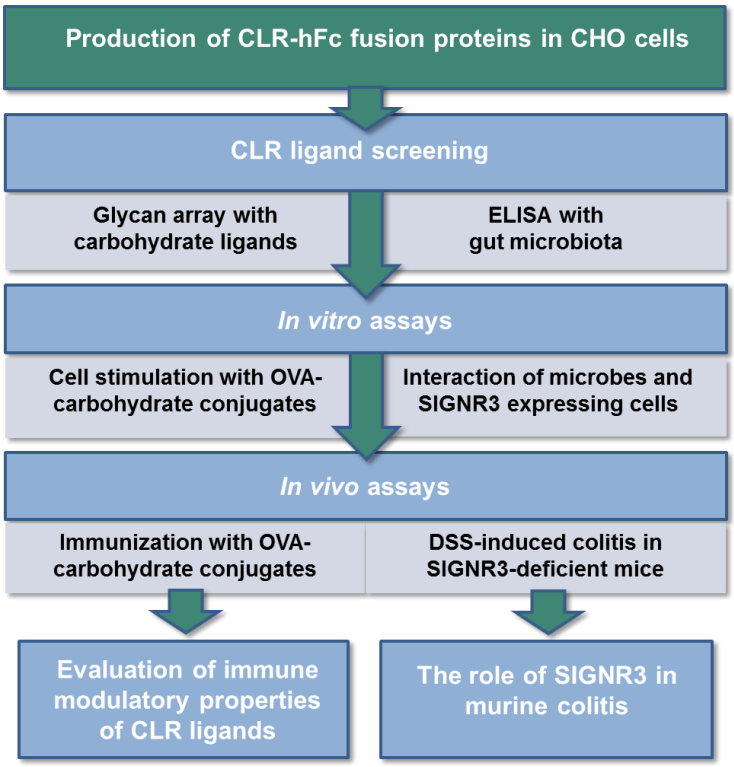

Figure 4.1 Overview of the different steps of the platform (left) and the analysis of the CLR SIGNR3 in murine colitis (right).

4.2 Production of CLR-hFc proteins

4.2.1 Cloning and expression of fusion proteins

As a tool to screen for immunomodulatory properties of CLR ligands, fusion proteins consisting of the extracellular region of a murine CLR fused to the Fc part of human IgG_1 were generated. The construction of chimeric IgG fusion proteins was first described in the late 1980s (Capon et al., 1989; Gascoigne et al., 1987). One advantage of CLR-hFc fusion proteins is that they are secreted as homodimers linked by sulfide bonding between the cysteine residues in the hinge region of the hFc (Figure 3.1)(Capon et al., 1989; Hollenbaugh and Aruffo, 2002). Certain CLRs

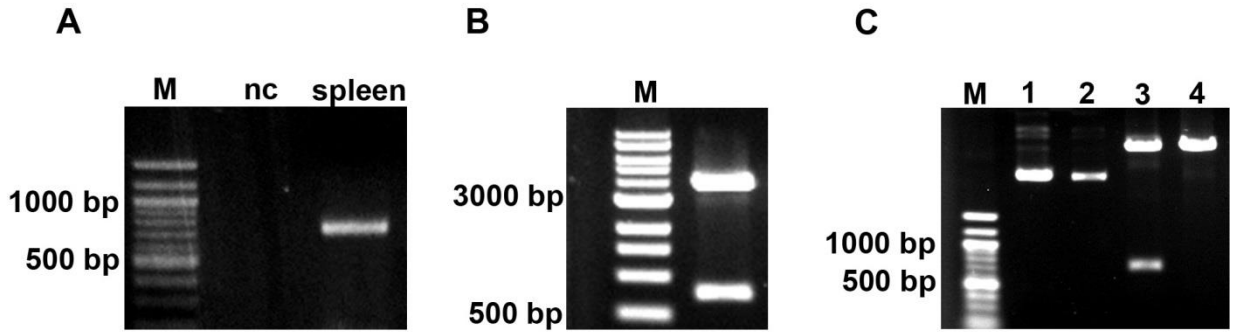

Figure 4.2 Cloning of the MGL1-hFc construct

Products of each cloning step were analyzed on a 1.5 % agarose gel, stained with EtBr and visualized under UV light. *A,* The extracellular region of MGL1 was amplified by PCR (749 bp) and ligated into the cloning vector pDrive. *B,* Digestion of MGL1 in pDrive, by the restriction enzymes *Ecor*V and *Nco*I . *C,* Analytic double digestion of MGL1 in pFuse-hIgG1-Fc2 with the same enzymes as in B. Shown are undigested plasmids (1 and 2), digested plasmids with insert successfully ligated (3) or without any insert (4). M, marker; nc, negative control.

such as Dectin-1 and Clec2 naturally form dimers in the cell membrane (Sancho et al., 2009), thus, the dimerization of the fusion proteins resembles the native state of these CLRs. In addition, the dimerization of two CRDs increases the avidity compared to a monovalent protein. Moreover, CLR-hFc fusion proteins can be detected in parallel both during the production and in experimental assays.

Since the CLRs MGL1, Clec9a and SIGNR3 were all expressed in spleen and $CD11c^+$ cells, cDNA transcribed from murine splenic mRNA was used to amplify the extracellular regions. The quality of the cDNA was first controlled by amplifying the coding sequence of the β-actin transcript (data not shown). By performing a gradient PCR analyzed on an agarose gel, the optimal annealing temperature was established for each primer pair (Table 3.1). Each amplicon was first ligated into the cloning vector pDrive by TA-cloning. Primers used for the PCR included restriction sites at the 5'end (see Table 3.1). By digestion with specific restriction enzymes, the insert was cut out from the cloning vector, followed by ligation into the expression vector pFuse-hIgG1-hFc2 (Figure 3.1B). In this way, the CLR extracellular region was inserted in frame with the hFc coding sequence. Each cloning step was examined by agarose gel analysis. A representative example of cloning of a CLR-fusion protein is shown in Figure 4.2. The cDNAs coding for each CLR-hFc protein and the corresponding amino acid sequences are presented in the appendix. For the production of MGL1-hFc and Clec9a-hFc, CHO cells stably expressing the fusion proteins were produced. For this purpose, vectors were linearized by *Not*I and transfected

into CHO cells. Stable subclones (Figure 4.3) were grown in bioreactors and the fusion proteins were purified from the supernatant over a protein G column. Protein concentration was measured by BCA and a range of 150-300 µg of each fusion protein was produced in a bioreactor. The SIGNR3-hFc fusion protein was produced by transiently transfected FreeStyle™ CHO-S Cell and purified like the other proteins. About 100 µg SIGNR3-hFc per 30 ml transiently transfected cells were produced. The SIGNR3-hFc fusion protein was generated by Timo Johannssen.

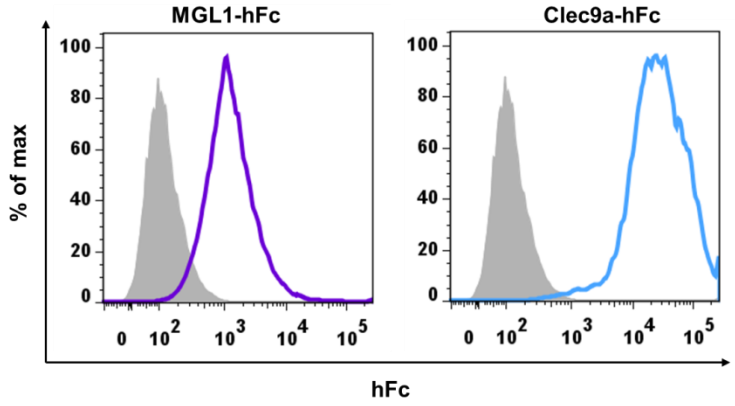

Figure 4.3 Stable subclones of CLR-hFc expressing CHO cells

Intracellular staining of the CLR-hFc in transfected CHO subclones was performed with a phycoerythrin-labeled antibody against the hFc part and cells were analyzed by flow cytometry. Shown are stable stable subclones of CHO cells expressing MGL1-hFc and Clec9a-hFc.

4.2.2 Characterization and functionality of the CLR-hFc fusion proteins

To characterize the fusion proteins, they were separated by SDS-PAGE followed by western blot analysis or Coomassie staining of the gel. To facilitate the analysis of several fusion proteins on the same western blot membrane, an antibody against the hFc part was used. Using this antibody is also of advantage if a commercial antibody is not available. Coomassie gel staining and western blot analysis of MGL1-hFc show one single band representing the expected calculated size of 54.2 kDa of the fusion proteins (Figure 4.4A and C). In accordance with this, ES-MS/MS analysis of MGL1-hFc revealed that the main peptides were from MGL1 and the hIgG (appendix). Similar to the MGL1-hFc fusion protein, a band representing the expected molecular weight of 44.7 kDa was detected by analysis of SIGNR3-hFc (Figure 4.4B and D). When Clec9a-hFc was analyzed by western blot and Coomassie staining, a protein around the size of 50 kDa was detected. This protein correlates with the calculated MW of 46.7 kDa for Clec9a-hFc. In addition, multiple bands with different sizes were detected (Figure 4.4A).

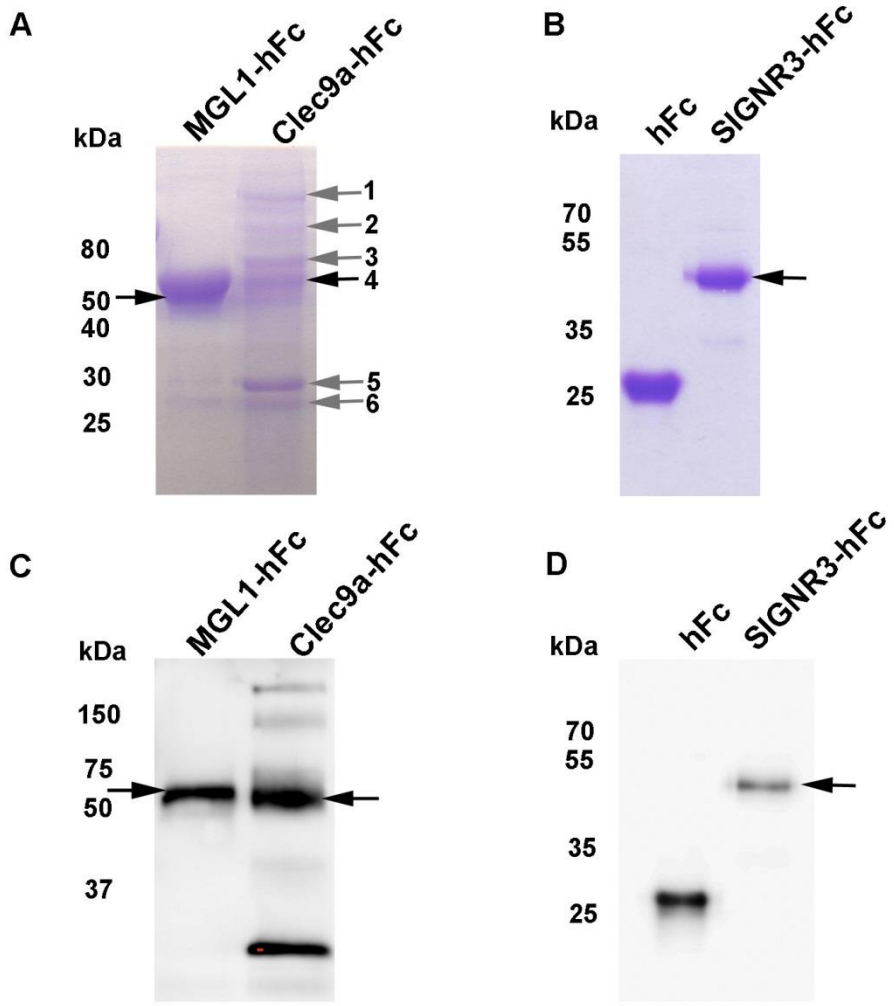

Figure 4.4 Characterization of fusion proteins

CLR-hFc fusion proteins were separated by SDS-PAGE and analyzed by Coomassie gel staining (*A* and *B*) or western blot using a HRP-labeled antibody against the hFc part (*C* and *D*). Black arrows show bands representing the fusion protein representing the calculated molecular weights of 46.7 kDa (Clec9a-hFc), 54.2 Da (MGL1-hFc), and 44.7 kDa (SIGNR3-hFc). Bands of interest from Clec9a-hFc and MGL1-hFc (*A*, black + grey arrows) were cut out, tryptically digested and analyzed by LC/MS-MS.

ES-MS/MS analyses show that all but one of the analyzed protein bands contained mainly peptides from Clec9a and hIgG (appendix). These analyses confirm the identity of the generated Clec9a-hFc fusion protein and suggest that the additional bands proteins represent proteins with post-translational modifications, such as glycosylation, thus increasing the molecular weight. The proteins of less MW are presumably degradation products.

As a general control of the functionality and carbohydrate binding capabilities of the produced fusion proteins, the interactions of MGL1-hFc and the reported MGL1 ligands

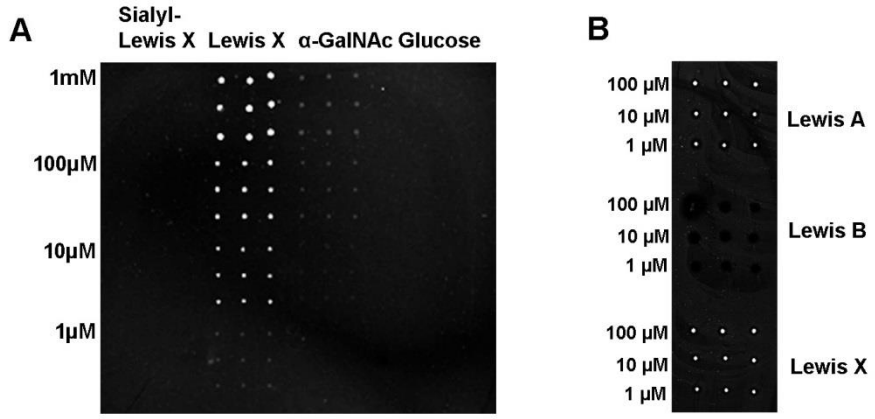

Figure 4.5 Functionality test of MGL1-hFc

A, Glycan array using MGL1-hFc show binding to Lewis X and α-GalNAc, but not to sialyl-Lewis X or glucose.

B, The MGL1-hFc also binds Lewis A but not Lewis B, α-GalNAc, α-N-acetylgalactosamine.

Lewis X (Gal(β1-4)[Fuc(α1-3)]GlcNAc), Lewis A (Gal(β1-3)[Fuc(α1-4)]GlcNAc) and α-GalNAc (Singh et al., 2009; Tsuiji et al., 2002) were examined. Synthetic Lewis X, Lewis A, Lewis B, α-GalNAc, sialyl Lewis X or glucose were immobilized on epoxy slides. Incubation with MGL1-hFc protein and detection with a fluorescently labeled antibody against the hFc part revealed binding to Lewis X at all concentrations printed (1μM-1mM). In addition, MGL1-hFc bound to α-GalNAc (printed at 0.1-1mM), but not to the negative controls sialyl Lewis X or glucose at any concentration tested (Figure 4.5A). Binding was also detected to all printed concentrations of Lewis A, but not to the specificity control Lewis B (Figure 4.5B). Thus, the CRD of MGL1-hFc is functional and binds the same carbohydrate ligands as native MGL1. No binding of Clec9a-hFc to Lewis A, Lewis B or Lewis X was detected (data not shown). The functionality of SIGNR3-hFc was analyzed by ELISA and a significant binding of SIGNR3-hFc to the known ligand zymosan (Takahara et al., 2004) was detected, as described in a later section (Figure 4.15).

Thus, the identity and functionality of CLR-hFc fusion proteins were confirmed. The fusion proteins presented here are members of a library of CLR-hFc fusion proteins belonging to the subgroup II and V of the CTLD superfamily (table 1.2) expressing one CRD in the extracellular region. Ligand binding to MGL1-hFc and SIGNR3-hFc was proven, demonstrating the functionality of CLR-hFc fusion proteins. Thus, the hFc tag does not appear to influence the activity of the CRD of the CLRs, which can be helpful when ligands are yet not well defined.

4.3 Screening of the immune modulatory properties of carbohydrate CLR ligands

4.3.1 Glycan array

The carbohydrate recognition is specific for each myeloid CLR (Sancho and Reis e Sousa, 2012), and for some CLRs, carbohydrate ligands have yet to be determined. Lewis X, Lewis A and α-GalNAc have been identified as ligands for MGL1 (Table 1.1) (Singh et al., 2009; Tsuiji et al., 2002). To date, no carbohydrate ligands are known for Clec9a. To identify potential novel ligands for Clec9a and MGL1, a glycan array was used to screen for binding to synthetic carbohydrates. After printing the carbohydrates and quenching of any unreacted groups, the CLR-hFc proteins were incubated, followed by detection with a fluorescently labeled antibody against the hFc part.

Interactions of the CLR-hFc fusion proteins with the different carbohydrate structures are summarized in Figure 4.6 and Table 4.1. As expected, MGL1-hFc bound to nearly all structures bearing a terminal galactose, but not to terminal glucose or *N*-acetylglucosamine (GlcNAc) residues (Figure 4.6A). Generally, stronger binding of MGL1-hFc was detected for β-linked compared to α-linked galactose (Figure 4.6 and Table 4.1). Clec9a-hFc bound to PIM_1 and PIM_4 (structure No. 45 and 48) as well as to a tetrasaccharide with terminal mannose (structure No 27). Generally, no binding was detected to the three blood antigens tested (Figure 4.6B). MGL1-hFc and Clec9a-hFc, along with four other CLR-hFc proteins from the CLR-hFc library, bound to the majority of heparin structures (Figure 4.6B and data not shown). In addition, hFc alone bound strongly to natural heparin (structure No. 16, Figure 4.6B). Similarly, both MGL1-hFc and Clec9a-hFc bound to sulfated galactose (structure No. 28 and 29). Since sulfated structures and the heparins are negatively charged (Capila and Linhardt, 2002), the interactions with of these sugars with the CLR-hFc fusion proteins are presumably caused by charge-charge interactions, thus were considered unspecific.

Interestingly, MGL1-hFc and Clec9a-hFc bound to the tumor antigen carbohydrate Gb5 (structure No. 50, Figure 4.6). Binding analysis of this carbohydrate to five additional CLR-hFc fusion proteins of the existing library revealed that Clec12b-hFc also bound to Gb5, whereas Dectin-1-hFc, MCL-hFc, DCIR-hFc and MICL-hFc did not (Figure 4.7A, CLR-hFc fusion

proteins produced by Maha Maglinao). None of the CLR-hFc fusion proteins tested bound to the related structure Globo-H. Gb5 and Globo-H have the same pentasaccharide core structure, but Globo-H possesses an additional terminal fucose (Figure 4.7B). This terminal fucose hinders the binding of fusion proteins, thus the recognition of the terminal galactose on the Gb5 seems to be crucial for binding to MGL1-hFc, Clec9a-hFc and Clec12b-hFc. In addition, MGL1-hFc and Clec9a-hFc bound to 1,3-lactosamine (structure No 18, figure 4.7A), whereas no such binding was detected for Dectin-1-hFc, MCL-hFc, DCIR-hFc, MICL-hFc or Clec12b-hFc.

Three carbohydrate CLR-ligand hits from the glycan array were selected to establish the next steps of the platform. These were the above mentioned Gb5 (structure No. 50, Figure 4.7), 1,3-lactosamine (structure No. 18, Figure 4.7) as well as Lewis X (Figure 4.5). Notably, MGL1-hFc was the exclusive binder for Lewis X of the CLR-hFc fusion proteins tested here. Similarly, binding signals to Gb5 as well as to 1,3-lactosamine were strongest for MGL1-hFc, although Clec9a-hFc and Clec12b-hFc also bound.

Table 4.1 Binding of MGL1-hFc and Clec9a-hFc to carbohydrate structures by glycan array.

No.	Structure	MGL1-hFc	Clec9-hFc
1	Neu5Ac(α1-3)Gal(β1-3)GlcNAc(β1-3)Gal(β1-4)Glcβ1-$O(CH_2)_6NH_2$	-	-
2	Neu5Ac(α1-3)Gal(β1-4)GlcNAc(β1-3)Gal(β1-4)Glcβ1-$O(CH_2)_6NH_2$	-	-
3	Neu5Ac(α1-6)Gal(β1-3)GlcNAc(β1-3)Gal(β1-4)Glcβ1-$O(CH_2)_6NH_2$	-	-
4	Neu5Ac(α1-6)Gal(β1-4)GlcNAc(β1-3)Gal(β1-4) Glcβ1-$O(CH_2)_6NH_2$	-	-
5	Neu5Ac(α1-3)Gal(β1-4)GlcNAc6Sβ1-O $(CH_2)_6NH_2$	-	-
6	Neu5Ac(α1-3)Gal(β1-4)Glcβ1-$O(CH_2)_6NH_2$	-	-
7	Neu5Ac(α1-6)Gal(β1-4)Glcβ1-$O(CH_2)_6NH_2$	-	-
9	GlcNS(6S)(α1-4)IdoA(2S)(α1-4)GlcNS(6S)(α1-4) IdoA(2S)(α1-4)GlcNS(6S)(α1-4) IdoA(2S)α1-O $(CH_2)_5SO_2(CH_2)_2NH_2$	+	++
10	GlcNAc(6S)(α1-4)IdoA(2S)(α1-4)GlcNAc(6S) (α1-4)IdoA(2S)(α1-4)GlcNAc(6S)(α1-4)IdoA (2S)α1-$O(CH_2)_5NH_2$	-	++
11	GlcNS(α1-4)IdoA(α1-4)GlcNS(α1-4)IdoA(α1-4) GlcNS(α1-4)IdoAα1- $O(CH_2)_5NH_2$	-	-
12	GlcNAc(α1-4)IdoA(α1-4)GlcNAc(α1-4)IdoA (α1-4) GlcNAc(α1-4)IdoAα1-$O(CH_2)_5NH_2$	-	-
13	IdoA(2S)(α1-4)GlcNS(α1-4)IdoA(2S)(α1-4) GlcNS(α1-4)IdoA(2S)(α1-4)GlcNSα1-O $(CH_2)_5NH_2$	+	+
14	IdoA(2S)(α1-4)GlcNAc(α1-4)IdoA(2S)(α1-4) GlcNAc(α1-4)IdoA(2S)(α1-4)GlcNAcα1-O $(CH_2)_5NH_2$	+	++
15	IdoA(2S)(4S)(α1-$O(CH_2)_5SO_2(CH_2)_2NH_2$	++	++
16	Natural Heparin 5 kDa	+	+
17	Gal(β1-4)Glcβ1-$O(CH_2)_5SH$	++	-
18	Gal(β1-3)GlcNAcβ1-$O(CH_2)_5SH$	++	-
19	Gal(β1-4)GlcNAcβ1-$O(CH_2)_5SH$	+++	-
20	GalNAc(β1-4)GlcNAcβ1-$O(CH_2)_5SH$	+	-
21	Gal(β1-3)GalNAcβ1-$O(CH_2)_5SH$	+++	+
22	Gal(β1-2)Galβ1-$O(CH_2)_5SH$	+++	-
23	Gal(β1-3)Gal(β1-4)Glcβ1-$O(CH_2)_5SH$	+++	-
24	Fuc(α1-2)Gal(β1-4)GlcNAcβ1-$O(CH_2)_5SH$	-	-
25	GalNAc(α1-3)Fuc(α1-2)Gal(β1-4)GlcNAcβ1-O $(CH_2)_5SH$	-	-
26	Gal(α1-3)Fuc(α1-2)Gal(β1-4)GlcNAcβ1-O $(CH_2)_5SH$	-	-
27	Man(α1-3)Fuc(α1-2)Gal(β1-4)GlcNAc(β1-$O(CH_2)_5SH$	-	+
28	Gal(3S)β1-$O(CH_2)_5NHC(NH)(CH_2)_3SH$	-	++
29	Gal(6S)β1-$O(CH_2)_5NHC(NH)(CH_2)_3SH$	-	++
31	GlcNAcβ1-$O(CH_2)_5SH$	-	++

32	Gal(β1-4)GlcNAc(β1-2)Glcα1-O$(CH_2)_5$SH	+	+
33	Man(α1-2)Manα1-O$(CH_2)_5$SH	-	-
34	Man(α1-2)Man(α1-6)[Man(α1-2)Man(α1-3)] Man(α1-6)[Man(α1-2)Man(α1-2)Man(α1-3)] Manα1-$(OCH_2CH_2)_3$SH	-	-
36	Man(α1-2)Man(α1-2)Manα1-O$(CH_2)_6$SH	-	-
37	Man(α1-6)Man(α1-6)[Man(α1-2)]Man(α1-6) Man(α1-6)Manα1-O$(CH_2)_6$SH	-	-
38	Man(α1-2)Man(α1-6)Man(α1-6)Manα1-O $(CH_2)_6$SH	-	-
39	Ara(α1-6)Ara(α1-3)[Ara(α1-6)]Ara(α1-6)Ara(α1-6)Ara(α1-2)[Man(α1-6)]Man(α1-6)[Man(α1-2)] Man(α1-6) Man(α1-6) Manα1-O$(CH_2)_6$SH	-	-
40	Gal(α1-3)[Gal(β1-4)]GlcNAc(α1-4)ManNAc(β1-4)[Gal(α1-4)]GlcNAcβ1-O$(CH_2)_5$SH	++	++
41	Glc(β1-4)Glcβ1-O$(CH_2)_5$SH	-	+
42	GlcNAc(α1-2)Glcα1-O$(CH_2)_5$SH	-	++
43	Fuc(α1-O$(CH_2)_5$SH	++	+++
45	Man(α1-2)*myo*-Ins(1-$OPO_3H(CH_2)_6$SH PIM_1	-	+
46	Man(α1-2)[Man(α1-6)]*myo*-Ins(1-$OPO_3H(CH_2)_6$SH PIM_2	-	-
47	Man(α1-6)Man(α1-6)[Man(α1-2)]*myo*-Ins1-$OPO_3H(CH_2)_6$SH PIM_3	-	-
48	Man(α1-6)Man(α1-6)Man(α1-6)[Man(α1-2)]*myo*-Ins1-$OPO_3H(CH_2)_6$SH PIM_4	-	+
49	Fuc(α1-2)Gal(β1-3)GalNAc(β1-3)Gal(α1-4)Gal(β1-4)Glcβ1-O$(CH_2)_5$SH Globo-H	-	-
50	Gal(β1-3)GalNAc(β1-3)Gal(α1-4)Gal (β1-4)Glcβ1-O$(CH_2)_5$SH Gb-5 or SSEA-3	+++	+
51	Glcβ1-O$(CH_2)_2NH_2$	-	+
52	Galβ1-O$(CH_2)_2NH_2$	++	+

Semiquantitative score for binding signals: very strong (+++), strong(++), moderate (+), no binding (-).

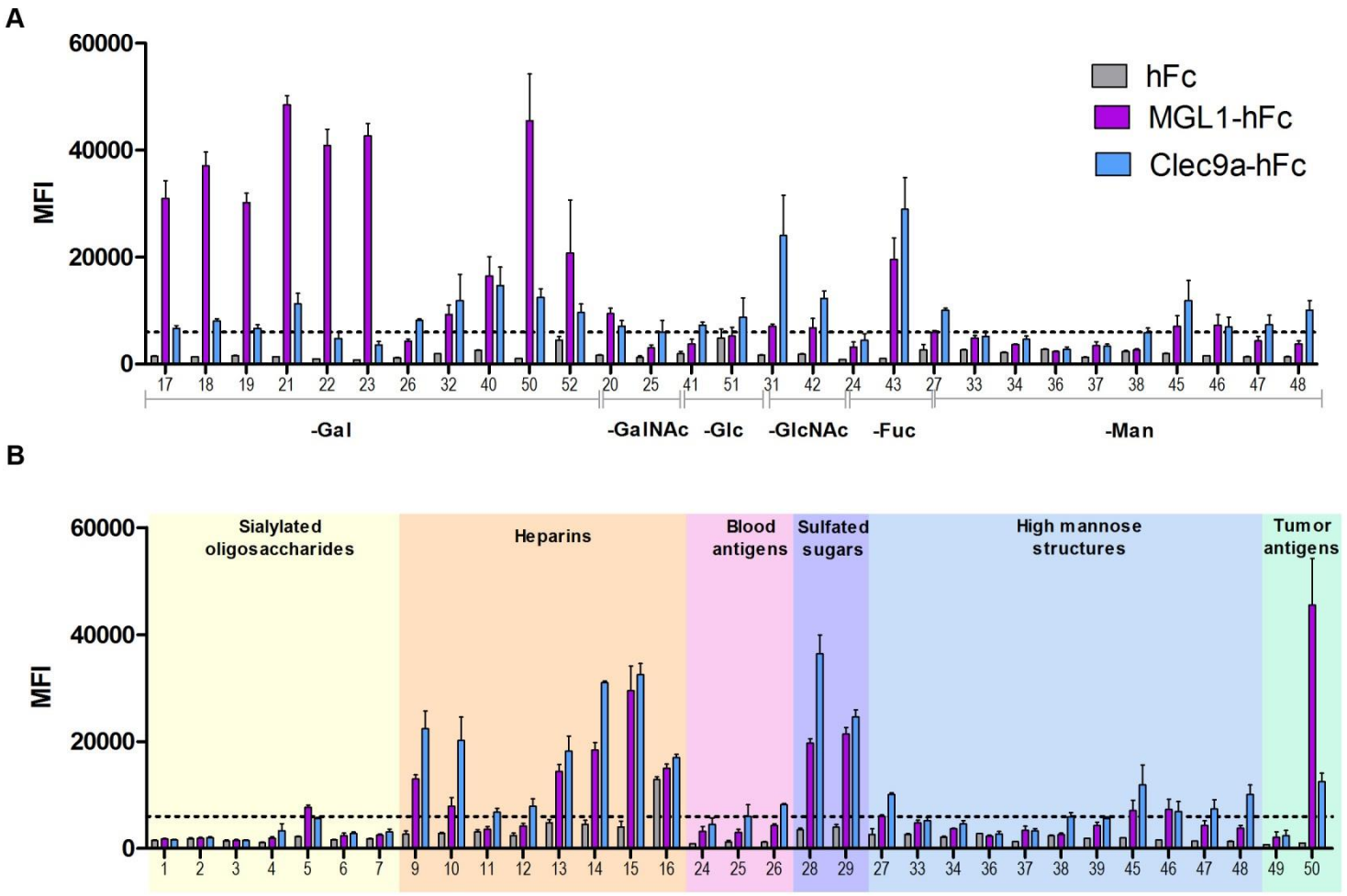

Figure 4.6 Screening of synthetic CLR carbohydrate ligands

The two fusion proteins Clec9a-hFc and MGL1-hFc were applied to glycan array to screen for synthetic carbohydrate ligands. hFc was used as a specificity control. *A*, Binding of the CLR-hFc fusion proteins to carbohydrates with different terminal sugars. *B*, Binding to different carbohydrate patterns. Error bars represent + SEM. Gal, Galactose; GalNAc, N-acetylgalactosamine; Glc, glucose; GlcNAc, *N*-acetylglucosamine; Fuc, fucose; Man, mannose.

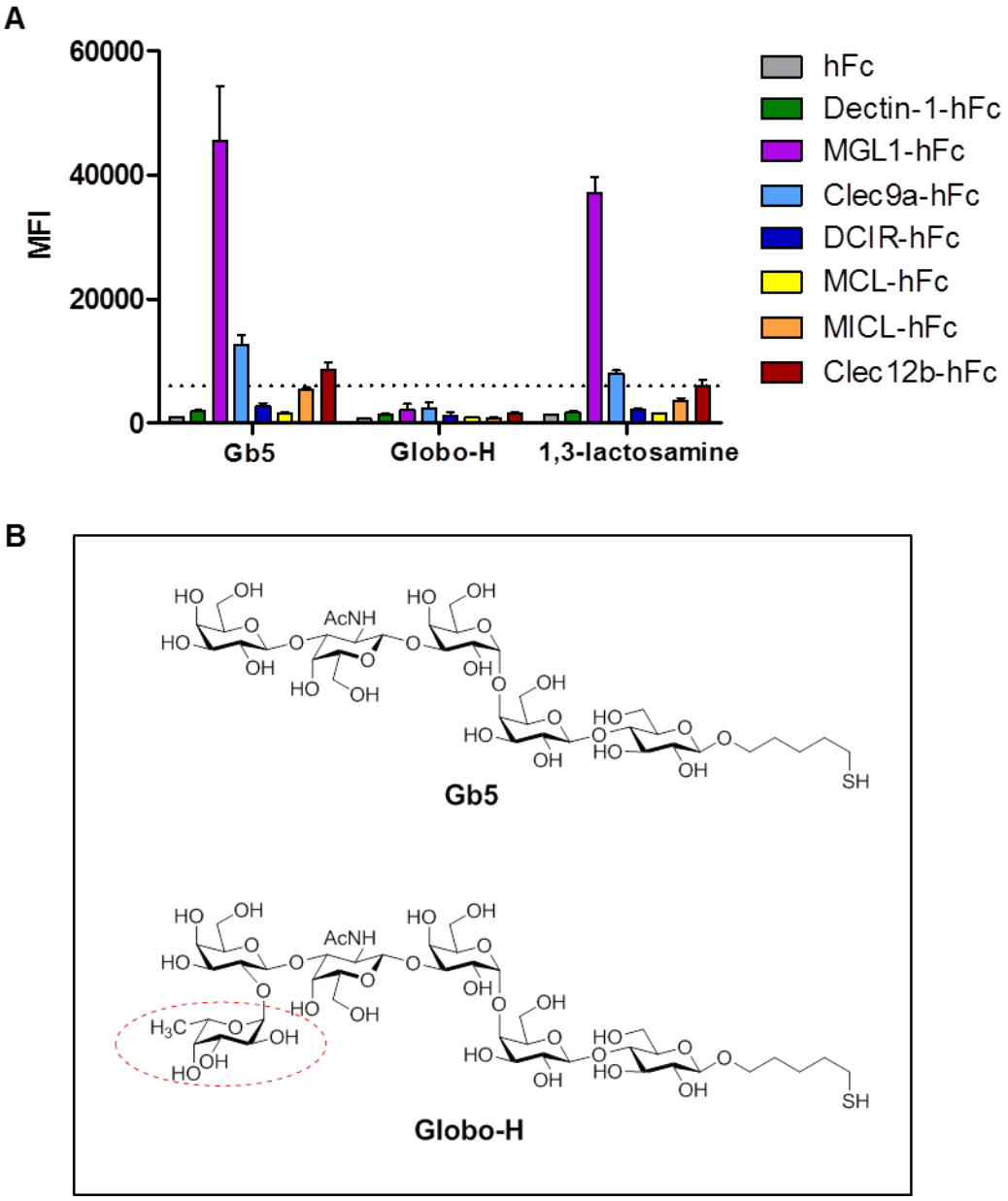

Figure 4.7 Binding of CLR-hFc fusion proteins to carbohydrates

A, Binding pattern of the CLR-hFc fusion proteins to the tumor antigens Gb5 and Globo-H as well as to the disaccharide 1,3-lactosamine. Dectin-1-hFc, DCIR-hFc, MCL-hFc, MICL-hFc and Clec12b-hFc were produced by the same method as described here for Clec9a-hF and MGL1-hFc. *B*, The carbohydrate structure of Gb5 and Globo-H differ in one terminal fucose of Globo-H (marked).

4.3.2 *In vitro* and *in vivo* assays

CLR-ligand interactions can shape immune responses. This can be achieved either by CLR-mediated endocytosis and enhanced antigen presentation (Burgdorf et al., 2007; van Kooyk, 2008) or by activation of signaling pathways leading to activation or suppression of APC functions (Brown, 2006; Richard et al., 2006). In this thesis, one objective was to perform analysis of the *in vitro* and *in vivo* immunomodulatory properties of the identified CLR ligands. The frequency of T cells that are specific for an antigen is normally very low. Using transgenic T cells with a single TCR specific for an antigen allows to study specific T cell effector functions. In this thesis, cells from OT-II mice expressing a transgenic TCR specific for the $OVA_{323-339}$ peptide presented by MHC class-II $I\text{-}A^b$ molecule were used. To examine whether targeting CLRs on dendritic cells influences the ability to activate T cells, OVA was conjugated to three of the CLR ligands identified by glycan array. The OVA-carbohydrate conjugates were then used for pulsing dendritic cells *in vitro* before adding OT-II T cells. To analyze the *in vivo* immunomodulatory properties of carbohydrate CLR ligands, OT-II cells were adoptively transferred into C57BL/6 wild-type and mice were then immunized with the OVA-carbohydrate conjugates. By performing these studies, CLR ligands with immunomodulatory potential can be identified. The analysis of immunomodulatory properties of CLR ligands was a collaborative approach performed jointly with Maha Maglinao. The results regarding *in vitro* and *in vivo* are also described in (Maglinao, 2013).

4.3.2.1 Characterization of OVA-conjugates

To conjugate the CLR carbohydrate ligands Lewis X, 1,3-lactosamine and Gb5 to OVA, the DSAP linker was used. To avoid the formation of carbohydrate dimers, the sugar was added dropwise to a 10-fold molar excess of linker. After allowing all present carbohydrates to react with the linker, unbound linker was extracted by addition of a large excess of chloroform. Carbohydrate-linker was mixed with OVA in phosphate buffer and incubated overnight. OVA-conjugates were then purified and rebuffered into PBS by centrifugation in an amicon concentrator.

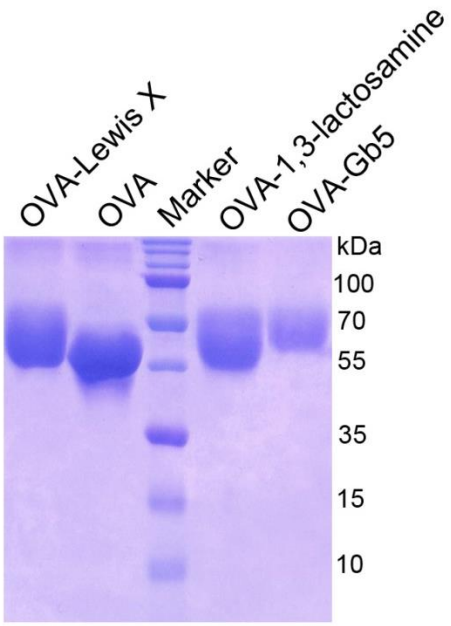

Figure 4.8 OVA-carbohydrate conjugates

OVA conjugated to Lewis X, 1,3-lactosamine or Gb5 was analyzed by SDS-PAGE and subsequent Coomassie staining.

To characterize the OVA-carbohydrate conjugates, a SDS-PAGE was performed followed by Coomassie gel staining. The results obtained revealed an increased size of the OVA-carbohydrate conjugates compared with OVA alone (Figure 4.8). MALDI-TOF-MS analysis showed an average of 4.6-4.8 carbohydrate molecules per OVA molecule (Figure 4.9). To test if the conjugated carbohydrates were available for binding, their interaction with MGL1-hFc was tested. Incubation of MGL1-hFc to plate-coated OVA-Lewis X and OVA-1,3-lactosamine demonstrated that the OVA-carbohydrate conjugates are indeed recognized by MGL1-hFc but not by the control hFc (Figure 4.10). These OVA-carbohydrate conjugates were used for *in vitro* and *in vivo* assays.

4.3.2.2 *In vitro* stimulation and DC/T cell co-culture

To examine whether CLR targeting by antigens influences uptake and the ability to activate T cells, a co-culture experiment with $CD11c^+$ splenic cells from C57/BL6 mice and T cells from OT-II transgenic mice was performed. MACS-purified $CD11c^+$ cells were pulsed with OVA-carbohydrate conjugates. Subsequently, OT-II T cells were added and T cell activation was determined by means of cytokine production and the expression of activation markers.

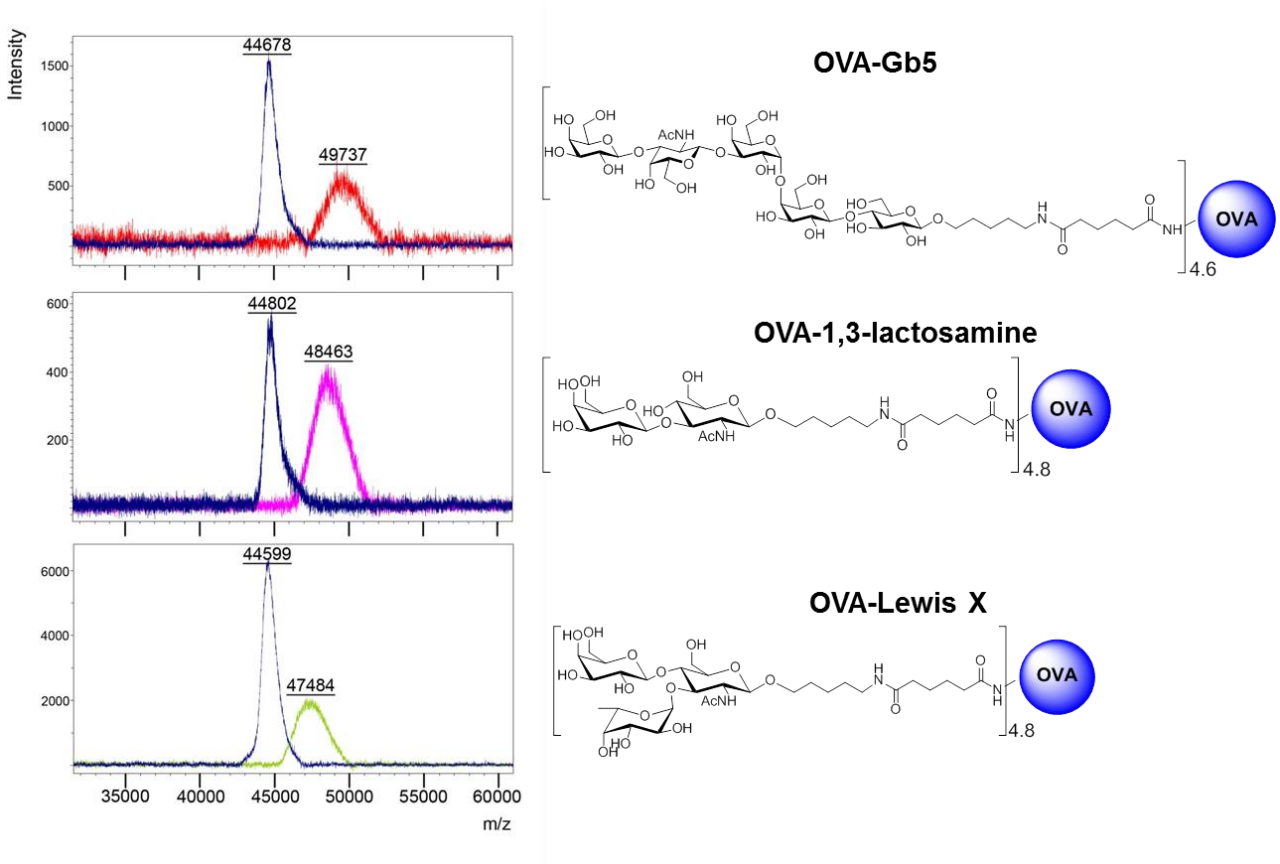

Figure 4.9 Characterization of the OVA-carbohydrate conjugates

MALDI analysis of OVA (blue) conjugated to Gb5 (red, upper panel), 1,3-lactosamine (pink, middle panel) or Lewis X (green, lower panel), revealed that an average of 4.6-4.8 sugars per OVA molecules were conjugated. Schemes of OVA-carbohydrate conjugates are shown next to the corresponding MALDI-analysis.

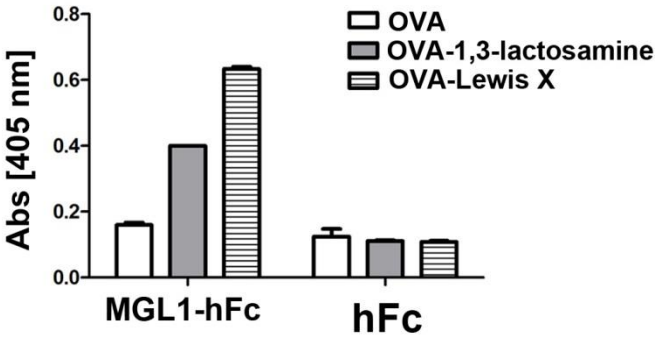

Figure 4.10 Binding of MGL-hFc to OVA-carbohydrate conjugates

Specific binding of MGL1-hFc, but not hFc, to OVA-Lewis X and OVA-1,3-lactosamine was demonstrated by ELISA. Binding was performed in 96-well plates in duplicates.

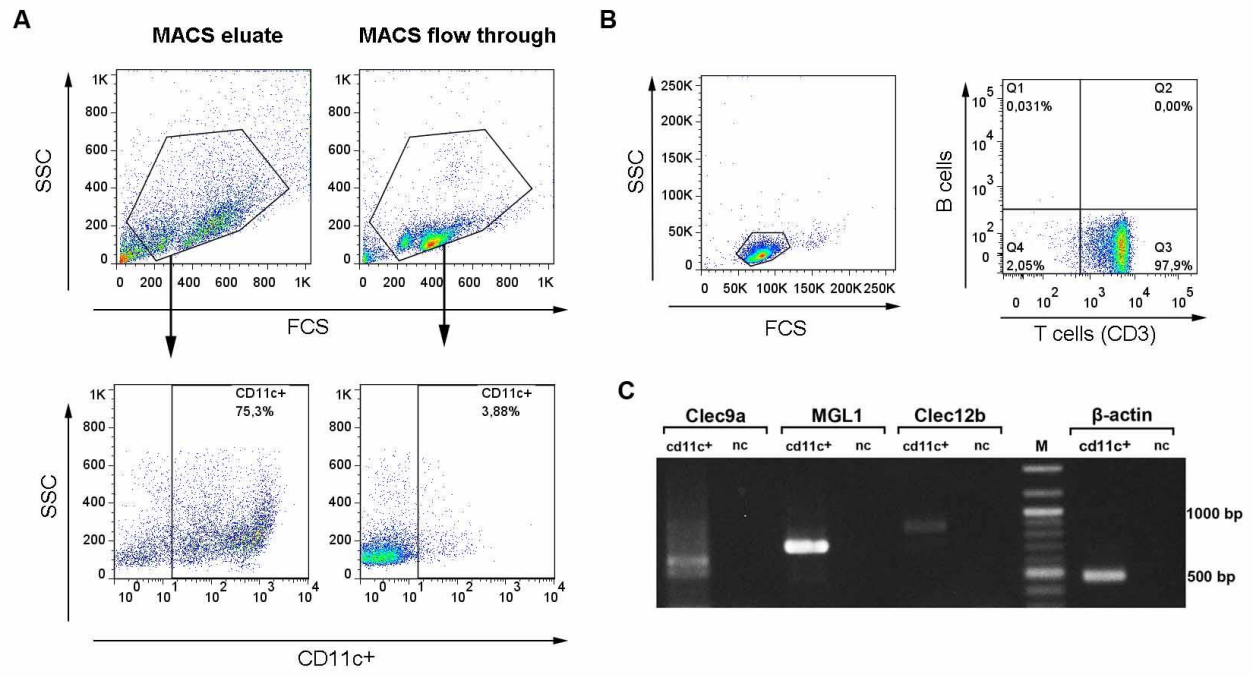

Figure 4.11 MACS purified CD11c$^+$ cells and OT-II T cells.

A, CD11c$^+$ cells purified by MACS were stained with APC-labeled antibody against CD11c. Flow cytometry analysis of MACS purified CD11c$^+$ cells show a CD11c$^+$ purity of 75%. *B*, T cells were purified from OT-II splenic cells by MACS separation. Staining with fluorescently labeled antibodies against the T cell receptor associated molecule CD3 and analysis by flow cytometry demonstrate a T cell purity of 97.9 %. *C*, The expression of CLRs by MACS purified CD11c$^+$ cells was analyzed by RT-PCR, demonstrating the presence of mRNA coding for Clec9a, MGL1 and Clec12b. Primers for β-actin were used as a positive control. SSC, side scatter; FSC, forward scatter; M, marker; nc, negative control without any cDNA.

The purity of MACS-purified CD11c$^+$ cells was about 75% (Figure 4.11A). RT-PCR analysis of RNA extracted from these CD11c$^+$ cells demonstrated the presence of mRNA coding for MGL1, Clec9a and Clec12b (Figure 4.11C). MACS purified CD11c$^+$ cells were pulsed with 30 µg/ml OVA or OVA carbohydrate conjugates before addition of MACS purified OT-II T cells (purity 98%, Figure 4.11B). Analysis of activation markers on CD11c$^+$ cells and T cells as well as cytokine concentrations in cell supernatants was performed after 72 h. Cells stimulated with OVA up-regulated the T cell activation marker CD69, but there was no significant difference between cells stimulated with conjugated or unconjugated OVA (data not shown). Interestingly, a significantly higher level of the cytokine IL-2 was produced by cells stimulated with OVA-carbohydrate conjugates than by cells stimulated with OVA alone (Figure 4.12). IL-2 is a

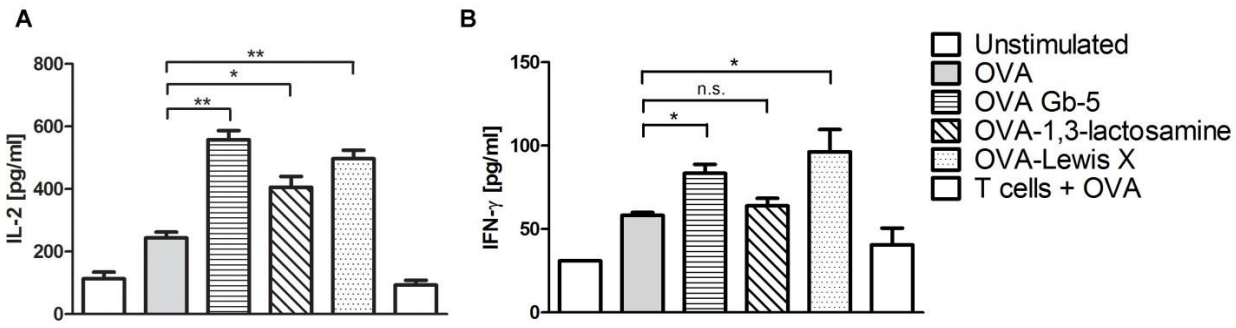

Figure 4.12

Splenic CD11c$^+$ cells were pulsed with the OVA-carbohydrate conjugates OVA-Gb5, OVA-1,3-lactosamine or OVA-Lewis X followed by co-culture with OT-II T cells for 72 h. The concentration of the T cell cytokines IL-2 *(A)* and IFN-γ *(B)* was measured in the supernatant by ELISA or CBA, respectively. Stimulation with all three OVA conjugates induced a significant increase of IL-2 levels compared with OVA alone. In addition, stimulation with OVA-Gb5 and OVA-Lewis X resulted in significant higher production of IFN-γ. Statistical analysis was performed by a two tailed, unpaired, student's t test. *$p<0.05$,** $p<0.01$, n.s, not significant.

cytokine produced mainly by T cells upon activation, leading to autocrine stimulation and T cell proliferation. IFN-γ production was significantly increased when cells were stimulated with OVA-Gb5 or OVA-Lewis X. IFN-γ is produced mainly by Th1 cells. There were no detectable levels of the Th2 cytokine IL-4 in any of the supernatants (data not shown).

These studies demonstrate that the OVA-carbohydrate conjugates are able to influence the T cell response *in vitro*. The significant increase of IL-2 compared with OVA alone suggests that OVA-carbohydrate conjugates augmented T cell proliferation. Moreover, pulsing dendritic cells with the conjugates led to increased IFN-γ production, which may suggest that CD4$^+$ T cell differentiation is polarized into Th1.

4.3.2.3 *In vivo* immunization

To further analyze the immunomodulatory effects of the OVA-carbohydrate conjugates observed in the *in vitro* assay, immunization of mice with the conjugates was performed. To generate a specific immune response against OVA, adoptive transfer of OT-II cells into wild-type C57BL/6 mice was performed before immunization with OVA-carbohydrate conjugates.

Mice were prime-boost immunized and sacrificed on day 27. Spleen cells were re-stimulated with $OVA_{323-339}$ for 18 h before cytokine producing cells were analyzed by ELISpot

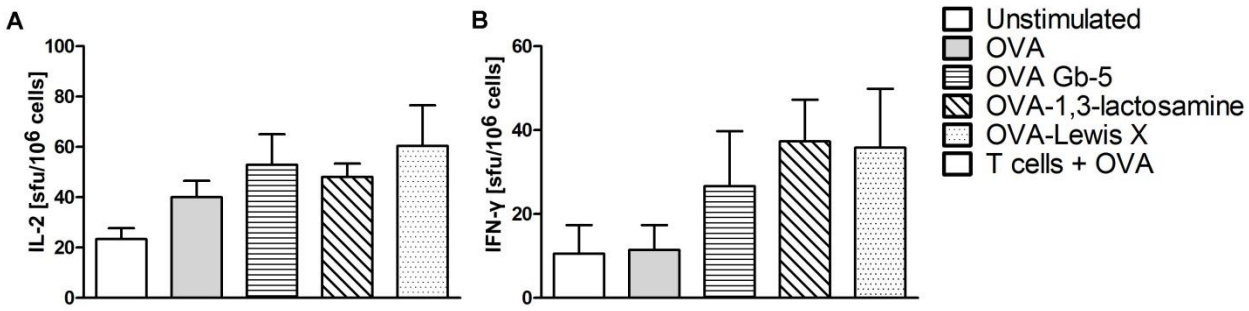

Figure 4.13 Cytokine producing splenic cells

Analysis of splenic cells from mice immunized with OVA or OVA-carbohydrate conjugates. Cells were stimulated with $OVA_{323-339}$ for 18 h before ELISpot analysis of IL-2 producing cells (*A*) and IFN-γ producing cells (*B*). Statistical analysis with two-tailed, unpaired, student's t test revealed no significant difference between OVA and OVA conjugates.

assay. Similar to the cytokine production in the supernatant in the *in vitro* assay, by tendency an increase of T cells producing IL-2 and IFN-γ cells were detected in spleen cells from mice immunized with the OVA-carbohydrate conjugates (Figure 4.13). No IL-4 producing cells were detected (data not shown). Analysis of the antibody titers in sera of immunized mice showed that significantly less anti-OVA-antibodies were produced upon immunization with OVA conjugated to Gb5 or 1,3-lactosamine. This difference was observed for the dilutions 1:50, 1:100 and 1:200 (Figure 4.14A and B). In addition to total anti-OVA IgGs, the presence of the IgG isotypes IgG_1 and IgG_{2a} was examined. Similar results as for the total IgG were obtained for anti-OVA-IgG_1 antibody (Figure 4.14C), whereas no detectable levels of IgG_{2a} were present (data not shown). These data suggest that immunization of the tested OVA-carbohydrate conjugates induces Th1 responses, reflected by the expansion of IFN-γ producing cells. Moreover, the decrease of OVA-specific antibodies suggests a reduced Th2 response upon immunization with the OVA-carbohydrate conjugates. Thus, modification of an antigen by CLR carbohydrate ligands can modulate the Th1/Th2 balance.

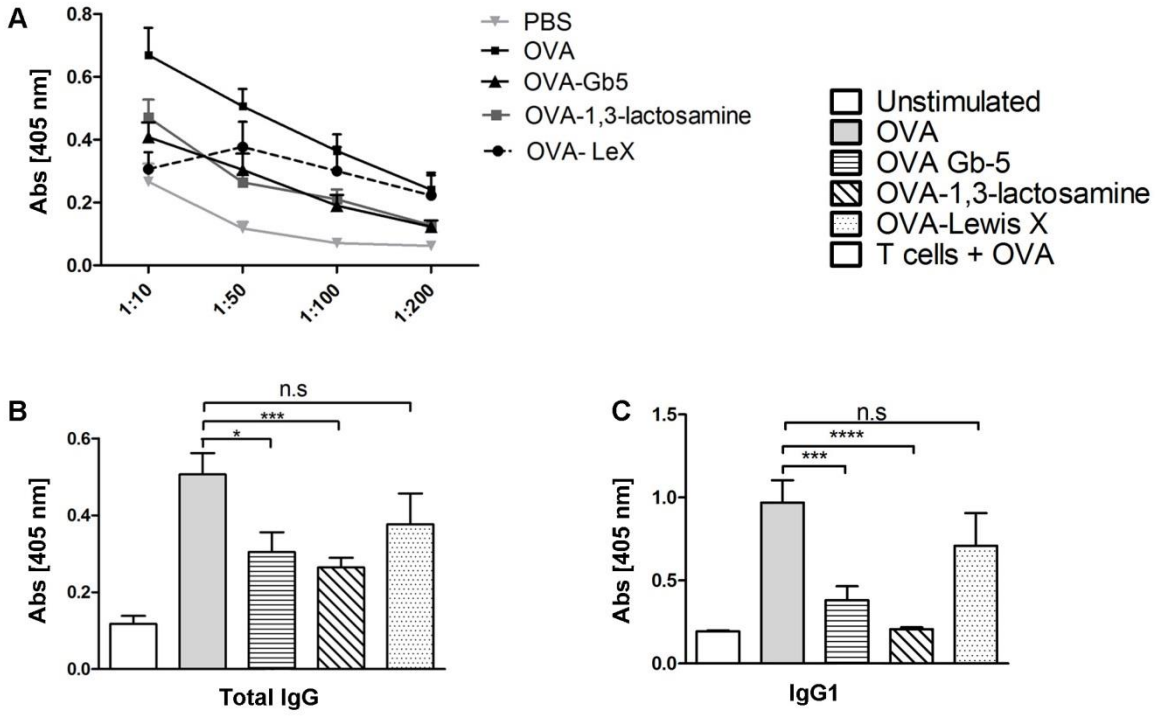

Figure 4.14 Analysis of OVA antibodies present in serum

A, Titration of OVA serum antibodies detected with antibodies against total IgG (H+L). *B,* Dilution 1:50 from A, with statistical analysis performed by a two tailed, unpaired, student's t test. *$p<0.05$,** $p<0.01$, n.s, not significant.

C, The composition of IgG1 antibodies. IgG2 antibodies were below detection level.

Taken together, in this thesis I present the establishment of a platform suitable for screening of immunomodulatory properties of CLR carbohydrate ligands. The first step was the identification of CLR carbohydrate ligands using CLR-hFc fusion proteins. This was followed by the assessment of the *in vitro* and *in vivo* immunomodulatory properties of the carbohydrates. In this thesis, novel CLR ligands were identified and immunomodulatory properties of candidate carbohydrate ligands were tested. By using this platform, further CLR ligands with immunomodulatory properties can be identified and the mechanism by which the CLR ligands act as immune modulators can be analyzed.

4.4 Screening of CLR binding to gut microbiota

4.4.1 CLR binding to gut microbiota

The generated CLR-hFc fusion proteins proved to be useful tools in the identification of novel CLR carbohydrates ligands by glycan array. To test if the CLR-hFc fusion proteins were also useful to screen for microbial ligands, the interaction of SIGNR3 with the fungal cell wall component zymosan (Takahara et al., 2004) was examined. ELISA-based interaction studies demonstrated that, indeed, an interaction between zymosan and SIGNR3 could be detected using SIGNR3-hFc (Figure 4.15A).

To analyze the interaction of CLRs with intestinal commensals, heat inactivated gut microbiota were coated on microtiter wells. After blocking with BSA, plates were incubated with the fusion proteins MGL1-hFc, Clec9a-hFc and SIGNR3-hFc. Of the CLRs analyzed here, MGL1 is the only CLR reported to be involved in the recognition of microbiota and this interaction regulates the intestinal inflammation in DSS-induced colitis (Saba et al., 2009). Accordingly, significant binding of MGL1-hFc to the gut microbiota was detected (Figure 4.15A). Interestingly, the binding of both Clec9a-hFc and SIGNR3-hFc to the gut microbiota

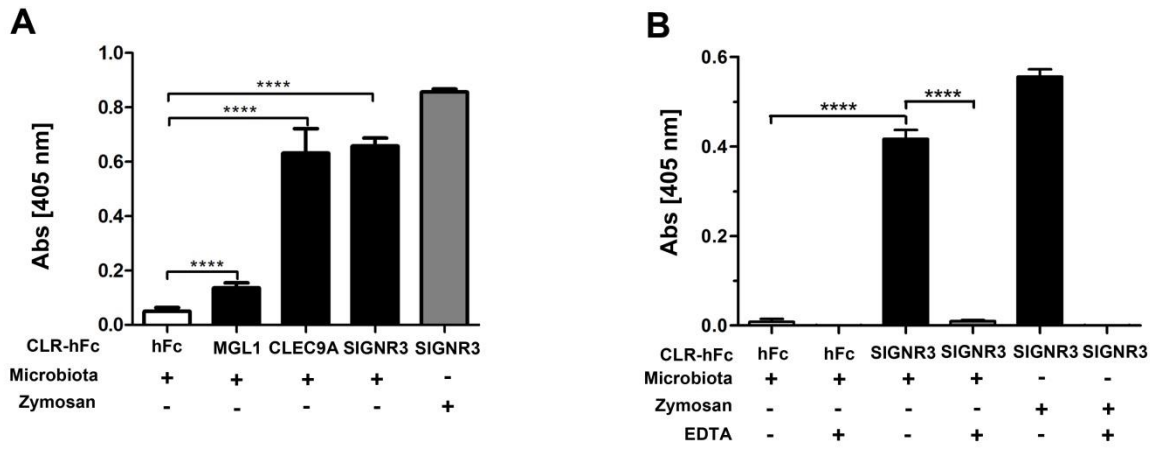

Figure 4.15 Screening of CLR binding to gut microbiota

A, Binding of the CLR-hFc fusion proteins MGL1-hFc, Clec9a-hFc and SIGNR3-hFc to heat inactivated gut microbiota was analyzed by ELISA. *B,* Binding of SIGNR3-hFc to microbiota or zymosan washed with lectin buffer or 25 mM EDTA buffer indicates that the binding is Ca^{2+}-dependent. Data are presented as mean + SEM. The p-values were determined using unpaired student's t-test. Where the mean was zero, no statistical test was performed. *p<0.05 ****p<0.0001

exceeded that of MGL1-Fc (Figure 4.15A). Clec9a has been reported to bind to dead cells and F-actin (Ahrens et al., 2012; Sancho et al., 2009; Zhang et al., 2012) and to date, no interaction with microbes or carbohydrate structures has been reported. Thus, the binding of Clec9a-hFc to microbes detected in this thesis might represent Clec9a recognition of dead microbes. SIGNR3 has been reported to bind to pathogenic mycobacterial lipoglycans and is involved in the innate immune response during *M. tuberculosis* infection (Tanne et al., 2009). Recently, SIGNR3 was reported to play an immunoregulative role in the macrophage response to *Leishmania infantum* (Lefevre et al., 2013). However, to date, no defined SIGNR3 ligands in the murine gut microflora were reported. Thus, the revealed interaction of SIGNR3 with gut microbes expands the known ligand repertoire of SIGNR3. Therefore, one objective in this thesis was to further analyze the recognition of gut microbes by SIGNR3, and to evaluate the impact of this interaction in intestinal immunity.

CLR-ligand interaction is, for many CLRs, Ca^{2+}-dependent (Sancho and Reis e Sousa, 2012). To analyze whether the interaction of SIGNR3 with the gut microbiota detected by ELISA

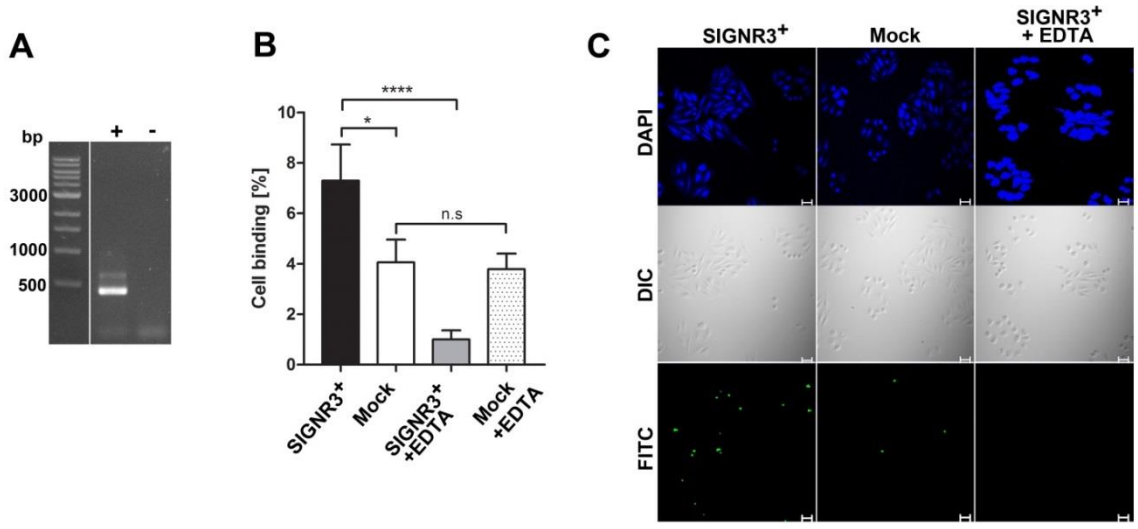

Figure 4.16 Binding of FITC-labeled microbes to SIGNR3-transfected cells

A, RT-PCR analysis of mRNA of transfected cells demonstrates the presence of SIGNR3 in transiently transfected (+) cells, but not in untransfected cells (–). *B,* Binding of FITC-labeled microbes to SIGNR3- or mock transfected CHO cells, demonstrates a significant binding between FITC-labeled microbes to SIGNR3-transfected cells. This binding was significantly decreased when cells were washed in 25 mM EDTA buffer. Data are presented as mean + SEM. The *p*-values were determined using unpaired student's t-test. **p*<0.05 *****p*<0.0001. *C,* Representative images of transfected CHO cells (blue) incubated with FITC-labeled microbiota (green) and washed with 25 mM EDTA. Transfection rate was 10-15 %. Scale bar = 20 µm. DIC; differential interference contrast.

was Ca^{2+}-dependent, washing with EDTA-buffer was performed. This treatment completely abolished the interaction of SIGNR3-hFc with zymosan as well as with gut microbiota, indicating Ca^{2+}-dependency (Figure 4.15B). To further analyze the interaction of SIGNR3 and the gut microbes, the binding of FITC-labeled gut antigens to CHO cells transiently transfected with pUNO-SIGNR3 was analyzed. RT-PCR analysis demonstrated that transfected cells expressed SIGNR3 mRNA after 24 h (Figure 4.16A). Since there is no functional commercial available antibody against SIGNR3, an indirect test was performed to evaluate the transfection rate. Accordingly, transfection rate with another pUNO-CLR vector was ~12 % (data not shown), suggesting a similar transfection rate for pUNO-SIGNR3. Similar to the ELISA binding assay, significant binding of FITC-labeled gut microbiota to CHO cells transiently expressing SIGNR3 was detected. Notably, this interaction was almost completely abolished when cells were washed in 25 mM EDTA, but not when washing was performed with buffer containing Ca^{2+} ions (Figure 4.16B and C). Together with the ELISA-based binding studies, these data suggest a Ca^{2+} dependent interaction of SIGNR3 and gut microbiota.

MGL1 has been reported to bind to commensal bacteria (Saba et al., 2009). Another CLR, Dectin-1 recognizes fungi present in the gut (Iliev et al., 2012). To analyze which phylum of commensal microbes SIGNR3 recognizes, co-staining of the gut microbes with SIGNR3-hFc and an antifungal-antibody was performed by Timo Johannssen. Flow cytometry analysis of stained cells revealed that SIGNR3-hFc bound to >60 % of the fungal population of the gut

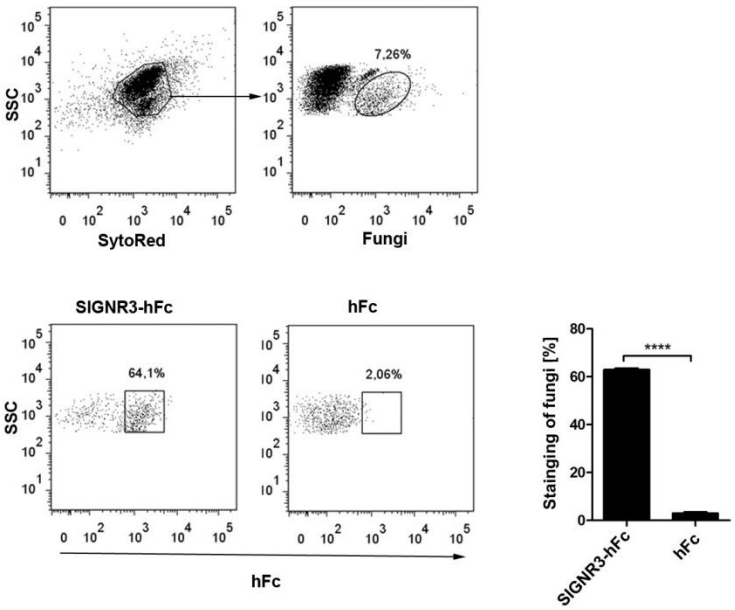

Figure 4.17 SIGNR3 interaction with commensal fungi

SytoRed labeled gut microbes were stained with an anti-fungal antibody (upper panel of dot plots). Co-staining with SIGNR3-hFc revealed that SIGNR3-hFc reconized >60 % of the fungi whereas only marginal binding was detected by staining with hFc (lower panel of dot plots). Graph represents statistical analysis of the percentage of protein binding. Data are presented as mean + SEM. The *p*-values were determined using unpaired student's t-test. ****$p<0.0001$

microbes (Figure 4.17). Thus, in this thesis, a Ca^{2+} dependent binding of SIGNR3 to commensal microbiota, mainly fungi, was revealed.

4.4.2 Murine colitis

The CLR Dectin-1 recognizes fungal populations present in the gut microbiota, and this interaction influences the intestinal immune response during colitis (Iliev et al., 2012). Since SIGNR3 also recognizes commensal fungi, I sought to analyze the impact of SIGNR3 in DSS-induced colitis. In this model, commensal microbes that are normally restricted to the outer mucosal layer penetrate the inner mucosal layer and are recognized by local immune cells. This recognition then leads to the initiation of an inflammatory response against the commensals (Johansson et al., 2011; Johansson et al., 2010).

Expression analysis of SIGNR3 revealed the presence of SIGNR3 mRNA in spleen and MLN cells from wild-type, but not $SIGNR3^{-/-}$, mice (Figure 4.18A). In addition, a weak band representing SIGNR3 mRNA was detected in the colon from wild-type mice (Figure 4.18A). These findings demonstrate the presence of the SIGNR3 mRNA transcript in intestinal tissue. Genetic analysis of the $SIGNR3^{-/-}$ mice was performed during breeding (Figure 4.18B) and mice with homozygous deletion of the SIGNR3 gene were used for colitis experiment.

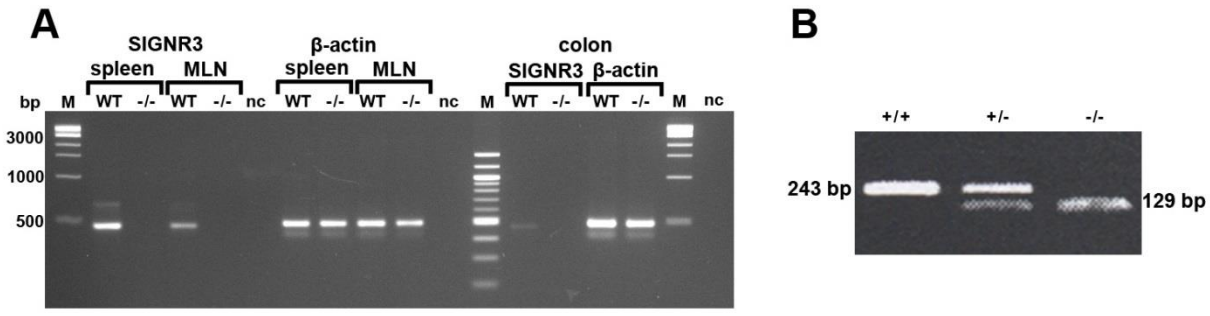

Figure 4.18 Analysis of SIGNR3 mRNA and genotyping of $SIGNR3^{-/-}$ mice

A, RT-PCR analysis of spleen, MLN and colon from wild-type (WT) and $SIGNR3^{-/-}$ mice using primers for β-actin and SIGNR3 demonstrates the presence of SIGNR3 mRNA in spleen, MLN and colon of wild-type (WT) mice. M, marker; nc, negative control. *B*, Representative results from genotyping of wild-type ($^{+/+}$), heterozygous ($^{+/-}$) and SIGNR3 deficient mice ($^{-/-}$).

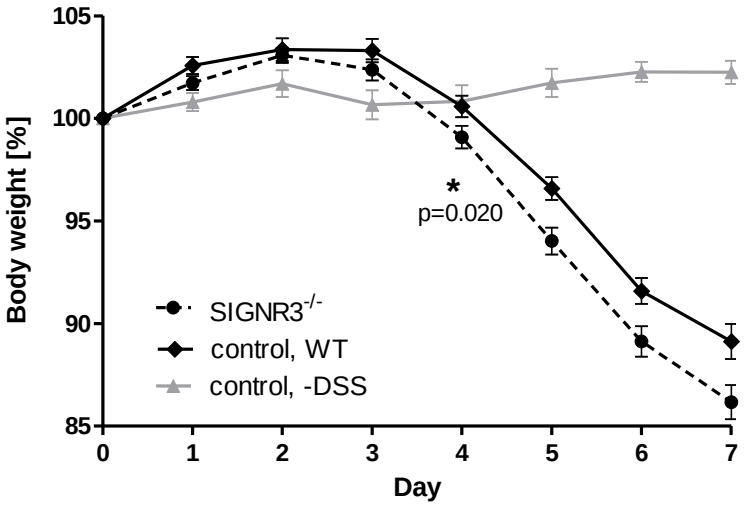

Figure 4.19 Weight loss

Wild-type (WT) and SIGNR3$^{-/-}$ mice were fed 3% DSS supplemented to the drinking water for seven consecutive days. Weight was recorded daily. SIGNR3$^{-/-}$ mice lost significantly more weight from day four on (n=31 for SIGNR3$^{-/-}$ mice, n=30 for wild-type mice, n=19 untreated (-DSS) mice). A summary of four independent experiments is shown. Data are expressed as mean + SEM. For statistical analysis a mixed linear model was used taking multiple measurements per mouse into account and the structure of these measurements was assumed to be autoregressive. A significant difference in weight was observed between the two groups from day 4 to 7 (*$p<0.05$).

Four days after DSS-induced colitis, both wild-type and SIGNR3$^{-/-}$ mice lost considerably weight compared with the untreated mice (Figure 4.19). This is a result of intestinal inflammation leading to malnutrition. Notably, the weight loss at day 4-7 was significantly more pronounced in DSS-treated SIGNR3$^{-/-}$ mice than wild-type mice (Figure 4.19). In addition, both strains displayed marked colitis symptoms at day 7 (Figure 4.20). To evaluate the grade of colitis symptoms, a disease activity index (DAI) was assigned to each mouse. The DAI reflects a grading of the stool consistency, presence of blood in feces, and weight loss. Interestingly, the DAI score was significantly higher in the SIGNR3$^{-/-}$ mice compared with wild-type mice (Figure 4.20A). Similarly, the stool score reflecting the incidence of diarrhea was significantly increased in SIGNR3$^{-/-}$ mice compared with wild-type mice (Figure 4.20B). These findings demonstrate that SIGNR3$^{-/-}$ mice suffer from exacerbated colitis, suggesting the involvement of SIGNR3 in the regulation of DSS-induced intestinal inflammation. No weight loss or colitis symptoms were observed in untreated wild-type mice (Figure 4.19 and 4.20) or SIGNR3$^{-/-}$ mice (data not shown). The colon in all mice treated with DSS was significantly shorter than colon

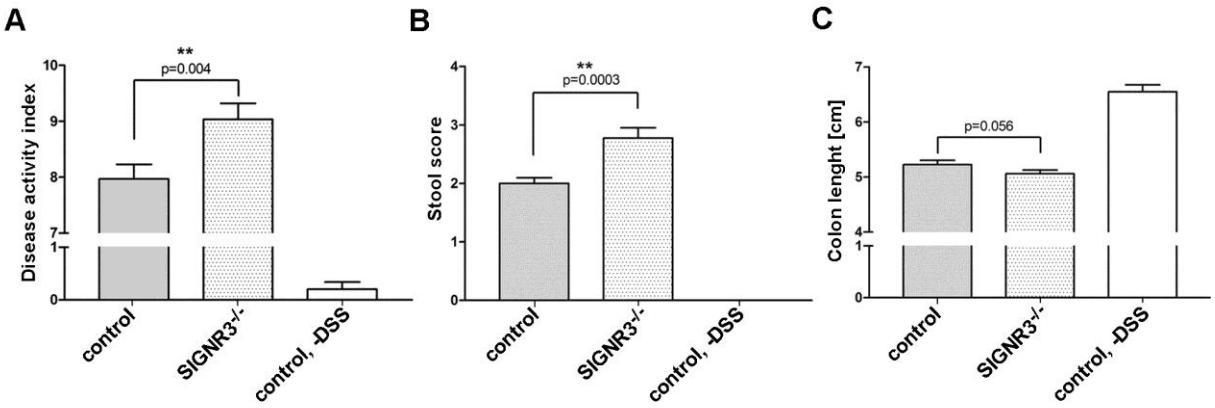

Figure 4.20 Colitis symptoms

Colitis symptoms detected seven days after DSS-induction of colitis in wild-type and SIGNR3$^{-/-}$ mice. A significant increase of disease activity index (DAI) *(A)* and stool score *(B)* were detected in SIGNR3$^{-/-}$ mice. Colons were shortened in both wild-type and SIGNR3$^{-/-}$ mice *(C).* A summary of four independent experiments is shown. Data are expressed as mean + SEM. The *p*-values were determined using unpaired Student's t-test. Significance is indicated by asterisks (*), *p<0.05, **p<0.01

from untreated wild-type mice, indicating severe intestinal inflammation. No significant difference in colon shortening was observed between SIGNR3$^{-/-}$ mice and wild-type mice (Figure 4.20C). This finding might demonstrate that the maximum colon shortening due to inflammation was reached.

4.4.2.1 Histological analyses

To further analyze the impact of inflammation on DSS-treated mice, histological analysis of colon was performed. Staining by hematoxylin and eosin (H&E) revealed a severe, acute, multifocal to coalescent, partly transmural ulcerative colitis in wild-type and SIGNR3$^{-/-}$ mice treated with DSS (Figure 4.21A). Both groups had severe submucosal edema and adjacent steatitis. However, the percentage of altered tissue was markedly increased in SIGNR3$^{-/-}$ mice compared to wild-type mice (Figure 4.21B). Interestingly, tissue damage and ulceration were exacerbated in SIGNR3$^{-/-}$ mice both in the oral and rectal part of the colon, whereas the middle colon part was equally affected in SIGNR3$^{-/-}$ and wild-type mice (Figure 4.21B). Untreated SIGNR3$^{-/-}$ did not display any histological abnormalities (data not shown). In conclusion, histological evaluation indicates that SIGNR3$^{-/-}$ mice are more susceptible to DSS-induced colitis than wild-type mice (Eriksson et al., 2013).

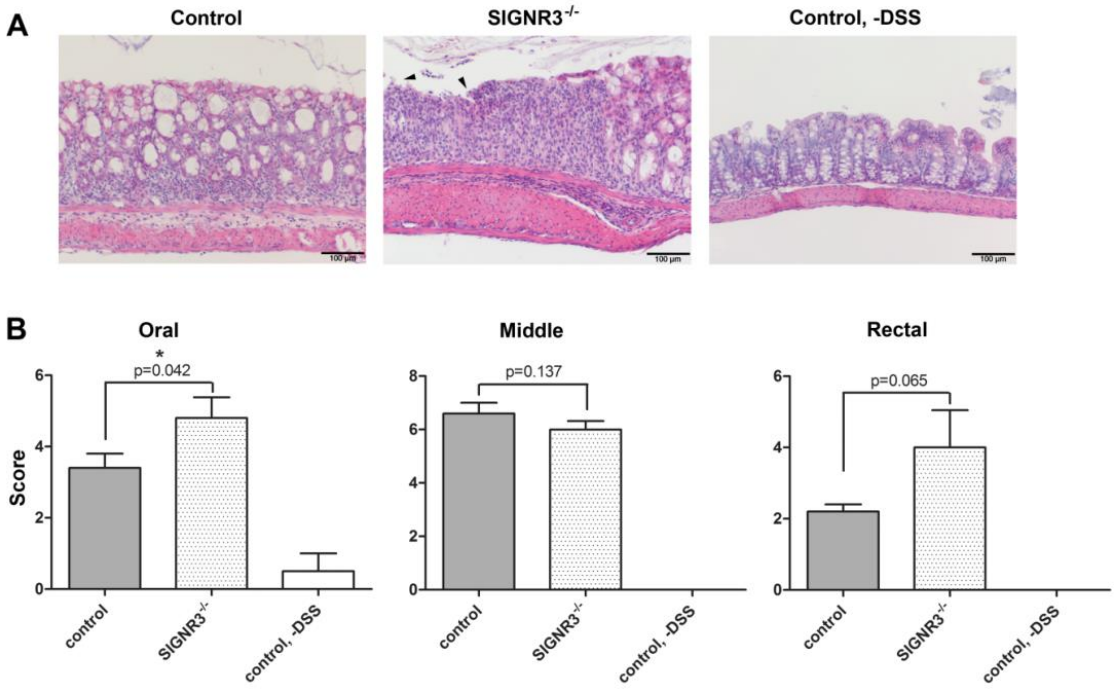

Figure 4.21 Histological analysis of colon tissue

After seven days of DSS treatment, paraffin sections of colon of each mouse were prepared and stained with hematoxylin and eosin (H&E). A histopathological evaluation of each section was performed in a blinded manner. *A*, H&E stained sections from colon of C57BL/6 wild-type, SIGNR3$^{-/-}$ mice and untreated control mice. Arrows show examples of mucosal ulceration. *B*, Each colon was divided into three segments of identical length (oral, middle, rectal) and each segment of the colon was analyzed separately. The degree of infiltration of inflammatory cells and mucosal erosion/ulceration was graded from none (score 0) to mild (score 1), moderate (score 3) or severe (score 4). Data are expressed as mean + SEM (n=5). The *p*-values were determined using unpaired Student's t-test. Significance is indicated by asterisks (*), *$p<0.05$

4.4.2.2 Analysis of local cytokine production in colon

To address the immunological mechanisms that led to the increased inflammation in SIGNR3$^{-/-}$ mice during DSS colitis, the local cytokines in the colon were measured. Pro-inflammatory cytokines such as TNF-α, IL-1β, and IL-6 were detectable in both SIGNR3$^{-/-}$ and wild-type mice upon induction of DSS colitis (Figure 4.22), whereas the concentrations of IL-10, IL-12p40 and IL-17A were below the detection level in both mouse strains. The concentrations of all tested cytokines were below the detection level in untreated wild-type and SIGNR3-deficient mice (data not shown). Interestingly, TNF-α levels were significantly higher in colon of SIGNR3$^{-/-}$ mice during DSS colitis, indicating that SIGNR3 plays an immunoregulatory role during colonic inflammation.

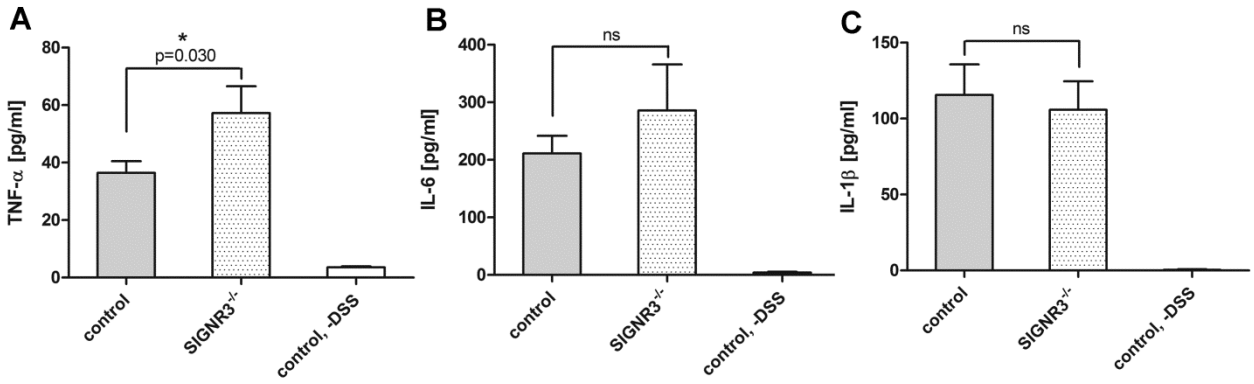

Figure 4.22 Cytokines in colon homogenates

Cytokines in colon homogenates from WT and SIGNR3$^{-/-}$ mice fed with 3% DSS were analyzed by cytometric bead array. The levels of TNF-α *(A)*, IL-6 *(B)*, and IL-1β *(C)* were measured (n=8 for DSS-treated SIGNR3$^{-/-}$ and WT mice, n=5 for untreated wild-type mice). Data are expressed as mean + SEM. The *p*-values were determined using unpaired Student's t-test. Significance is indicated by asterisks (*), *p<0.05.

To conclude, SIGNR3 binds to fungi present in the gut microbiota and the impact of this interaction was analyzed by DSS-induced colitis in SIGNR3$^{-/-}$ mice. Increased weight loss, worsened colitis symptoms as well as higher histopathological scores were observed in SIGNR3$^{-/-}$ mice compared with wild-type mice demonstrating that SIGNR3 influences the intestinal immunity during colitis. These data, along with the increased TNF-α concentration in the colon, suggest that SIGNR3 modulates the intestinal immune response during DSS-induced colitis (Eriksson et al., 2013).

In the first part of this PhD thesis, methods used to screen for CLR carbohydrate ligands and their potential immunomodulatory effect are presented. In the second part of this PhD thesis the interaction of CLRs with gut microbiota and the role of SIGNR3 in murine colitis are presented. Together, these data demonstrate the potential for future targeting of CLRs with carbohydrate ligands in the context of inflammation.

5 DISCUSSION

5.1 Overview of the CLR-ligand platform

CLRs and their carbohydrate ligands are involved in autoimmune related disease models (Fujikado et al., 2008; Iliev et al., 2012) and infection models (Tanne et al., 2009; Vazquez-Mendoza et al., 2013). Still, the ligands and the impact of these interactions on the immune response are not known for the majority of CLRs. One aim of this thesis was to establish a platform to facilitate screening of CLR-ligand interactions and their impact *in vitro* and *in vivo*. For this purpose, a library of fusion proteins consisting of the extracellular region of selected myeloid CLRs and the hFc part were generated. The advantage of using a library of CLR-hFc fusion proteins produced in the same way is that specificity and selectivity of the CLR-ligand interactions can be compared. Here, I present the production of three of these CLR-hFc fusion proteins followed by their biochemical characterization. CLR-hFc fusion proteins were used to screen for synthetic carbohydrate ligands and novel CLRs ligands were identified. The immunomodulatory properties of the identified interactions were analyzed by *in vitro* and *in vivo* experiments. Three selected carbohydrate ligands of MGL1 were able to modulate T cell activation and differentiation both *in vitro* and *in vivo*, demonstrated by an increased IL-2 and IFN-γ production by T cells co-cultured with stimulated $CD11c^+$ cells.

5.2 Production of CLR-hFc fusion proteins

As a tool for the analysis of CLR-ligand interactions, functional fusion proteins consisting of the extracellular region of the respective CLRs and the Fc part of the human IgG_1 were generated. The extracellular region of the CLRs MGL1, Clec9a and SIGNR3 were cloned into an expression vector (Figure 3.1A) followed by CLR-hFc fusion protein production in CHO cells. Producing recombinant fusion proteins in CHO cells has the advantage that folding and glycosylation are similar to the native murine protein (Dinnis and James, 2005). Fc-fusion proteins are established tools to analyze receptor-ligand interactions (Capon et al., 1989; Gascoigne et al., 1987; Higgins et al., 1999; Hollenbaugh and Aruffo, 2002; Lepenies, 2007). However, many of these receptors are type I proteins with their extracellular region in their *N*-terminal part (Bennett et al., 1991; Higgins et al., 1999; Lepenies, 2007). The CLRs analyzed in this thesis are type II proteins, with

their extracellular region in the *C*-terminal part. Although these kinds of Fc fusion proteins have been used in other studies (Hsu et al., 2009), I aimed at confirming that the CLR-hFc proteins were properly folded thus have a functional carbohydrate binding capacity. As expected, specific binding of MGL1-hFc to the reported ligands Lewis X, Lewis A and α-GalNAc could be detected by glycan array (Figure 4.5), demonstrating the functionality of MGL1-hFc. Similarly, the functionality of the SIGNR3-hFc was demonstrated by binding to its known ligand zymosan (Figure 4.13A).

The fusion proteins produced in this thesis were mainly used for the identification of novel CLR ligands. However, there are numerous biological and physicochemical applications for Fc fusion proteins (Table 5.1). For example, Fc fusion proteins containing the extracellular part of co-stimulatory molecules may affect the co-stimulatory signal required for T cell activation (Figure 1.1). Injection of CTLA-4-Fc (that binds CD80/CD86) in mice was reported to prevent the development of autoimmune diabetes (Lenschow et al., 1995). The CTLA-4-Fc fusion protein was found to block the CD80/CD86-CD28 interaction and to promote T cell tolerance, and is now approved for clinical therapy after renal transplantation (El-Charabaty et al., 2012). Other examples of how fusion proteins can be used to block co-stimulatory pathways are listed in table 5.1. Similar to this thesis, lectin-Fc fusion proteins have been used for the identification of novel ligands by glycan array and ELISA (Bochner et al., 2005; Hsu et al., 2009). In addition, these fusion proteins are useful for staining carbohydrate ligands in tissue sections (Guo et al., 2011) as well as western blot analysis (van Sorge et al., 2009). The CLR-hFc proteins produced in this thesis can be used for several of these applications.

There are numerous advantages of an Fc tag over other protein tagging systems. One of the main advantages is that the Fc fusion proteins form stable dimers and have a longer plasma half-life than in a monomeric form (Capon et al., 1989). Dimerization is also useful for lectin-sugar interactions since these are normally relatively weak. Simultaneous interactions of multiple proteins can compensate for low affinity and provide a stronger interaction (Collins and Paulson, 2004). In addition, Fc receptors expressed by phagocytic immune cells can bind to the Fc fusion protein and thereby mediate uptake or killing of the binding partner of the fusion protein (Abbas, 2003; Capon et al., 1989).

The generated CLR-hFc fusion proteins can also be useful to analyze the affinity and kinetics of the binding of novel ligands by using surface plasmon resonance (SPR) (Duverger et al., 2010; Grunstein et al., 2011). Furthermore, using the CLR-hFc fusion proteins for structural

analysis of the CLR-ligand interaction by e.g. co-crystallization can reveal information about ligand binding sites and carbohydrate structures important for binding (Chatwell et al., 2008; Drickamer, 1999; Feinberg et al., 2011).

Table 5.1 Examples of applications of IgG-fusion proteins

Application	Fc protein	Comments	References
Analysis of protein ligand interaction			
Screening of ligands	Siglec-8-Fc CLR-Fc CD4-Fc	Identification of ligands by the use of glycan array and ELISA	(Ashkenazi et al., 1990; Bochner et al., 2005; Capon et al., 1989; Hsu et al., 2009)
Staining of tissue sections	Siglec-F-Fc	Binding to ligands on sections of murine lung	(Guo et al., 2011)
Detection of ligands in western blot	MGL-Fc	Identification of ligands in bacteria	(van Sorge et al., 2009)
Analysis of ligand receptor interaction	LFA3-Fc	Surface plasmon resonance (SPR)	(Majeau et al., 1999)
***In vivo* immune modulation**			
Dampening of immune responses *in vivo*	CTLA-4-Fc	Binding of CD80/CD86 prevents development of autoimmune diabetes	(Lenschow et al., 1995)
Promotion of T cell tolerance in renal transplantation	CTLA-4-Fc	Phase III clinical trials	(El-Charabaty et al., 2012)
T cell regulation	OX40-Fc	Amelioration of T-cell dependent murine colitis	(Higgins et al., 1999)
Promotion of immune response	Tim-3-Fc	Blocking of binding of Galectin-9 to T cells leads to improved murine immune response after influenza A virus infection.	(Sharma et al., 2011)

5.3 Screening of immune modulatory properties of CLR ligands

5.3.1 Screening of CLR carbohydrate ligands

To identify novel CLR ligands, the CLR-hFc fusion proteins were used to screen for binding to a wide range of synthetic carbohydrate structures using glycan array. As expected, MGL1-hFc bound to all structures containing a terminal galactose, not only confirming the existence of a functional CRD in the MGL1-hFc fusion protein, but also that these CLR-hFc proteins are applicable to glycan array screening (Figure 4.6). Glycan array is a useful method to analyze the rather weak interactions between carbohydrates and lectins. Since highly concentrated carbohydrates are printed as small nanospots, multivalency allows for lectin-carbohydrate interactions to take place (Horlacher et al., 2010; Lee et al., 2011). Another advantage of the glycan array technology is that only small amounts of synthetic sugars are needed (Horlacher et al., 2010). By applying the generated CLR-hFc proteins in glycan array, the identification of novel carbohydrate ligands was accomplished. One of the carbohydrates that was recognized by MGL1-hFc was the tumor antigen Gb5, also called stage specific embryonic antigen-3 (SSEA-3). Similar to the MGL1-ligand Lewis X (also known as SSEA-1), Gb5 is present during embryonic stages (Muramatsu and Muramatsu, 2004). In addition, both of these antigens are found on tumor cells such as testicular cancer (Olie et al., 1996). High abundance of Gb5 is found on both renal and breast carcinoma cells (Heimburg-Molinaro et al., 2011). Transformation of a normal tissue cell to a tumor cell often involves aberrant glycosylation leading to the cell surface presence of tumor-associated carbohydrate antigens such as Gb5 and Lewis X (Heimburg-Molinaro et al., 2011). Tumor cells have different ways of evading immune responses, by mechanisms including down-regulation of tumor antigen expression and Treg dampening of immune responses (Drake et al., 2006; Zou, 2006). Directing immune responses against cells expressing certain tumor-associated carbohydrates exclusively expressed by tumors can be useful for developing tumor-specific vaccines or immunotherapies (Heimburg-Molinaro et al., 2011; Singh et al., 2011).

In addition to the high abundance on the surface of certain tumor cells, Lewis X is present in the cell wall of pathogens such as *Helicobacter pylori* and *Schistosoma mansoni* (Heimburg-Molinaro et al., 2011; Ko et al., 1990). The surface expression of Lewis X by *S. mansoni* prevents the immune system from recognizing parasitic trematode larvae upon infection in a human or animal host (Ko et al., 1990). *Schistosoma* antigens containing Lewis X negatively regulate the

peripheral blood mononuclear cell (PMBC) response against the parasite via IL-10 induction (Velupillai et al., 2000). These studies demonstrate that carbohydrate antigens have indeed the potential to modulate immune responses.

5.3.2 Screening of immune modulatory properties of CLR ligands

To analyze the immune modulatory properties of chosen CLR ligands discovered by glycan array, the OT-II system was used. By conjugating the CLR carbohydrate ligands Lewis X, Gb5 and 1,3-lactosamine to OVA, OVA-specific cellular and humoral responses were modulated. T cell activation was enhanced, reflected by a significant increase of the IL-2 production demonstrated by *in vitro* co-culture experiments (Figure 4.12A). In addition, the increase of IFN-γ *in vitro* (Figure 4.12B) that was by tendency also observed *in vivo*, suggests that these CLR-ligands polarize $CD4^+$ T cell differentiation into Th1. This conclusion is also corroborated by the reduced production of OVA-specific antibodies *in vivo*, since Th1 cells mainly promote immune responses against intracellular antigens. The Th1 polarization seen here is similar to other studies using carbohydrates (Ahlen et al., 2012; Napoletano et al., 2012; Singh et al., 2011). For instance, by conjugating the mannose receptor (MR)-ligands 3-sulfo-Lewis A and tri-GlcNac to OVA, cross presentation was enhanced and Th cell differentiation into IFN-γ-producing cells was increased (Singh et al., 2011). IFN-γ promotes macrophage activation and is also important for the generation of potent $CD8^+$ T cell responses and for their recruitment to tumor sites (Wong et al., 2008).

In the OT-II model used in this thesis, the OVA is taken up by APCs and the $OVA_{323-339}$ peptide is loaded on MHC-II molecules and presented to OT-II T cells (Robertson et al., 2000). Glycosylation of a MHC-II binding peptide can affect the binding of MHC-II molecules as well as T cell activation (Gad et al., 2003; Galli-Stampino et al., 1997). In the case of $OVA_{323-339}$, the T cell activation is decreased by glycosylation (Ishioka et al., 1992). To prevent carbohydrate conjugation to the $OVA_{323-339}$ peptide, the DSAP linker reacting with the primary amine in the side chain of lysine residues on the OVA surface was used. Since the $OVA_{323-339}$ peptide (ISQAVHAAHAEINEAGR) loaded on the MHC-II molecule does not contain a lysine residue (Robertson et al., 2000), the conjugation of sugar should not affect the peptide loading on MHC-class II or peptide-TCR interactions (Ishioka et al., 1992). Thus, it can be excluded that the immune modulatory effects detected by the OVA-carbohydrate conjugates tested in this thesis are

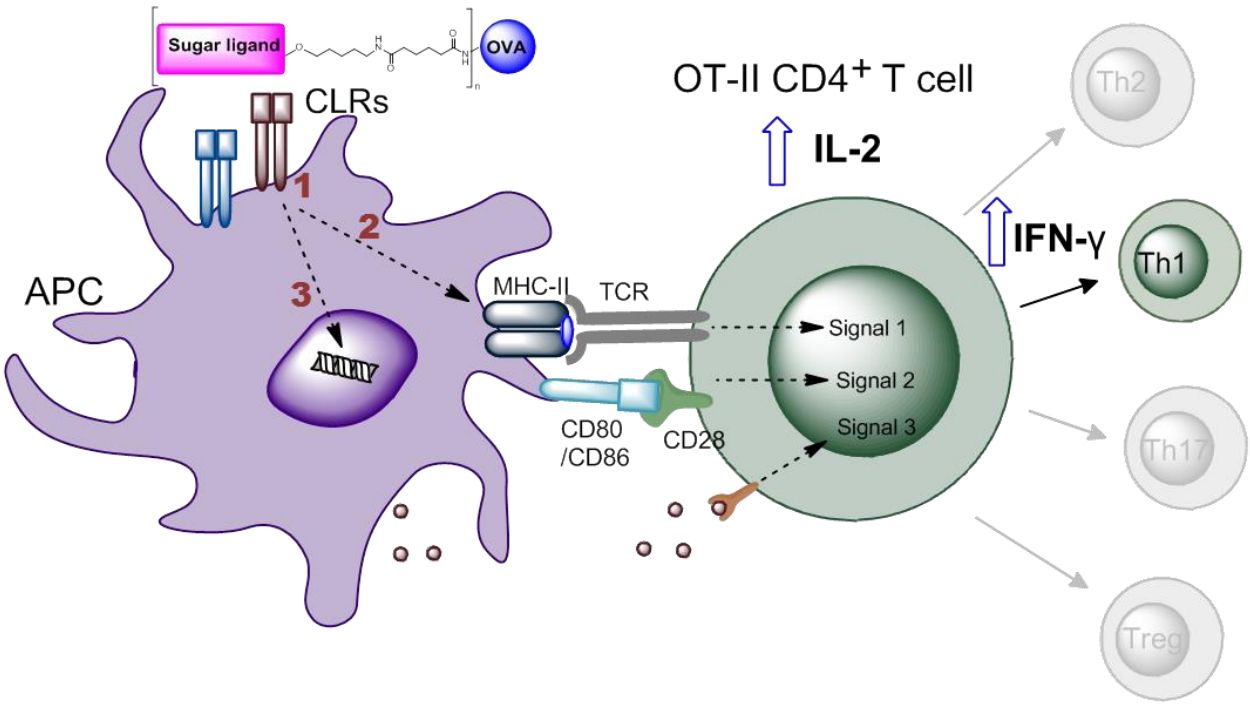

Figure 5.1 OVA-carbohydrate conjugates can modulate OT-II T cell activation and differentiation
OVA conjugated to CLR ligands increase T cell activation demonstrated by an increased production of the cytokines IL-2 and IFN-γ. $CD11c^+$ DCs bind and endocytose the OVA-sugar conjugates. The OVA-carbohydrate conjugates might influence the endocytic uptake of OVA(1), intracellular trafficking (2) or intracellular signaling (3).

due to glycosylation of the $OVA_{323-339}$ peptide. Accordingly, the IL-2 increase and the modulation of Th1/Th2 cell differentiation observed are due to changes in the kinetics of OVA uptake/processing or altered intracellular signaling (Figure 5.1).

Of all tested CLR-hFc proteins, MGL1-hFc, Clec9a-hFc and Clec12b-hFc showed binding to Gb5 and 1,3-lactosamine in the glycan array (Figure 4.7). The mRNA coding for each of these CLRs was detected in splenic $CD11c^+$ cells, indicating that these CLRs are expressed by DCs. However, the signaling motifs of these CLRs are highly diverse (Figure 1.2). Clec9a signals via a hemITAM (Sancho and Reis e Sousa, 2012). On the contrary, Clec12b contains an intracellular ITIM suggesting an immune regulatory role for this receptor (Hoffmann et al., 2007) and, to date, the signaling motifs of MGL1 are not reported. Due to these highly various CLR signaling pathways, it is unlikely that the effects of the carbohydrate targeting *in vitro* and *in vivo* are due to simultaneous binding to all of these CLRs. Binding of MGL1-hFc to Gb5 and 1,3-lactosamine in the glycan array resulted in the highest fluorescence signal. In addition, of the tested CLR-hFc fusion proteins, MGL1-hFc was the exclusive binder to Lewis X. Similar to the

result in the present thesis, co-culture of T cells and bone marrow derived dendritic cells stimulated with GalNAc antigens induced T cell proliferation and activation of both $CD4^+$ and $CD8^+$ T cells along with the induction of IFN-γ and IL-17A production (Denda-Nagai et al., 2010). This effect was dependent of MGL2, the second murine homologue of human MGL. Moreover, the engagement of the human MGL by GalNAc antigens induced phosphorylation of extracellular signal-regulated kinase 1,2 (ERK1,2) and NF-kB activation, indicating that MGL engagement promotes DC activation (Napoletano et al., 2012). In addition, MGL interaction with CD45 on effector T cells negatively regulated TCR-mediated signaling and T cell-dependent cytokine response (van Vliet et al., 2006a). Thus, these reports suggest that human MGL and its murine homologues are involved in the regulation of T cell responses. This is in agreement with the increased T cell production of IL-2 observed after stimulation with OVA conjugated to MGL1 ligands.

Previous studies demonstrate that targeting of antigens to the CLRs MR (Burgdorf et al., 2007) or DEC-205 (Dudziak et al., 2007) mediates enhanced antigen uptake. In addition, the intracellular trafficking can be directed by CLR-specific delivery (Burgdorf et al., 2007). However, in these studies antibody-mediated targeting was performed. In this thesis, I show that certain CLR carbohydrate ligands can be used to direct immune responses. In addition, the platform presented here including the generation of CLR-hFc fusion proteins and the *in vitro* and *in vivo* assays can be used to identify further CLR carbohydrate ligands with immune modulatory properties.

5.4 The role of CLRs in intestinal inflammation

5.4.1 Recognition of microbiota by CLRs

The CLR-hFc proteins produced in this thesis were used to screen for ligands in gut microbiota. MGL1 binds to the commensal bacterial strains *Streptococcus spp.* and *Lactobacillus spp.* (Saba et al., 2009). As expected, a significant binding of MGL1-hFc to gut microbiota was detected by ELISA. One of the CLRs binding even stronger to the gut microbes than MGL1 was SIGNR3 (Figure 4.13). This binding was confirmed by binding of fluorescently labeled gut microbes to SIGNR3-transfected cells (Figure 4.15). To date, SIGNR3 has been reported to bind to pathogenic mycobacterial lipoglycans (Tanne et al., 2009) as well as the yeast cell wall component zymosan (Takahara et al., 2004). Similar to the human DC-SIGN, SIGNR3 also binds to *C. albicans* (Cambi et al., 2003; Takahara et al., 2004). Co-staining of the microbes with SIGNR3-hFc and an anti-fungal antibody showed that SIGNR3 binds indeed mainly to fungal gut microbes. Although *C. albicans* is present in the human gut microbiota it is not a part of the healthy murine gut microbiota (Jawhara et al., 2008; Pope and Cole, 1982). A previous study demonstrated that the three main fungal populations in C75BL/6 mice kept under SPF conditions were *C. tropicalis, S. cerevisiae* and *Trichosporonales spp.* (Iliev et al., 2012). Since the SIGNR3-hFc stained over 60 % of the commensal fungi, it is likely that SIGNR3 recognizes one or more of these strains. The fungal cell wall consists of different layers rich of carbohydrates. The outermost layer consists mainly of high mannan followed by layers of β-glucans and chitin. The different layers and carbohydrates are recognized by certain CLRs. Dectin-1 mainly recognizes fungal cell wall β-glucans, whereas the CLRs Dectin-2, MR and Mincle bind the mannan layer (Hardison and Brown, 2012). The interaction of SIGNR3 and microbiota is also similar to other PRRs. NOD2 and TLR4 recognize microbial antigens such as muramyl dipeptide and LPS in the gut and are involved in maintaining the balance between controlled responses to pathogens and overwhelming innate immune activation (Rakoff-Nahoum et al., 2004; Watanabe et al., 2004).

In this thesis, I show that SIGNR3 is involved in the recognition of intestinal microbiota, mainly fungi. These results demonstrate that CLR-hFc fusion proteins are useful to screen for microbial ligands to elucidate their role in infection and inflammation.

5.4.2 SIGNR3 in murine colitis

To analyze the impact of the interaction of SIGNR3 and gut microbiota on intestinal immunity, I employed the DSS colitis model. This model allows commensal microbes that are normally restricted to the outer mucosal layer to penetrate the inner mucosal layer. Consequently, these microbes interact with epithelial cells and local innate immune cells, initiating an inflammatory response against the commensals (Johansson et al., 2011; Johansson et al., 2010). Thus, this model is widely used to study the role of the interaction of commensal microbiota and intestinal innate immunity (Schölmerich 2000). Upon colitis induction, SIGNR3$^{-/-}$ mice exhibited a more severe weight loss and aggravated colitis symptoms such as severe diarrhea, cell infiltration into the colon, and mucosal ulceration compared to wild-type mice (Figure 4.18-4.20). This observation is consistent with several reports where mice lacking other PPRs e.g. TLRs, NOD2 and certain CLRs presented exacerbated colitis symptoms (Iliev et al., 2012; Müller et al., 2010; Rakoff-Nahoum et al., 2004; Saba et al., 2009; Watanabe et al., 2006). Similar to the present study, mice lacking NOD2 are more susceptible to colitis (Watanabe et al., 2006). Although the binding to its microbial ligand muramyl dipeptide activates NF-κB signal pathways resulting in proinflammatory cytokine production (Inohara et al., 2001), this receptor is also involved in controlling an overwhelming adaptive immune response (Strober et al., 2008). The mechanism of the NOD2 involvement in gut homeostasis has been debated (Saleh and Trinchieri, 2011). One mechanism suggested to be involved is NOD2 inhibition of TLR-driven inflammation in the gut (Watanabe et al., 2004). Consequently, lack of homeostatic gut control by NOD2 results in increased susceptibility to intestinal inflammation in mice as well as in humans (Ogura et al., 2001; Strober et al., 2008).

Recent studies have shown a role for CLRs in the immune regulation of gut inflammation. Mice lacking Dectin-1 are more susceptible to chemically induced colitis, due to an altered immune response to fungal microbiota (Iliev et al., 2012). In addition, MGL1 has a protective role in colitis, demonstrated by more severe inflammation in MGL1$^{-/-}$ mice during colitis (Saba et al., 2009). In contrast to these studies, mice lacking SIGNR1 exhibited an ameliorated form of murine colitis implicating that this receptor is rather involved in the pro-inflammatory response than in immune regulation during colitis (Saunders et al., 2010).

Since certain CLRs signal via common adaptor molecules, such as Syk (Figure 1.2) (Sancho and Reis e Sousa, 2012), it is possible that other CLRs involved in the regulation of the intestinal homeostasis partially compensate the lack of SIGNR3. However, I here provide

evidence that one single CLR has a marked influence on colitis pathogenesis, which suggests a non-redundant role of SIGNR3 in murine colitis.

Upon colitis induction, TNF-α production was increased in the colon of SIGNR3$^{-/-}$ mice compared to wild-type mice. This proinflammatory cytokine plays a key role in the pathogenesis of IBD (Apostolaki et al., 2010; Neurath et al., 1997) and administration of TNF-α-neutralizing antibodies is an approved medical therapy for IBD patients (Engel and Neurath, 2010). Notably, mice lacking Dectin-1 also display higher TNF-α levels in the colon after induction of colitis (Iliev et al., 2012). Similar to Dectin-1, SIGNR3 has an intracellular hemITAM and was suggested to signal via Syk and activation of either of these CLRs has been reported to induce TNF-α production (Sancho and Reis e Sousa, 2012; Tanne et al., 2009). The interaction of SIGNR3 and fungi in the gut during DSS-induced colitis seem to mediate immune regulation. The lack of SIGNR3-induced regulation during colitis in SIGNR3$^{-/-}$mice possibly leads to an increase of the fungal load similar to the increased fungal invasion in colonic tissue in Dectin-1$^{-/-}$ mice during colitis (Iliev et al., 2012). As a consequence, intestinal inflammation and local TNF-α production might be increased in SIGNR3$^{-/-}$ mice. In accordance with the study by Iliev *et al.*, the findings in this thesis demonstrate that besides Dectin-1, SIGNR3 is also involved in the regulation of pro-inflammatory cytokine production in murine colitis.

Increasing evidence points to a role for fungi in the pathogenesis of IBD (Ott et al., 2008). The fungal composition of the microbiota was reported to be different in patients and healthy controls, suggesting the involvement of fungi in IBD (Ott et al., 2008). In addition anti-*Saccharomyces cerevisiae* antibodies (ASCA) are frequently found in patients with CD (Sutton et al., 2000; Walker et al., 2004) as well as in mice after DSS-colitis (Iliev et al., 2012; Jawhara et al., 2008; Müller et al., 2010). The findings in this thesis demonstrate that SIGNR3 recognizes fungal microbiota and plays an immune regulatory role in colitis. To further analyze the involvement of fungi in murine colitis, mice can be treated with anti-fungals such as fluconazole before DSS-induction of colitis. Taken together, these findings highlight the importance of the CLR SIGNR3 in commensal recognition and maintenance of homeostasis in intestinal immunity.

6. SUMMARY

C-type lectin receptors (CLR) and their carbohydrate ligands are involved in several different inflammatory processes. Still, for some CLRs, ligands need to be identified and the impact of CLR-ligand interactions on the immune response is not known for the majority of CLRs. The aim of this PhD thesis was to establish a platform to facilitate screening of CLR-ligand interactions and to analyze their impact *in vitro* and *in vivo*. To this end, the extracellular regions of MGL1, Clec9a and SIGNR3 were expressed as fusion proteins with the Fc part of human IgG_1. Fusion proteins were produced in CHO cells followed by their biochemical characterization. Binding of CLR-hFc fusion proteins to synthetic carbohydrate ligands was screened using glycan array. Three candidate carbohydrate ligands binding to MGL1-hFc were selected for analysis *in vitro* and *in vivo* and were conjugated to ovalbumin (OVA). Pulsing dendritic cells with OVA-carbohydrate conjugates before co-culture with OT-II T cells resulted in an increased IL-2 and IFN-γ production by T cells. Similarly, by trend an increase of the IL-2 and IFN-γ producing T cell populations was detected upon immunization with OVA-carbohydrate conjugates. In addition, the production of OVA-specific antibodies was reduced in mice immunized with OVA-carbohydrate conjugates. These findings demonstrate that it is possible to use CLR carbohydrate ligands to influence OVA-specific T cell responses *in vitro* and *in vivo*. Moreover, this platform is a suitable tool to identify CLR carbohydrate ligands with immune modulatory properties.

Recent observations suggest that the interaction of gut microbes and certain CLRs, such as Dectin-1 and MGL1, influence the intestinal inflammation. To analyze whether further CLRs recognize gut commensals, the generated CLR-hFc proteins were used to screen for microbiota ligands. One CLR-hFc fusion proteins that bound to fungi in the microbiota was SIGNR3. To analyze if this interaction impacted the intestinal immunity against microbiota, the dextran sulfate sodium (DSS) model of colitis was employed. $SIGNR3^{-/-}$ mice exhibited an increased weight loss associated with more severe colitis symptoms compared to wild-type control mice. The increased inflammation in $SIGNR3^{-/-}$ mice was accompanied by a higher level of TNF-α in colon. These findings highlight the importance of CLRs in intestinal immunity and demonstrate for the first time an immune regulatory role for SIGNR3 in colitis.

To conclude, well characterized CLR-hFc fusion proteins are useful tools for the identification of novel carbohydrate ligands as well as microbial ligands. *In vitro* stimulation assays along with immunization studies revealed the immune modulatory role of certain

carbohydrate ligands. In addition, an immune regulatory role of the CLR SIGNR3 in murine intestinal inflammation during colitis was discovered. Together these findings highlight the importance of CLRs and their ligand recognition in innate immunity.

7. ZUSAMMENFASSUNG

C-Typ Lektinrezeptoren (CLRs) und ihre Kohlenhydrat-Liganden sind bei der Entstehung der Mehrzahl von Entzündungsherden beteiligt. Liganden sind für einige CLRs jedoch noch nicht identifiziert und auch der Einfluss der CLR-Liganden-Interaktion auf die Immunantwort ist für die meisten CLRs nicht geklärt. Ein Ziel dieser Doktorarbeit war die Etablierung einer Plattform von CLR-hFc Fusionsproteinen, um in kurzer Zeit eine Mehrzahl von Interaktionen zwischen CLRs und möglichen Liganden zu testen und deren Bedeutung *in vitro* und *in vivo* zu analysieren. Zu diesem Zweck wurden MGL1, Clec9a und SIGNR3 als Fusionsproteine bestehend aus der jeweiligen extrazellulären Region und dem humanen IgG_1 Fc-Teil exprimiert. Die Fusionsproteine wurden in CHO-Zellen produziert und anschließend biochemisch charakterisiert. Mittels Glykan-Array-Technologie wurden sie dann auf ihre Bindung zu synthetischen Kohlenhydrat-Liganden untersucht. Drei Kohlenhydrat-Liganden zeigten hierbei positive Bindungen zu MGL1. Sie wurden für weitere *in vitro* und *in vivo* Analysen ausgewählt und zu diesem Zweck an Ovalbumin (OVA) konjugiert. Nach Beladung von dendritischen Zellen mit den OVA-Kohlenhydrat-Konjugaten und anschließender Ko-Kultivierung mit OT-II T-Zellen zeigte sich eine erhöhte IL-2 und IFN-γ Produktion durch die T-Zellen. Die Immunisierung von Mäusen mit den OVA-Kohlenhydrat-Konjugaten ergab tendenziell ebenfalls eine erhöhte Anzahl an IL-2 und IFN-γ produzierenden T-Zellpopulationen. Weiterhin war die Produktion von OVA-spezifischen Antikörpern in den mit den OVA-Kohlenhydrat-Konjugaten immunisierten Mäusen geringer. Diese Ergebnisse zeigen, dass die OVA-Kohlenhydrat-Konjugate die T-Zellantwort *in vitro* und *in vivo* beeinflussen können. Daher ist die im Rahmen dieser Doktorarbeit etablierte Plattform sehr nützlich, um CLR-Liganden mit immunmodulierenden Eigenschaften zu identifizieren.

Kürzlich erschienene Publikationen weisen darauf hin, dass die Interaktion zwischen Mikroorganismen im Darm und bestimmten CLRs, wie z.B. Dectin-1 und MGL1, einen Einfluss auf die Entzündungsentstehung im Darm im Colitis-Verlauf haben. Um zu untersuchen, ob noch weitere CLRs kommensale Darm-Mikroorganismen erkennen, wurden die im Rahmen dieser Doktorarbeit generierten CLR-hFc Fusionsproteine auf Bindung zu Darmmikrobiota getestet. Hierbei wies SIGNR3 eine positive Bindung auf. Um zu untersuchen, ob diese Interaktion Einfluss auf die darmassoziierte Immunität gegen Mikrobiota hat, wurde das Dextran-Natriumsulfat (DSS)-induzierte Colitis-Modell in der Maus verwendet. Hierbei wiesen die

SIGNR3$^{-/-}$ Mäuse im Vergleich zu den Wildtyp-Mäusen einen erhöhten Gewichtsverlust auf, der einher ging mit stärker ausgeprägten Colitis-typischen Symptomen. Der erhöhte Entzündungsgrad in SIGNR3$^{-/-}$ Mäusen war verbunden mit im Darm lokal vermehrter TNF-α Produktion. Diese Ergebnisse heben hervor, wie wichtig CLRs für die darmassoziierte Immunität sind, und demonstrieren zum ersten Mal eine immunregulatorische Rolle für SIGNR3 im Krankheitsverlauf der Colitis.

Zusammenfassend sind die im Rahmen dieser Doktorarbeit produzierten und charakterisierten CLR-hFc Fusionsproteine sehr nützlich für die Identifikation von neuen Kohlenhydrat-Liganden oder von mikrobiellen Liganden. Die *in vitro* Stimulationsstudien sowie Immunisierungsstudien ergaben, dass einige Kohlenhydrat-Liganden immunmodulatorische Eigenschaften besitzen. Weiterhin wurde für SIGNR3 eine immunregulatorische Rolle in der Entstehung einer akuten Darmentzündung im Verlauf der murinen Colitis entdeckt. Insgesamt heben diese Ergebnisse die wichtige Rolle von CLRs und ihre Ligand-Erkennung in der angeborenen Immunität hervor.

REFERENCES

Abbas, K.A.L., H.A. (2003). Cellular and Molecular Immunology, Elsevier Science, Saunders, (Fifth edition edn).

Adams, E.W., Ratner, D.M., Bokesch, H.R., McMahon, J.B., O'Keefe, B.R., and Seeberger, P.H. (2004). Oligosaccharide and glycoprotein microarrays as tools in HIV glycobiology; glycan-dependent gp120/protein interactions. *Chem Biol* 11, 875-881.

Adams, E.W., Ratner, D.M., Seeberger, P.H., and Hacohen, N. (2008). Carbohydrate-mediated targeting of antigen to dendritic cells leads to enhanced presentation of antigen to T cells. *Chembiochem* 9, 294-303.

Ahlen, G., Strindelius, L., Johansson, T., Nilsson, A., Chatzissavidou, N., Sjoblom, M., Rova, U., and Holgersson, J. (2012). Mannosylated mucin-type immunoglobulin fusion proteins enhance antigen-specific antibody and T lymphocyte responses. *PLoS One* 7, e46959.

Ahrens, S., Zelenay, S., Sancho, D., Hanc, P., Kjaer, S., Feest, C., Fletcher, G., Durkin, C., Postigo, A., Skehel, M., *et al.* (2012). F-actin is an evolutionarily conserved damage-associated molecular pattern recognized by DNGR-1, a receptor for dead cells. *Immunity* 36, 635-645.

Apostolaki, M., Armaka, M., Victoratos, P., and Kollias, G. (2010). Cellular mechanisms of TNF function in models of inflammation and autoimmunity. *Curr Dir Autoimmun* 11, 1-26.

Ashkenazi, A., Presta, L.G., Marsters, S.A., Camerato, T.R., Rosenthal, K.A., Fendly, B.M., and Capon, D.J. (1990). Mapping the CD4 binding site for human immunodeficiency virus by alanine-scanning mutagenesis. *Proc Natl Acad Sci U S A* 87, 7150-7154.

Banchereau, J., and Steinman, R.M. (1998). Dendritic cells and the control of immunity. *Nature* 392, 245-252.

Barnden, M.J., Allison, J., Heath, W.R., and Carbone, F.R. (1998). Defective TCR expression in transgenic mice constructed using cDNA-based alpha- and beta-chain genes under the control of heterologous regulatory elements. *Immunol Cell Biol* 76, 34-40.

Belkaid, Y. (2007). Regulatory T cells and infection: a dangerous necessity. *Nat Rev Immunol* 7, 875-888.

Bennett, B.D., Bennett, G.L., Vitangcol, R.V., Jewett, J.R., Burnier, J., Henzel, W., and Lowe, D.G. (1991). Extracellular domain-IgG fusion proteins for three human natriuretic peptide receptors. Hormone pharmacology and application to solid phase screening of synthetic peptide antisera. *J Biol Chem* 266, 23060-23067.

Bochner, B.S., Alvarez, R.A., Mehta, P., Bovin, N.V., Blixt, O., White, J.R., and Schnaar, R.L. (2005). Glycan array screening reveals a candidate ligand for Siglec-8. *J Biol Chem* 280, 4307-4312.

Bonifaz, L., Bonnyay, D., Mahnke, K., Rivera, M., Nussenzweig, M.C., and Steinman, R.M. (2002). Efficient targeting of protein antigen to the dendritic cell receptor DEC-205 in the steady state leads to antigen presentation on major histocompatibility complex class I products and peripheral CD8+ T cell tolerance. *J Exp Med* 196, 1627-1638.

Bonifaz, L.C., Bonnyay, D.P., Charalambous, A., Darguste, D.I., Fujii, S., Soares, H., Brimnes, M.K., Moltedo, B., Moran, T.M., and Steinman, R.M. (2004). In vivo targeting of antigens to maturing dendritic cells via the DEC-205 receptor improves T cell vaccination. *J Exp Med* 199, 815-824.

Boonyarattanakalin, S., Liu, X., Michieletti, M., Lepenies, B., and Seeberger, P.H. (2008). Chemical synthesis of all phosphatidylinositol mannoside (PIM) glycans from Mycobacterium tuberculosis. *J Am Chem Soc* 130, 16791-16799.
Boscardin, S.B., Hafalla, J.C., Masilamani, R.F., Kamphorst, A.O., Zebroski, H.A., Rai, U., Morrot, A., Zavala, F., Steinman, R.M., Nussenzweig, R.S., and Nussenzweig, M.C. (2006). Antigen targeting to dendritic cells elicits long-lived T cell help for antibody responses. *J Exp Med* 203, 599-606.
Bosse, F., Marcaurelle, L.A., and Seeberger, P.H. (2002). Linear synthesis of the tumor-associated carbohydrate antigens Globo-H, SSEA-3, and Gb3. *J Org Chem* 67, 6659-6670.
Bouma, G., and Strober, W. (2003). The immunological and genetic basis of inflammatory bowel disease. *Nat Rev Immunol* 3, 521-533.
Brown, G.D. (2006). Dectin-1: a signalling non-TLR pattern-recognition receptor. *Nat Rev Immunol* 6, 33-43.
Burgdorf, S., Kautz, A., Bohnert, V., Knolle, P.A., and Kurts, C. (2007). Distinct pathways of antigen uptake and intracellular routing in CD4 and CD8 T cell activation. *Science* 316, 612-616.
Burnet, F.M. (1976). A modification of Jerne's theory of antibody production using the concept of clonal selection. *CA Cancer J Clin* 26, 119-121.
Cambi, A., Gijzen, K., de Vries l, J., Torensma, R., Joosten, B., Adema, G.J., Netea, M.G., Kullberg, B.J., Romani, L., and Figdor, C.G. (2003). The C-type lectin DC-SIGN (CD209) is an antigen-uptake receptor for Candida albicans on dendritic cells. *Eur J Immunol* 33, 532-538.
Caminschi, I., Lahoud, M.H., and Shortman, K. (2009). Enhancing immune responses by targeting antigen to DC. *Eur J Immunol* 39, 931-938.
Caminschi, I., Proietto, A.I., Ahmet, F., Kitsoulis, S., Shin Teh, J., Lo, J.C., Rizzitelli, A., Wu, L., Vremec, D., van Dommelen, S.L., *et al.* (2008). The dendritic cell subtype-restricted C-type lectin Clec9A is a target for vaccine enhancement. *Blood* 112, 3264-3273.
Capila, I., and Linhardt, R.J. (2002). Heparin-protein interactions. *Angewandte Chemie* 41, 391-412.
Capon, D.J., Chamow, S.M., Mordenti, J., Marsters, S.A., Gregory, T., Mitsuya, H., Byrn, R.A., Lucas, C., Wurm, F.M., Groopman, J.E., and et al. (1989). Designing CD4 immunoadhesins for AIDS therapy. *Nature* 337, 525-531.
Carvalho, F.A., Aitken, J.D., Vijay-Kumar, M., and Gewirtz, A.T. (2012). Toll-like receptor-gut microbiota interactions: perturb at your own risk! *Annu Rev Physiol* 74, 177-198.
Cash, H.L., Whitham, C.V., Behrendt, C.L., and Hooper, L.V. (2006). Symbiotic bacteria direct expression of an intestinal bactericidal lectin. *Science* 313, 1126-1130.
Chatwell, L., Holla, A., Kaufer, B.B., and Skerra, A. (2008). The carbohydrate recognition domain of Langerin reveals high structural similarity with the one of DC-SIGN but an additional, calcium-independent sugar-binding site. *Mol Immunol* 45, 1981-1994.
Chen, G., Shaw, M.H., Kim, Y.G., and Nunez, G. (2009). NOD-like receptors: role in innate immunity and inflammatory disease. *Annu Rev Pathol* 4, 365-398.
Chen, G.Y., and Nunez, G. (2009). Gut Immunity: a NOD to the commensals. *Curr Biol* 19, R171-174.
Chen, Y., Inobe, J., Marks, R., Gonnella, P., Kuchroo, V.K., and Weiner, H.L. (1995). Peripheral deletion of antigen-reactive T cells in oral tolerance. *Nature* 376, 177-180.
Chomczynski, P., and Sacchi, N. (1987). Single-step method of RNA isolation by acid guanidinium thiocyanate-phenol-chloroform extraction. *Anal Biochem* 162, 156-159.
Collins, B.E., and Paulson, J.C. (2004). Cell surface biology mediated by low affinity multivalent protein-glycan interactions. *Curr Opin Chem Biol* 8, 617-625.

Cruz, L.J., Tacken, P.J., Pots, J.M., Torensma, R., Buschow, S.I., and Figdor, C.G. (2012). Comparison of antibodies and carbohydrates to target vaccines to human dendritic cells via DC-SIGN. *Biomaterials* 33, 4229-4239.
Czerkinsky, C.C., Nilsson, L.A., Nygren, H., Ouchterlony, O., and Tarkowski, A. (1983). A solid-phase enzyme-linked immunospot (ELISPOT) assay for enumeration of specific antibody-secreting cells. *J Immunol Methods* 65, 109-121.
Delves, P.J., and Roitt, I.M. (2000). The immune system. First of two parts. *N Engl J Med* 343, 37-49.
DeNardo, G.L., Bradt, B.M., Mirick, G.R., and DeNardo, S. (2003). Human antiglobulin response to foreign antibodies: therapeutic benefit? *Cancer Immunol Immunother* 52, 309-316.
Denda-Nagai, K., Aida, S., Saba, K., Suzuki, K., Moriyama, S., Oo-Puthinan, S., Tsuiji, M., Morikawa, A., Kumamoto, Y., Sugiura, D., *et al.* (2010). Distribution and function of macrophage galactose-type C-type lectin 2 (MGL2/CD301b): efficient uptake and presentation of glycosylated antigens by dendritic cells. *J Biol Chem* 285, 19193-19204.
Dieleman, L.A., Ridwan, B.U., Tennyson, G.S., Beagley, K.W., Bucy, R.P., and Elson, C.O. (1994). Dextran sulfate sodium-induced colitis occurs in severe combined immunodeficient mice. *Gastroenterology* 107, 1643-1652.
Dinnis, D.M., and James, D.C. (2005). Engineering mammalian cell factories for improved recombinant monoclonal antibody production: lessons from nature? *Biotechnol Bioeng* 91, 180-189.
Dooms, H., and Abbas, A.K. (2006). Control of CD4+ T-cell memory by cytokines and costimulators. *Immunol Rev* 211, 23-38.
Drake, C.G., Jaffee, E., and Pardoll, D.M. (2006). Mechanisms of immune evasion by tumors. *Adv Immunol* 90, 51-81.
Drickamer, K. (1999). C-type lectin-like domains. *Curr Opin Struct Biol* 9, 585-590.
Dudziak, D., Kamphorst, A.O., Heidkamp, G.F., Buchholz, V.R., Trumpfheller, C., Yamazaki, S., Cheong, C., Liu, K., Lee, H.W., Park, C.G., *et al.* (2007). Differential antigen processing by dendritic cell subsets in vivo. *Science* 315, 107-111.
Duverger, E., Lamerant-Fayel, N., Frison, N., and Monsigny, M. (2010). Carbohydrate-lectin interactions assayed by SPR. *Methods Mol Biol* 627, 157-178.
El-Charabaty, E., Geara, A.S., Ting, C., El-Sayegh, S., and Azzi, J. (2012). Belatacept: a new era of immunosuppression? *Expert Rev Clin Immunol* 8, 527-536.
Engel, M.A., and Neurath, M.F. (2010). New pathophysiological insights and modern treatment of IBD. *J Gastroenterol* 45, 571-583.
Eriksson, M., Johannssen, T., Smolinski, D.v., Gruber, A.D., Seeberger, P.H., and Lepenies, B. (2013). The C-type lectin receptor SIGNR3 binds to fungi present in commensal microbiota and influences immune regulation in experimental colitis. *Front Immunol, In press*.
Feinberg, H., Taylor, M.E., Razi, N., McBride, R., Knirel, Y.A., Graham, S.A., Drickamer, K., and Weis, W.I. (2011). Structural basis for langerin recognition of diverse pathogen and mammalian glycans through a single binding site. *J Mol Biol* 405, 1027-1039.
Fujikado, N., Saijo, S., Yonezawa, T., Shimamori, K., Ishii, A., Sugai, S., Kotaki, H., Sudo, K., Nose, M., and Iwakura, Y. (2008). Dcir deficiency causes development of autoimmune diseases in mice due to excess expansion of dendritic cells. *Nat Med* 14, 176-180.
Gad, M., Jensen, T., Gagne, R., Komba, S., Daugaard, S., Kroman, N., Meldal, M., and Werdelin, O. (2003). MUC1-derived glycopeptide libraries with improved MHC anchors are strong antigens and prime mouse T cells for proliferative responses to lysates of human breast cancer tissue. *Eur J Immunol* 33, 1624-1632.

Galli-Stampino, L., Meinjohanns, E., Frische, K., Meldal, M., Jensen, T., Werdelin, O., and Mouritsen, S. (1997). T-cell recognition of tumor-associated carbohydrates: the nature of the glycan moiety plays a decisive role in determining glycopeptide immunogenicity. *Cancer Res* 57, 3214-3222.
Galustian, C., Park, C.G., Chai, W., Kiso, M., Bruening, S.A., Kang, Y.S., Steinman, R.M., and Feizi, T. (2004). High and low affinity carbohydrate ligands revealed for murine SIGN-R1 by carbohydrate array and cell binding approaches, and differing specificities for SIGN-R3 and langerin. *Int Immunol* 16, 853-866.
Gascoigne, N.R., Goodnow, C.C., Dudzik, K.I., Oi, V.T., and Davis, M.M. (1987). Secretion of a chimeric T-cell receptor-immunoglobulin protein. *Proc Natl Acad Sci U S A* 84, 2936-2940.
Grunstein, D., Maglinao, M., Kikkeri, R., Collot, M., Barylyuk, K., Lepenies, B., Kamena, F., Zenobi, R., and Seeberger, P.H. (2011). Hexameric supramolecular scaffold orients carbohydrates to sense bacteria. *J Am Chem Soc* 133, 13957-13966.
Guo, J.P., Brummet, M.E., Myers, A.C., Na, H.J., Rowland, E., Schnaar, R.L., Zheng, T., Zhu, Z., and Bochner, B.S. (2011). Characterization of expression of glycan ligands for Siglec-F in normal mouse lungs. *Am J Respir Cell Mol Biol* 44, 238-243.
Hagemeyer, C.E., von Zur Muhlen, C., von Elverfeldt, D., and Peter, K. (2009). Single-chain antibodies as diagnostic tools and therapeutic agents. *Thromb Haemost* 101, 1012-1019.
Hanashima, S., Castagner, B., Esposito, D., Nokami, T., and Seeberger, P.H. (2007). Synthesis of a sialic acid alpha(2-3) galactose building block and its use in a linear synthesis of sialyl Lewis X. *Org Lett* 9, 1777-1779.
Hardison, S.E., and Brown, G.D. (2012). C-type lectin receptors orchestrate antifungal immunity. *Nat Immunol* 13, 817-822.
Hart, A.L., Al-Hassi, H.O., Rigby, R.J., Bell, S.J., Emmanuel, A.V., Knight, S.C., Kamm, M.A., and Stagg, A.J. (2005). Characteristics of intestinal dendritic cells in inflammatory bowel diseases. *Gastroenterology* 129, 50-65.
Heimburg-Molinaro, J., Lum, M., Vijay, G., Jain, M., Almogren, A., and Rittenhouse-Olson, K. (2011). Cancer vaccines and carbohydrate epitopes. *Vaccine* 29, 8802-8826.
Heinsbroek, S.E., Oei, A., Roelofs, J.J., Dhawan, S., Te Velde, A., Gordon, S., and de Jonge, W.J. (2012). Genetic deletion of dectin-1 does not affect the course of murine experimental colitis. *BMC Gastroenterol* 12, 33.
Higashi, N., Fujioka, K., Denda-Nagai, K., Hashimoto, S., Nagai, S., Sato, T., Fujita, Y., Morikawa, A., Tsuiji, M., Miyata-Takeuchi, M., *et al.* (2002). The macrophage C-type lectin specific for galactose/N-acetylgalactosamine is an endocytic receptor expressed on monocyte-derived immature dendritic cells. *J Biol Chem* 277, 20686-20693.
Higgins, L.M., McDonald, S.A., Whittle, N., Crockett, N., Shields, J.G., and MacDonald, T.T. (1999). Regulation of T cell activation in vitro and in vivo by targeting the OX40-OX40 ligand interaction: amelioration of ongoing inflammatory bowel disease with an OX40-IgG fusion protein, but not with an OX40 ligand-IgG fusion protein. *J Immunol* 162, 486-493.
Hoffmann, S.C., Schellack, C., Textor, S., Konold, S., Schmitz, D., Cerwenka, A., Pflanz, S., and Watzl, C. (2007). Identification of CLEC12B, an inhibitory receptor on myeloid cells. *J Biol Chem* 282, 22370-22375.
Hollenbaugh, D., and Aruffo, A. (2002). Construction of immunoglobulin fusion proteins. *Curr Protoc Immunol* Chapter 10, Unit 10 19A.
Hooper, L.V., Littman, D.R., and Macpherson, A.J. (2012). Interactions between the microbiota and the immune system. *Science* 336, 1268-1273.

Horlacher, T., Oberli, M.A., Werz, D.B., Krock, L., Bufali, S., Mishra, R., Sobek, J., Simons, K., Hirashima, M., Niki, T., and Seeberger, P.H. (2010). Determination of carbohydrate-binding preferences of human galectins with carbohydrate microarrays. *Chembiochem* 11, 1563-1573.
Hoshikawa, H., Sawamura, T., Kakutani, M., Aoyama, T., Nakamura, T., and Masaki, T. (1998). High affinity binding of oxidized LDL to mouse lectin-like oxidized LDL receptor (LOX-1). *Biochem Biophys Res Commun* 245, 841-846.
Hovius, J.W., de Jong, M.A., den Dunnen, J., Litjens, M., Fikrig, E., van der Poll, T., Gringhuis, S.I., and Geijtenbeek, T.B. (2008). Salp15 binding to DC-SIGN inhibits cytokine expression by impairing both nucleosome remodeling and mRNA stabilization. *PLoS Pathog* 4, e31.
Hsu, T.L., Cheng, S.C., Yang, W.B., Chin, S.W., Chen, B.H., Huang, M.T., Hsieh, S.L., and Wong, C.H. (2009). Profiling carbohydrate-receptor interaction with recombinant innate immunity receptor-Fc fusion proteins. *J Biol Chem* 284, 34479-34489.
Huang, H., Ostroff, G.R., Lee, C.K., Specht, C.A., and Levitz, S.M. (2010). Robust stimulation of humoral and cellular immune responses following vaccination with antigen-loaded beta-glucan particles. *MBio* 20, 1 e00164-10.
Ichii, S., Imai, Y., and Irimura, T. (1997). Tumor site-selective localization of an adoptively transferred T cell line expressing a macrophage lectin. *J Leukoc Biol* 62, 761-770.
Ichii, S., Imai, Y., and Irimura, T. (2000). Initial steps in lymph node metastasis formation in an experimental system: possible involvement of recognition by macrophage C-type lectins. *Cancer Immunol Immunother* 49, 1-9.
Iliev, I.D., Funari, V.A., Taylor, K.D., Nguyen, Q., Reyes, C.N., Strom, S.P., Brown, J., Becker, C.A., Fleshner, P.R., Dubinsky, M., *et al.* (2012). Interactions between commensal fungi and the C-type lectin receptor Dectin-1 influence colitis. *Science* 336, 1314-1317.
Inohara, N., Ogura, Y., Chen, F.F., Muto, A., and Nunez, G. (2001). Human Nod1 confers responsiveness to bacterial lipopolysaccharides. *J Biol Chem* 276, 2551-2554.
Ishioka, G.Y., Lamont, A.G., Thomson, D., Bulbow, N., Gaeta, F.C., Sette, A., and Grey, H.M. (1992). MHC interaction and T cell recognition of carbohydrates and glycopeptides. *J Immunol* 148, 2446-2451.
Jawhara, S., Thuru, X., Standaert-Vitse, A., Jouault, T., Mordon, S., Sendid, B., Desreumaux, P., and Poulain, D. (2008). Colonization of mice by Candida albicans is promoted by chemically induced colitis and augments inflammatory responses through galectin-3. *J Infect Dis* 197, 972-980.
Joffre, O., Nolte, M.A., Sporri, R., and Reis e Sousa, C. (2009). Inflammatory signals in dendritic cell activation and the induction of adaptive immunity. *Immunol Rev* 227, 234-247.
Joffre, O.P., Sancho, D., Zelenay, S., Keller, A.M., and Reis e Sousa, C. (2010). Efficient and versatile manipulation of the peripheral CD4+ T-cell compartment by antigen targeting to DNGR-1/CLEC9A. *Eur J Immunol* 40, 1255-1265.
Johansson, M.E., Ambort, D., Pelaseyed, T., Schutte, A., Gustafsson, J.K., Ermund, A., Subramani, D.B., Holmen-Larsson, J.M., Thomsson, K.A., Bergstrom, J.H., *et al.* (2011). Composition and functional role of the mucus layers in the intestine. *Cell Mol Life Sci* 68, 3635-3641.
Johansson, M.E., Gustafsson, J.K., Sjoberg, K.E., Petersson, J., Holm, L., Sjovall, H., and Hansson, G.C. (2010). Bacteria penetrate the inner mucus layer before inflammation in the dextran sulfate colitis model. *PLoS One* 5, e12238.

Kapsenberg, M.L. (2003). Dendritic-cell control of pathogen-driven T-cell polarization. *Nat Rev Immunol* 3, 984-993.
Khader, S.A., Bell, G.K., Pearl, J.E., Fountain, J.J., Rangel-Moreno, J., Cilley, G.E., Shen, F., Eaton, S.M., Gaffen, S.L., Swain, S.L., *et al.* (2007). IL-23 and IL-17 in the establishment of protective pulmonary CD4+ T cell responses after vaccination and during Mycobacterium tuberculosis challenge. *Nat Immunol* 8, 369-377.
Khazaeli, M.B., Conry, R.M., and LoBuglio, A.F. (1994). Human immune response to monoclonal antibodies. *J Immunother Emphasis Tumor Immunol* 15, 42-52.
Ko, A.I., Drager, U.C., and Harn, D.A. (1990). A Schistosoma mansoni epitope recognized by a protective monoclonal antibody is identical to the stage-specific embryonic antigen 1. *Proc Natl Acad Sci U S A* 87, 4159-4163.
Kolarich, D., Jensen, P.H., Altmann, F., and Packer, N.H. (2012). Determination of site-specific glycan heterogeneity on glycoproteins. *Nat Protoc* 7, 1285-1298.
Kropshofer, H., Vogt, A.B., Moldenhauer, G., Hammer, J., Blum, J.S., and Hammerling, G.J. (1996). Editing of the HLA-DR-peptide repertoire by HLA-DM. *Embo J* 15, 6144-6154.
Lahoud, M.H., Ahmet, F., Kitsoulis, S., Wan, S.S., Vremec, D., Lee, C.N., Phipson, B., Shi, W., Smyth, G.K., Lew, A.M., *et al.* (2011). Targeting antigen to mouse dendritic cells via Clec9A induces potent CD4 T cell responses biased toward a follicular helper phenotype. *J Immunol* 187, 842-850.
Lee, R.T., Hsu, T.L., Huang, S.K., Hsieh, S.L., Wong, C.H., and Lee, Y.C. (2011). Survey of immune-related, mannose/fucose-binding C-type lectin receptors reveals widely divergent sugar-binding specificities. *Glycobiology* 21, 512-520.
Lefevre, L., Lugo-Villarino, G., Meunier, E., Valentin, A., Olagnier, D., Authier, H., Duval, C., Dardenne, C., Bernad, J., Lemesre, J.L., *et al.* (2013). The C-type Lectin Receptors Dectin-1, MR, and SIGNR3 Contribute Both Positively and Negatively to the Macrophage Response to Leishmania infantum. *Immunity* 38, 1038-1049.
Lemischka, I.R., Raulet, D.H., and Mulligan, R.C. (1986). Developmental potential and dynamic behavior of hematopoietic stem cells. *Cell* 45, 917-927.
Lenschow, D.J., Ho, S.C., Sattar, H., Rhee, L., Gray, G., Nabavi, N., Herold, K.C., and Bluestone, J.A. (1995). Differential effects of anti-B7-1 and anti-B7-2 monoclonal antibody treatment on the development of diabetes in the nonobese diabetic mouse. *J Exp Med* 181, 1145-1155.
Lepenies, B. (2007). Funktion der Koinhibitoren CTLA-4 und BTLA bei der T-Zellregulation im Verlauf der Blutphase der experimentellen Malaria, PhD thesis, Department of Biology, University of Hamburg.
Lepenies, B., Lee, J., and Sonkaria, S. (2013). Targeting C-type lectin receptors with multivalent carbohydrate ligands. *Ad. DrugDelivRev.* doi: 10.1016/j.addr.2013.05.007
Ley, R.E., Peterson, D.A., and Gordon, J.I. (2006). Ecological and evolutionary forces shaping microbial diversity in the human intestine. *Cell* 124, 837-848.
Loftus, E.V., Jr. (2004). Clinical epidemiology of inflammatory bowel disease: Incidence, prevalence, and environmental influences. *Gastroenterology* 126, 1504-1517.
Lutz, M.B. (2012). Therapeutic potential of semi-mature dendritic cells for tolerance induction. *Front Immunol* 3, 123.
Macho Fernandez, E., Valenti, V., Rockel, C., Hermann, C., Pot, B., Boneca, I.G., and Grangette, C. (2011). Anti-inflammatory capacity of selected lactobacilli in experimental colitis is driven by NOD2-mediated recognition of a specific peptidoglycan-derived muropeptide. *Gut* 60, 1050-1059.

Macpherson, A.J., and Uhr, T. (2004). Induction of protective IgA by intestinal dendritic cells carrying commensal bacteria. *Science* 303, 1662-1665.
Maglinao, M. (2013). C-type Lectin Receptors in Cell-specific Targeting and Malaria Infection, PhD-thesis, Department of Biology, Chemistry, and Pharmacy, Freie Universität Berlin.
Majeau, G.R., Whitty, A., Yim, K., Meier, W., and Hochman, P.S. (1999). Low affinity binding of an LFA-3/IgG1 fusion protein to CD2+ T cells is independent of cell activation. *Cell Adhes Commun* 7, 267-279.
Mattson, G., Conklin, E., Desai, S., Nielander, G., Savage, M.D., and Morgensen, S. (1993). A practical approach to crosslinking. *Mol Biol Rep* 17, 167-183.
Mayer, L., and Shao, L. (2004). Therapeutic potential of oral tolerance. *Nat Rev Immunol* 4, 407-419.
Medzhitov, R. (2001). Toll-like receptors and innate immunity. *Nat Rev Immunol* 1, 135-145.
Mizuochi, S., Akimoto, Y., Imai, Y., Hirano, H., and Irimura, T. (1998). Immunohistochemical study on a macrophage calcium-type lectin in mouse embryos: transient expression in chondroblasts during endochondral ossification. *Glycoconj J* 15, 397-404.
Mocsai, A., Ruland, J., and Tybulewicz, V.L. (2010). The SYK tyrosine kinase: a crucial player in diverse biological functions. *Nat Rev Immunol* 10, 387-402.
Monks, C.R., Freiberg, B.A., Kupfer, H., Sciaky, N., and Kupfer, A. (1998). Three-dimensional segregation of supramolecular activation clusters in T cells. *Nature* 395, 82-86.
Mowat, A.M. (2003). Anatomical basis of tolerance and immunity to intestinal antigens. *Nat Rev Immunol* 3, 331-341.
Mukherjee, S., Partch, C.L., Lehotzky, R.E., Whitham, C.V., Chu, H., Bevins, C.L., Gardner, K.H., and Hooper, L.V. (2009). Regulation of C-type lectin antimicrobial activity by a flexible N-terminal prosegment. *J Biol Chem* 284, 4881-4888.
Müller, S., Schaffer, T., Flogerzi, B., Seibold-Schmid, B., Schnider, J., Takahashi, K., Darfeuille-Michaud, A., Vazeille, E., Schoepfer, A.M., and Seibold, F. (2010). Mannan-binding lectin deficiency results in unusual antibody production and excessive experimental colitis in response to mannose-expressing mild gut pathogens. *Gut* 59, 1493-1500.
Muramatsu, T., and Muramatsu, H. (2004). Carbohydrate antigens expressed on stem cells and early embryonic cells. *Glycoconj J* 21, 41-45.
Nagaoka, K., Takahara, K., Minamino, K., Takeda, T., Yoshida, Y., and Inaba, K. (2010). Expression of C-type lectin, SIGNR3, on subsets of dendritic cells, macrophages, and monocytes. *J Leukoc Biol* 88, 913-924.
Napoletano, C., Zizzari, I.G., Rughetti, A., Rahimi, H., Irimura, T., Clausen, H., Wandall, H.H., Belleudi, F., Bellati, F., Pierelli, L., *et al.* (2012). Targeting of macrophage galactose-type C-type lectin (MGL) induces DC signaling and activation. *Eur J Immunol* 42, 936-945.
Neurath, M.F., Fuss, I., Pasparakis, M., Alexopoulou, L., Haralambous, S., Meyer zum Buschenfelde, K.H., Strober, W., and Kollias, G. (1997). Predominant pathogenic role of tumor necrosis factor in experimental colitis in mice. *Eur J Immunol* 27, 1743-1750.
Ng, S.C., Benjamin, J.L., McCarthy, N.E., Hedin, C.R., Koutsoumpas, A., Plamondon, S., Price, C.L., Hart, A.L., Kamm, M.A., Forbes, A., *et al.* (2011). Relationship between human intestinal dendritic cells, gut microbiota, and disease activity in Crohn's disease. *Inflamm Bowel Dis* 17, 2027-2037.
O'Shea, J.J., and Paul, W.E. (2010). Mechanisms underlying lineage commitment and plasticity of helper CD4+ T cells. *Science* 327, 1098-1102.

Ogura, Y., Bonen, D.K., Inohara, N., Nicolae, D.L., Chen, F.F., Ramos, R., Britton, H., Moran, T., Karaliuskas, R., Duerr, R.H., *et al.* (2001). A frameshift mutation in NOD2 associated with susceptibility to Crohn's disease. *Nature* 411, 603-606.
Olie, R.A., Fenderson, B., Daley, K., Oosterhuis, J.W., Murphy, J., and Looijenga, L.H. (1996). Glycolipids of human primary testicular germ cell tumours. *Br J Cancer* 74, 133-140.
Orr, S.L., Le, D., Long, J.M., Sobieszczuk, P., Ma, B., Tian, H., Fang, X., Paulson, J.C., Marth, J.D., and Varki, N. (2012). A phenotype survey of thirty-six mutant mouse strains with gene targeted defects in glycosyltransferases or glycan-binding proteins. *Glycobiology* 23, 363-80.
Ott, S.J., Kuhbacher, T., Musfeldt, M., Rosenstiel, P., Hellmig, S., Rehman, A., Drews, O., Weichert, W., Timmis, K.N., and Schreiber, S. (2008). Fungi and inflammatory bowel diseases: Alterations of composition and diversity. *Scand J Gastroenterol* 43, 831-841.
Park, C.G., Takahara, K., Umemoto, E., Yashima, Y., Matsubara, K., Matsuda, Y., Clausen, B.E., Inaba, K., and Steinman, R.M. (2001). Five mouse homologues of the human dendritic cell C-type lectin, DC-SIGN. *Int Immunol* 13, 1283-1290.
Pope, L.M., and Cole, G.T. (1982). Comparative studies of gastrointestinal colonization and systemic spread by Candida albicans and nonlethal yeast in the infant mouse. *Scan Electron Microsc*, 1667-1676.
Powlesland, A.S., Ward, E.M., Sadhu, S.K., Guo, Y., Taylor, M.E., and Drickamer, K. (2006). Widely divergent biochemical properties of the complete set of mouse DC-SIGN-related proteins. *J Biol Chem* 281, 20440-20449.
Powrie, F., Leach, M.W., Mauze, S., Caddle, L.B., and Coffman, R.L. (1993). Phenotypically distinct subsets of CD4+ T cells induce or protect from chronic intestinal inflammation in C. B-17 scid mice. *Int Immunol* 5, 1461-1471.
Puck, T.T., Cieciura, S.J., and Robinson, A. (1958). Genetics of somatic mammalian cells. III. Long-term cultivation of euploid cells from human and animal subjects. *J Exp Med* 108, 945-956.
Rakoff-Nahoum, S., Paglino, J., Eslami-Varzaneh, F., Edberg, S., and Medzhitov, R. (2004). Recognition of commensal microflora by toll-like receptors is required for intestinal homeostasis. *Cell* 118, 229-241.
Reyes, A., Haynes, M., Hanson, N., Angly, F.E., Heath, A.C., Rohwer, F., and Gordon, J.I. (2010). Viruses in the faecal microbiota of monozygotic twins and their mothers. *Nature* 466, 334-338.
Richard, M., Thibault, N., Veilleux, P., Gareau-Page, G., and Beaulieu, A.D. (2006). Granulocyte macrophage-colony stimulating factor reduces the affinity of SHP-2 for the ITIM of CLECSF6 in neutrophils: a new mechanism of action for SHP-2. *Mol Immunol* 43, 1716-1721.
Robertson, J.M., Jensen, P.E., and Evavold, B.D. (2000). DO11.10 and OT-II T cells recognize a C-terminal ovalbumin 323-339 epitope. *J Immunol* 164, 4706-4712.
Rozen, S., and Skaletsky, H.J. (2000). Primer3 on the WWW for general users and for biologist programmers. In Bioinformatics Methods and Protocols: Methods in Molecular Biology. (Totowa, NJ: Humana Press), pp. 365-386.
Rubino, S.J., Selvanantham, T., Girardin, S.E., and Philpott, D.J. (2012b). Nod-like receptors in the control of intestinal inflammation. *Curr Opin Immunol* 24, 398-404.
Saba, K., Denda-Nagai, K., and Irimura, T. (2009). A C-type lectin MGL1/CD301a plays an anti-inflammatory role in murine experimental colitis. *Am J Pathol* 174, 144-152.
Saleh, M., and Trinchieri, G. (2011). Innate immune mechanisms of colitis and colitis-associated colorectal cancer. *Nat Rev Immunol* 11, 9-20.

Sancho, D., Joffre, O.P., Keller, A.M., Rogers, N.C., Martinez, D., Hernanz-Falcon, P., Rosewell, I., and Reis e Sousa, C. (2009). Identification of a dendritic cell receptor that couples sensing of necrosis to immunity. *Nature* 458, 899-903.
Sancho, D., and Reis e Sousa, C. (2012). Signaling by myeloid C-type lectin receptors in immunity and homeostasis. *Annu Rev Immunol* 30, 491-529.
Sartor, R.B. (2006). Mechanisms of disease: pathogenesis of Crohn's disease and ulcerative colitis. *Nat Clin Pract Gastroenterol Hepatol* 3, 390-407.
Sato, M., Kawakami, K., Osawa, T., and Toyoshima, S. (1992). Molecular cloning and expression of cDNA encoding a galactose/N-acetylgalactosamine-specific lectin on mouse tumoricidal macrophages. *J Biochem* 111, 331-336.
Saunders, S.P., Barlow, J.L., Walsh, C.M., Bellsoi, A., Smith, P., McKenzie, A.N., and Fallon, P.G. (2010). C-type lectin SIGN-R1 has a role in experimental colitis and responsiveness to lipopolysaccharide. *J Immunol* 184, 2627-2637.
Schlegel, M.K., Hütter, J., Eriksson, M., Lepenies, B., and Seeberger, P.H. (2011). Defined presentation of carbohydrates on a duplex DNA scaffold. *Chembiochem* 12, 2791-2800.
Schoenen, H., Bodendorfer, B., Hitchens, K., Manzanero, S., Werninghaus, K., Nimmerjahn, F., Agger, E.M., Stenger, S., Andersen, P., Ruland, J., *et al.* (2010). Cutting edge: Mincle is essential for recognition and adjuvanticity of the mycobacterial cord factor and its synthetic analog trehalose-dibehenate. *J Immunol* 184, 2756-2760.
Sharma, S., Sundararajan, A., Suryawanshi, A., Kumar, N., Veiga-Parga, T., Kuchroo, V.K., Thomas, P.G., Sangster, M.Y., and Rouse, B.T. (2011). T cell immunoglobulin and mucin protein-3 (Tim-3)/Galectin-9 interaction regulates influenza A virus-specific humoral and CD8 T-cell responses. *Proc Natl Acad Sci U S A* 108, 19001-19006.
Singh, S.K., Streng-Ouwehand, I., Litjens, M., Kalay, H., Saeland, E., and van Kooyk, Y. (2011). Tumour-associated glycan modifications of antigen enhance MGL2 dependent uptake and MHC class I restricted CD8 T cell responses. *Int J Cancer* 128, 1371-1383.
Singh, S.K., Streng-Ouwehand, I., Litjens, M., Weelij, D.R., Garcia-Vallejo, J.J., van Vliet, S.J., Saeland, E., and van Kooyk, Y. (2009). Characterization of murine MGL1 and MGL2 C-type lectins: distinct glycan specificities and tumor binding properties. *Mol Immunol* 46, 1240-1249.
Strober, W., Kitani, A., Fuss, I., Asano, N., and Watanabe, T. (2008). The molecular basis of NOD2 susceptibility mutations in Crohn's disease. *Mucosal Immunol* 1 Suppl 1, S5-9.
Sutton, C.L., Yang, H., Li, Z., Rotter, J.I., Targan, S.R., and Braun, J. (2000). Familial expression of anti-Saccharomyces cerevisiae mannan antibodies in affected and unaffected relatives of patients with Crohn's disease. *Gut* 46, 58-63.
Suzuki, N., Yamamoto, K., Toyoshima, S., Osawa, T., and Irimura, T. (1996). Molecular cloning and expression of cDNA encoding human macrophage C-type lectin. Its unique carbohydrate binding specificity for Tn antigen. *J Immunol* 156, 128-135.
Takahara, K., Yashima, Y., Omatsu, Y., Yoshida, H., Kimura, Y., Kang, Y.S., Steinman, R.M., Park, C.G., and Inaba, K. (2004). Functional comparison of the mouse DC-SIGN, SIGNR1, SIGNR3 and Langerin, C-type lectins. *Int Immunol* 16, 819-829.
Takeuchi, O., and Akira, S. (2010). Pattern recognition receptors and inflammation. *Cell* 140, 805-820.
Tanne, A., Ma, B., Boudou, F., Tailleux, L., Botella, H., Badell, E., Levillain, F., Taylor, M.E., Drickamer, K., Nigou, J., *et al.* (2009). A murine DC-SIGN homologue contributes to early host defense against Mycobacterium tuberculosis. *J Exp Med* 206, 2205-2220.

Tanne, A., and Neyrolles, O. (2010). C-type lectins in immune defense against pathogens: the murine DC-SIGN homologue SIGNR3 confers early protection against Mycobacterium tuberculosis infection. *Virulence* 1, 285-290.
Tewari, K., Flynn, B.J., Boscardin, S.B., Kastenmueller, K., Salazar, A.M., Anderson, C.A., Soundarapandian, V., Ahumada, A., Keler, T., Hoffman, S.L., *et al.* (2010). Poly(I:C) is an effective adjuvant for antibody and multi-functional CD4+ T cell responses to Plasmodium falciparum circumsporozoite protein (CSP) and alphaDEC-CSP in non human primates. *Vaccine* 28, 7256-7266.
Tsuiji, M., Fujimori, M., Ohashi, Y., Higashi, N., Onami, T.M., Hedrick, S.M., and Irimura, T. (2002). Molecular cloning and characterization of a novel mouse macrophage C-type lectin, mMGL2, which has a distinct carbohydrate specificity from mMGL1. *J Biol Chem* 277, 28892-28901.
Unger, W.W., van Beelen, A.J., Bruijns, S.C., Joshi, M., Fehres, C.M., van Bloois, L., Verstege, M.I., Ambrosini, M., Kalay, H., Nazmi, K., *et al.* (2012). Glycan-modified liposomes boost CD4+ and CD8+ T-cell responses by targeting DC-SIGN on dendritic cells. *J Control Release* 160, 88-95.
van Kooyk, Y. (2008). C-type lectins on dendritic cells: key modulators for the induction of immune responses. *Biochem Soc Trans* 36, 1478-1481.
van Kooyk, Y., Unger, W.W., Fehres, C.M., Kalay, H., and Garcia-Vallejo, J.J. (2013). Glycan-based DC-SIGN targeting vaccines to enhance antigen cross-presentation. *Mol Immunol* 55, 143-145.
van Sorge, N.M., Bleumink, N.M., van Vliet, S.J., Saeland, E., van der Pol, W.L., van Kooyk, Y., and van Putten, J.P. (2009). N-glycosylated proteins and distinct lipooligosaccharide glycoforms of Campylobacter jejuni target the human C-type lectin receptor MGL. *Cell Microbiol* 11, 1768-1781.
van Vliet, S.J., Gringhuis, S.I., Geijtenbeek, T.B., and van Kooyk, Y. (2006a). Regulation of effector T cells by antigen-presenting cells via interaction of the C-type lectin MGL with CD45. *Nat Immunol* 7, 1200-1208.
van Vliet, S.J., Saeland, E., and van Kooyk, Y. (2008). Sweet preferences of MGL: carbohydrate specificity and function. *Trends Immunol* 29, 83-90.
van Vliet, S.J., van Liempt, E., Geijtenbeek, T.B., and van Kooyk, Y. (2006b). Differential regulation of C-type lectin expression on tolerogenic dendritic cell subsets. *Immunobiology* 211, 577-585.
van Vliet, S.J., van Liempt, E., Saeland, E., Aarnoudse, C.A., Appelmelk, B., Irimura, T., Geijtenbeek, T.B., Blixt, O., Alvarez, R., van Die, I., and van Kooyk, Y. (2005). Carbohydrate profiling reveals a distinctive role for the C-type lectin MGL in the recognition of helminth parasites and tumor antigens by dendritic cells. *Int Immunol* 17, 661-669.
Vazquez-Mendoza, A., Carrero, J.C., and Rodriguez-Sosa, M. (2013). Parasitic infections: a role for C-type lectins receptors. *Biomed Res Int* 2013, 456352.
Velupillai, P., dos Reis, E.A., dos Reis, M.G., and Harn, D.A. (2000). Lewis(x)-containing oligosaccharide attenuates schistosome egg antigen-induced immune depression in human schistosomiasis. *Hum Immunol* 61, 225-232.
Vignali, D.A., Collison, L.W., and Workman, C.J. (2008). How regulatory T cells work. *Nat Rev Immunol* 8, 523-532.
Walker, L.J., Aldhous, M.C., Drummond, H.E., Smith, B.R., Nimmo, E.R., Arnott, I.D., and Satsangi, J. (2004). Anti-Saccharomyces cerevisiae antibodies (ASCA) in Crohn's disease are

associated with disease severity but not NOD2/CARD15 mutations. *Clin Exp Immunol* 135, 490-496.
Watanabe, T., Kitani, A., Murray, P.J., and Strober, W. (2004). NOD2 is a negative regulator of Toll-like receptor 2-mediated T helper type 1 responses. *Nat Immunol* 5, 800-808.
Watanabe, T., Kitani, A., Murray, P.J., Wakatsuki, Y., Fuss, I.J., and Strober, W. (2006). Nucleotide binding oligomerization domain 2 deficiency leads to dysregulated TLR2 signaling and induction of antigen-specific colitis. *Immunity* 25, 473-485.
Werninghaus, K., Babiak, A., Gross, O., Holscher, C., Dietrich, H., Agger, E.M., Mages, J., Mocsai, A., Schoenen, H., Finger, K., *et al.* (2009). Adjuvanticity of a synthetic cord factor analogue for subunit Mycobacterium tuberculosis vaccination requires FcRgamma-Syk-Card9-dependent innate immune activation. *J Exp Med* 206, 89-97.
Werz, D.B., Castagner, B., and Seeberger, P.H. (2007). Automated synthesis of the tumor-associated carbohydrate antigens Gb-3 and Globo-H: incorporation of alpha-galactosidic linkages. *J Am Chem Soc* 129, 2770-2771.
Wirtz, S., Neufert, C., Weigmann, B., and Neurath, M.F. (2007). Chemically induced mouse models of intestinal inflammation. *Nat Protoc* 2, 541-546.
Wong, S.B., Bos, R., and Sherman, L.A. (2008). Tumor-specific CD4+ T cells render the tumor environment permissive for infiltration by low-avidity CD8+ T cells. *J Immunol* 180, 3122-3131.
Yin, J., and Seeberger, P.H. (2010). Applications of heparin and heparan sulfate microarrays. *Methods Enzymol* 478, 197-218.
Yuita, H., Tsuiji, M., Tajika, Y., Matsumoto, Y., Hirano, K., Suzuki, N., and Irimura, T. (2005). Retardation of removal of radiation-induced apoptotic cells in developing neural tubes in macrophage galactose-type C-type lectin-1-deficient mouse embryos. *Glycobiology* 15, 1368-1375.
Zelenay, S., Keller, A.M., Whitney, P.G., Schraml, B.U., Deddouche, S., Rogers, N.C., Schulz, O., Sancho, D., and Reis e Sousa, C. (2012). The dendritic cell receptor DNGR-1 controls endocytic handling of necrotic cell antigens to favor cross-priming of CTLs in virus-infected mice. *J Clin Invest* 122, 1615-1627.
Zelensky, A.N., and Gready, J.E. (2005). The C-type lectin-like domain superfamily. *Febs J* 272, 6179-6217.
Zhang, J.G., Czabotar, P.E., Policheni, A.N., Caminschi, I., Wan, S.S., Kitsoulis, S., Tullett, K.M., Robin, A.Y., Brammananth, R., van Delft, M.F., *et al.* (2012). The dendritic cell receptor Clec9A binds damaged cells via exposed actin filaments. *Immunity* 36, 646-657.
Zou, W. (2006). Regulatory T cells, tumour immunity and immunotherapy. *Nat Rev Immunol* 6, 295-307.

LIST OF PUBLICATIONS

Schlegel MK, Hütter J, **Eriksson M**, Lepenies B, Seeberger PH, Defined Presentation of Carbohydrates on a Duplex DNA Scaffold, *Chembiochem*, 2011, Dec 16:12(18):2791-800

Eriksson M, Johannssen T, von Smolinski D, Gruber AD, Seeberger PH, Lepenies B, The C-type lectin receptor SIGNR3 binds to fungi present in commensal microbiota and influences immune regulation in experimental colitis. *Front Immunol*, *In press*.

Eriksson M*, Maglinao M*, Schlegel MK, Seeberger PH, Lepenies B, A Novel Platform to Screen for Immune Modulatory Properties of C-type Lectin Receptor Binding Carbohydrates, *In preparation.*

Eriksson M*, Maglinao M*, Serna S, Schlegel MK, Seeberger PH, Reichardt NC, Lepenies B, Biological Evaluation of Multivalent Lewis X MGL1 interactions, *In preparation*.

*authors contributed equally

APPENDIX

Gradient conditions for analytic column

Starting conditions for the analytical column were 2% solvent B (acetonitrile with 0.1% formic acid) and the flow rate on the analytical column was held at 5 µl/min throughout the experiment. After desalting the sample on the trap column, a gradient using an increasing solvent B concentration was applied. The gradient conditions were as follows: linear increase of buffer B from 2 to 30% (from 5 min to 61 min), further increase to 60% (61–76 min), followed by a steep increase to 90% (76–77 min). The column was held at 90% B for 5 min (77–82 min) before re-equilibrating the analytical column in 2% solvent B. Meanwhile, the trap column was re-equilibrated in 100% solvent A before injection of the next sample. Peptide trapping and reversed phase separation was performed at a column temperature of 45 °C.

Table A.1 MS operational parameters used in the present investigation

Ionization mode	**Positive mode ESI for (glyco)peptides**
Capillary exit	4500 V
ICC	On
Maximum accumulation time	50 ms
Target	200,000 (MS/MS)
Scan range	400-1500 *m/z* – for MS 100-2500 *m/z* for MS/MS
Isolation window	2.2 *m/z*
MS/MS fragmentation amplitude	60.0 %
Smart fragmentation option	On (start amplitude 30%—end amplitude 200%)

cDNA and amino acid sequences corresponding to the generated CLR-hFc fusion proteins

Sequences are marked in the following colors; IL-2 signal sequence (grey), extracellular region (blue), human Fc part (red) and amino acids linking the extracellular region and the hFc part (green).

MGL1-hFc

```
     1  atg tac agg atg caa ctc ctg tct tgc att gca cta agt ctt gca ctt gtc
          M   Y   R   M   Q   L   L   S   C   I   A   L   S   L   A   L   V
                      EcorV
    52  acg aat tcg ata tcc cag tta agg agg gac cta ggc acc ctg aga gcc act
          T   N   S   I   S   Q   L   R   R   D   L   G   T   L   R   A   T

   103  tta gac aac acc acc tcc aag ata aag gct gaa ttc cag tcc ctg gac tcc
          L   D   N   T   T   S   K   I   K   A   E   F   Q   S   L   D   S

   154  agg gct gac agc ttc gaa aaa ggg atc agt tct ctg aaa gtg gat gtg gag
          R   A   D   S   F   E   K   G   I   S   S   L   K   V   D   V   E

   205  gat cac agg cag gaa ctg cag gca ggc cga gac ttg agc cag aag gtg act
          D   H   R   Q   E   L   Q   A   G   R   D   L   S   Q   K   V   T

   256  tct ctg gag agc aca gtg gag aag agg gag cag gct ctc aaa aca gat ctg
          S   L   E   S   T   V   E   K   R   E   Q   A   L   K   T   D   L

   307  tct gat tta acc gac cat gtg caa cag ctg agg aag gac ttg aag gcc ctg
          S   D   L   T   D   H   V   Q   Q   L   R   K   D   L   K   A   L

   358  acg tgc cag ctg gcc aac ctc aag aac aac ggc tcg gaa gtg gcc tgc tgc
          T   C   Q   L   A   N   L   K   N   N   G   S   E   V   A   C   C

   409  ccg ctt cac tgg acg gag cat gaa ggc agc tgc tat tgg ttc tct gag tct
          P   L   H   W   T   E   H   E   G   S   C   Y   W   F   S   E   S

   460  gag aag tcg tgg cct gaa gct gac aag tac tgc cgg ctg gag aat tct cac
          E   K   S   W   P   E   A   D   K   Y   C   R   L   E   N   S   H

   511  ctg gtg gtg gtc aac tcc ctg gag gag cag aat ttt cta cag aat cgc tta
          L   V   V   V   N   S   L   E   E   Q   N   F   L   Q   N   R   L

   562  gcc aat gtg gtt agt tgg atc ggc cta acg gac caa aac ggg ccc tgg cga
          A   N   V   V   S   W   I   G   L   T   D   Q   N   G   P   W   R

   613  tgg gtg gat ggg acc gac ttt gag aaa ggc ttt aag aac tgg gcc cca ctg
          W   V   D   G   T   D   F   E   K   G   F   K   N   W   A   P   L

   664  cag cca gat aac tgg ttc gga cac gga ctg gga gga ggt gag gac tgt gcc
          Q   P   D   N   W   F   G   H   G   L   G   G   G   E   D   C   A

   715  cac atc act aca ggt ggt ccc tgg aat gat gat gtc tgc cag aga acc ttc
          H   I   T   T   G   G   P   W   N   D   D   V   C   Q   R   T   F
```

NcoI

```
766  cgc tgg atc tgt gag atg aag ctg gcc aag gag agc tcc atg gtt aga tct
       R   W   I   C   E   M   K   L   A   K   E   S   S   M   V   R   S

817  gac aaa act cac aca tgc cca ccg tgc cca gca cct gaa ctc ctg ggg gga
       D   K   T   H   T   C   P   P   C   P   A   P   E   L   L   G   G

868  ccg tca gtc ttc ctc ttc ccc cca aaa ccc aag gac acc ctc atg atc tcc
       P   S   V   F   L   F   P   P   K   P   K   D   T   L   M   I   S

919  cgg acc cct gag gtc aca tgc gtg gtg gtg gac gtg agc cac gaa gac cct
       R   T   P   E   V   T   C   V   V   V   D   V   S   H   E   D   P

970  gag gtc aag ttc aac tgg tac gtg gac ggc gtg gag gtg cat aat gcc aag
       E   V   K   F   N   W   Y   V   D   G   V   E   V   H   N   A   K

1021 aca aag ccg cgg gag gag cag tac aac agc acg tac cgt gtg gtc agc gtc
       T   K   P   R   E   E   Q   Y   N   S   T   Y   R   V   V   S   V

1072 ctc acc gtc ctg cac cag gac tgg ctg aat ggc aag gag tac aag tgc aag
       L   T   V   L   H   Q   D   W   L   N   G   K   E   Y   K   C   K

1123 gtc tcc aac aaa gcc ctc cca gcc ccc atc gag aaa acc atc tcc aaa gcc
       V   S   N   K   A   L   P   A   P   I   E   K   T   I   S   K   A

1174 aaa ggg cag ccc cga gaa cca cag gtg tac acc ctg ccc cca tcc cgg gag
       K   G   Q   P   R   E   P   Q   V   Y   T   L   P   P   S   R   E

1225 gag atg acc aag aac cag gtc agc ctg acc tgc ctg gtc aaa ggc ttc tat
       E   M   T   K   N   Q   V   S   L   T   C   L   V   K   G   F   Y

1276 ccc agc gac atc gcc gtg gag tgg gag agc aat ggg cag ccg gag aac aac
       P   S   D   I   A   V   E   W   E   S   N   G   Q   P   E   N   N

1327 tac aag acc acg cct ccc gtg ctg gac tcc gac ggc tcc ttc ttc ctc tac
       Y   K   T   T   P   P   V   L   D   S   D   G   S   F   F   L   Y

1378 agc aag ctc acc gtg gac aag agc agg tgg cag cag ggg aac gtc ttc tca
       S   K   L   T   V   D   K   S   R   W   Q   Q   G   N   V   F   S

1429 tgc tcc gtg atg cac gag gct ctg cac aac cac tac acg cag aag agc ctc
       C   S   V   M   H   E   A   L   H   N   H   Y   T   Q   K   S   L

1480 tcc ctg tct ccg ggt aaa tga
       S   L   S   P   G   K   -
```

Clec9a-hFc

```
     1  atg tac agg atg caa ctc ctg tct tgc att gca cta agt ctt gca ctt gtc
          M   Y   R   M   Q   L   L   S   C   I   A   L   S   L   A   L   V
              EcorI
    52  acg aat tcc cag gta tcc tct ctt gtc ttg gag cag cag gaa aga ctc atc
          T   N   S   Q   V   S   S   L   V   L   E   Q   Q   E   R   L   I

   103  caa cag gac aca gca ttg gtg aac ctt aca cag tgg cag agg aaa tac aca
          Q   Q   D   T   A   L   V   N   L   T   Q   W   Q   R   K   Y   T

   154  ctg gaa tac tgc caa gcc tta ctg cag aga tct ctc cat tca ggt agt gac
          L   E   Y   C   Q   A   L   L   Q   R   S   L   H   S   G   S   D

   205  tgc agc cct tgt cca cac aac tgg att cag aat gga aaa agt tgt tac tat
          C   S   P   C   P   H   N   W   I   Q   N   G   K   S   C   Y   Y

   256  gtc ttt gaa cgc tgg gaa atg tgg aac atc agt aag aag agc tgt tta aaa
          V   F   E   R   W   E   M   W   N   I   S   K   K   S   C   L   K

   307  gag ggc gct agt ctc ttt caa ata gac agc aaa gaa gaa atg gag ttc atc
          E   G   A   S   L   F   Q   I   D   S   K   E   E   M   E   F   I

   358  agc agt ata ggg aaa ctc aaa gga gga aat aaa tat tgg gtg gga gtg ttt
          S   S   I   G   K   L   K   G   G   N   K   Y   W   V   G   V   F

   409  caa gat gga atc agt gga tct tgg ttc tgg gaa gat ggc tct tct cct ctc
          Q   D   G   I   S   G   S   W   F   W   E   D   G   S   S   P   L

   460  tct gac ttg ttg cca gca gaa aga cag cga tca gcc ggc cag atc tgt gga
          S   D   L   L   P   A   E   R   Q   R   S   A   G   Q   I   C   G

   511  tac ctc aaa gat tct act ctc atc tca gat aag tgc gat agc tgg aaa tat
          Y   L   K   D   S   T   L   I   S   D   K   C   D   S   W   K   Y
                                                          NcoI
   562  ttt atc tgt gag aag aag gca ttt gga tcc tgc atc tcc atg gtt aga tct
          F   I   C   E   K   K   A   F   G   S   C   I   S   M   V   R   S

   613  gac aaa act cac aca tgc cca ccg tgc cca gca cct gaa ctc ctg ggg gga
          D   K   T   H   T   C   P   P   C   P   A   P   E   L   L   G   G

   664  ccg tca gtc ttc ctc ttc ccc cca aaa ccc aag gac acc ctc atg atc tcc
          P   S   V   F   L   F   P   P   K   P   K   D   T   L   M   I   S

   715  cgg acc cct gag gtc aca tgc gtg gtg gtg gac gtg agc cac gaa gac cct
          R   T   P   E   V   T   C   V   V   V   D   V   S   H   E   D   P

   766  gag gtc aag ttc aac tgg tac gtg gac ggc gtg gag gtg cat aat gcc aag
          E   V   K   F   N   W   Y   V   D   G   V   E   V   H   N   A   K

   817  aca aag ccg cgg gag gag cag tac aac agc acg tac cgt gtg gtc agc gtc
          T   K   P   R   E   E   Q   Y   N   S   T   Y   R   V   V   S   V

   868  ctc acc gtc ctg cac cag gac tgg ctg aat ggc aag gag tac aag tgc aag
          L   T   V   L   H   Q   D   W   L   N   G   K   E   Y   K   C   K
```

```
 919  gtc tcc aac aaa gcc ctc cca gcc ccc atc gag aaa acc atc tcc aaa gcc
        V   S   N   K   A   L   P   A   P   I   E   K   T   I   S   K   A

 970  aaa ggg cag ccc cga gaa cca cag gtg tac acc ctg ccc cca tcc cgg gag
        K   G   Q   P   R   E   P   Q   V   Y   T   L   P   P   S   R   E

1021  gag atg acc aag aac cag gtc agc ctg acc tgc ctg gtc aaa ggc ttc tat
        E   M   T   K   N   Q   V   S   L   T   C   L   V   K   G   F   Y

1072  ccc agc gac atc gcc gtg gag tgg gag agc aat ggg cag ccg gag aac aac
        P   S   D   I   A   V   E   W   E   S   N   G   Q   P   E   N   N

1123  tac aag acc acg cct ccc gtg ctg gac tcc gac ggc tcc ttc ttc ctc tac
        Y   K   T   T   P   P   V   L   D   S   D   G   S   F   F   L   Y

1174  agc aag ctc acc gtg gac aag agc agg tgg cag cag ggg aac gtc ttc tca
        S   K   L   T   V   D   K   S   R   W   Q   Q   G   N   V   F   S

1225  tgc tcc gtg atg cac gag gct ctg cac aac cac tac acg cag aag agc ctc
        C   S   V   M   H   E   A   L   H   N   H   Y   T   Q   K   S   L

1276  tcc ctg tct ccg ggt aaa tga
        S   L   S   P   G   K   -
```

SIGNR3-hFc

```
     1  atg tac agg atg caa ctc ctg tct tgc att gca cta agt ctt gca ctt gtc
          M   Y   R   M   Q   L   L   S   C   I   A   L   S   L   A   L   V
              EcorI
    52  acg aat tcc atg caa ctg aag gct gaa gtt cat gat ggc ttg tgc caa ccc
          T   N   S   M   Q   L   K   A   E   V   H   D   G   L   C   Q   P

   103  tgc gcc agg gac tgg aca ttc ttc aat gga agc tgt tac ttc ttc tcc aag
          C   A   R   D   W   T   F   F   N   G   S   C   Y   F   F   S   K

   154  tcc caa aga aat tgg cac aac tcc acc act gcc tgc cag gaa ctg ggg gcc
          S   Q   R   N   W   H   N   S   T   T   A   C   Q   E   L   G   A

   205  caa ctg gtc atc ata gag act gat gag gag cag act ttc ctg cag cag act
          Q   L   V   I   I   E   T   D   E   E   Q   T   F   L   Q   Q   T

   256  tct aag gct aga gga cca acc tgg atg ggt ctc tca gac atg cat aat gaa
          S   K   A   R   G   P   T   W   M   G   L   S   D   M   H   N   E

   307  gcc aca tgg cac tgg gtg gat ggc tca cct ctg tca ccc agc ttt aca cgc
          A   T   W   H   W   V   D   G   S   P   L   S   P   S   F   T   R

   358  tat tgg aat aga ggg gag ccc aac aat gtc ggt gat gaa gat tgt gca gag
          Y   W   N   R   G   E   P   N   N   V   G   D   E   D   C   A   E

   409  ttc tct ggg gat ggc tgg aat gat ctc agt tgt gat aaa cta ctt ttc tgg
          F   S   G   D   G   W   N   D   L   S   C   D   K   L   L   F   W
                                                          BglII
   460  atc tgt aag aaa gtt tca acc tca tca tgc acc acc aaa aga tct gac aaa
          I   C   K   K   V   S   T   S   S   C   T   T   K   R   S   D   K

   511  act cac aca tgc cca ccg tgc cca gca cct gaa ctc ctg ggg gga ccg tca
          T   H   T   C   P   P   C   P   A   P   E   L   L   G   G   P   S

   562  gtc ttc ctc ttc ccc cca aaa ccc aag gac acc ctc atg atc tcc cgg acc
          V   F   L   F   P   P   K   P   K   D   T   L   M   I   S   R   T

   613  cct gag gtc aca tgc gtg gtg gtg gac gtg agc cac gaa gac cct gag gtc
          P   E   V   T   C   V   V   V   D   V   S   H   E   D   P   E   V

   664  aag ttc aac tgg tac gtg gac ggc gtg gag gtg cat aat gcc aag aca aag
          K   F   N   W   Y   V   D   G   V   E   V   H   N   A   K   T   K

   715  ccg cgg gag gag cag tac aac agc acg tac cgt gtg gtc agc gtc ctc acc
          P   R   E   E   Q   Y   N   S   T   Y   R   V   V   S   V   L   T

   766  gtc ctg cac cag gac tgg ctg aat ggc aag gag tac aag tgc aag gtc tcc
          V   L   H   Q   D   W   L   N   G   K   E   Y   K   C   K   V   S

   817  aac aaa gcc ctc cca gcc ccc atc gag aaa acc atc tcc aaa gcc aaa ggg
          N   K   A   L   P   A   P   I   E   K   T   I   S   K   A   K   G
```

```
 868  cag ccc cga gaa cca cag gtg tac acc ctg ccc cca tcc cgg gag gag atg
        Q   P   R   E   P   Q   V   Y   T   L   P   P   S   R   E   E   M

 919  acc aag aac cag gtc agc ctg acc tgc ctg gtc aaa ggc ttc tat ccc agc
        T   K   N   Q   V   S   L   T   C   L   V   K   G   F   Y   P   S

 970  gac atc gcc gtg gag tgg gag agc aat ggg cag ccg gag aac aac tac aag
        D   I   A   V   E   W   E   S   N   G   Q   P   E   N   N   Y   K

1021  acc acg cct ccc gtg ctg gac tcc gac ggc tcc ttc ttc ctc tac agc aag
        T   T   P   P   V   L   D   S   D   G   S   F   F   L   Y   S   K

1072  ctc acc gtg gac aag agc agg tgg cag cag ggg aac gtc ttc tca tgc tcc
        L   T   V   D   K   S   R   W   Q   Q   G   N   V   F   S   C   S

1123  gtg atg cac gag gct ctg cac aac cac tac acg cag aag agc ctc tcc ctg
        V   M   H   E   A   L   H   N   H   Y   T   Q   K   S   L   S   L

1174  tct ccg ggt aaa tga
        S   P   G   K   -
```

EC-MS/MS Data searched against the SwissProt protein database with no restriction in Taxonomy Hits from protein search

MGL1-hFc

Row	Accession	Protein	MW [kDa]	pI	#Alt. Proteins	Scores	#Peptides	SC [%]	RMS90 [ppm]
1	MMGL_MOUSE	Macrophage asialoglycoprotein-binding protein 1 OS=Mus musculus GN=Mgl1 PE=1 SV=1	34.6	5.3	1	1154.6 (M:1154.6)	26	42.8	156.46
2	IGHG1_HUMAN	Ig gamma-1 chain C region OS=Homo sapiens GN=IGHG1 PE=1 SV=1	36.1	9.4	2	905.0 (M:905.0)	17	52.7	110.17
3	IGHG3_HUMAN	Ig gamma-3 chain C region OS=Homo sapiens GN=IGHG3 PE=1 SV=2	41.3	9.4	2	515.3 (M:515.3)	3	15.9	42.55
4	TRY1_BOVIN	Cationic trypsin OS=Bos taurus PE=1 SV=3	25.8	9.5	1	161.7 (M:161.7)	3	16.3	22.56

Clec9a-hFc band 1

Row	Accession	Protein	MW [kDa]	pI	#Alt. Proteins	Scores	#Peptides	SC [%]	RMS90 [ppm]
1	TRY1_BOVIN	Cationic trypsin OS=Bos taurus PE=1 SV=3	25.8	9.5	1	636.1 (M:636.1)	23	20.7	235.84
2	IGHG1_HUMAN	Ig gamma-1 chain C region OS=Homo sapiens GN=IGHG1 PE=1 SV=1	36.1	9.4	2	526.1 (M:526.1)	13	39.7	219.10
3	IGHG2_HUMAN	Ig gamma-2 chain C region OS=Homo sapiens GN=IGHG2 PE=1 SV=2	35.9	8.8	2	422.3 (M:422.3)	7	23.9	48.74
4	CLC9A_MOUSE	C-type lectin domain family 9 member A OS=Mus musculus GN=Clec9a PE=1 SV=1	27.0	6.0	1	355.5 (M:355.5)	7	28.6	42.89
5	RL19_MYCA1	50S ribosomal protein L19 OS=Mycobacterium avium (strain 104) GN=rplS PE=3 SV=1	12.9	10.7	4	51.1 (M:51.1)	1	7.1	130.12

Clec9a-hFc band 2

Row	Accession	Protein	MW [kDa]	pI	#Alt. Proteins	Scores	#Peptides	SC [%]	RMS90 [ppm]
1	IGHG1_HUMAN	Ig gamma-1 chain C region OS=Homo sapiens GN=IGHG1 PE=1 SV=1	36.1	9.4	2	661.7 (M:661.7)	20	45.5	208.77
2	TRY1_BOVIN	Cationic trypsin OS=Bos taurus PE=1 SV=3	25.8	9.5	1	478.2 (M:478.2)	24	20.7	194.85
3	CLC9A_MOUSE	C-type lectin domain family 9 member A OS=Mus musculus GN=Clec9a PE=1 SV=1	27.0	6.0	1	400.2 (M:400.2)	8	31.9	39.04
4	IGHG3_HUMAN	Ig gamma-3 chain C region OS=Homo sapiens GN=IGHG3 PE=1 SV=2	41.3	9.4	2	367.4	2	15.9	45.24

						(M:367.4)			
5	HS90B_HUMAN	Heat shock protein HSP 90-beta OS=Homo sapiens GN=HSP90AB1 PE=1 SV=4	83.2	4.8	21	276.5 (M:276.5)	5	9.1	59.29
6	LG3BP_RAT	Galectin-3-binding protein OS=Rattus norvegicus GN=Lgals3bp PE=1 SV=2	63.7	5.1	1	169.3 (M:169.3)	3	3.0	487.97
7	LG3BP_MESAU	Galectin-3-binding protein OS=Mesocricetus auratus GN=LGALS3BP PE=2 SV=1	64.4	5.0	1	91.5 (M:91.5)	1	2.6	66.38
8	RL19_MYCA1	50S ribosomal protein L19 OS=Mycobacterium avium (strain 104) GN=rplS PE=3 SV=1	12.9	10.7	4	53.5 (M:53.5)	1	7.1	130.12
9	K1C9_HUMAN	Keratin, type I cytoskeletal 9 OS=Homo sapiens GN=KRT9 PE=1 SV=3	62.0	5.0	1	51.0 (M:51.0)	1	1.4	93.79

Clec9a-hFc band 3

Row	Accession	Protein	MW [kDa]	pI	#Alt. Proteins	Scores	#Peptides	SC [%]	RMS90 [ppm]
1	ALBU_BOVIN	Serum albumin OS=Bos taurus GN=ALB PE=1 SV=4	69.2	5.8	13	1616.5 (M:1616.5)	30	52.2	23.79
2	IGHG1_HUMAN	Ig gamma-1 chain C region OS=Homo sapiens GN=IGHG1 PE=1 SV=1	36.1	9.4	2	389.1 (M:389.1)	12	29.4	114.97
3	FETUA_BOVIN	Alpha-2-HS-glycoprotein OS=Bos taurus GN=AHSG PE=1 SV=2	38.4	5.2	4	388.8 (M:388.8)	8	25.3	40.80
4	TRY1_BOVIN	Cationic trypsin OS=Bos taurus PE=1 SV=3	25.8	9.5	1	304.4 (M:304.4)	5	24.8	26.50
5	IGHG3_HUMAN	Ig gamma-3 chain C region OS=Homo sapiens GN=IGHG3 PE=1 SV=2	41.3	9.4	2	287.0 (M:287.0)	2	10.9	76.45
6	CLUS_RAT	Clusterin OS=Rattus norvegicus GN=Clu PE=1 SV=2	51.3	5.4	2	117.0 (M:117.0)	2	4.0	42.41
7	DHSA_MESAU	Succinate dehydrogenase [ubiquinone] flavoprotein subunit, mitochondrial (Fragment) OS=Mesocricetus auratus GN=SDHA PE=1 SV=1	60.0	5.8	9	60.1 (M:60.1)	2	2.0	495.75
8	PLTP_HUMAN	Phospholipid transfer protein OS=Homo sapiens GN=PLTP PE=1 SV=1	54.7	6.6	1	53.0 (M:53.0)	2	2.2	356.16
9	RL19_MYCA1	50S ribosomal protein L19 OS=Mycobacterium avium (strain 104) GN=rplS PE=3 SV=1	12.9	10.7	4	48.2 (M:48.2)	1	7.1	130.12

Clec9a Lane 4

Row	Accession	Protein	MW [kDa]	pI	#Alt. Proteins	Scores	#Peptides	SC [%]	RMS90 [ppm]
1	IGHG1_HUMAN	Ig gamma-1 chain C region OS=Homo sapiens GN=IGHG1 PE=1 SV=1	36.1	9.4	2	557.1 (M:557.1)	14	39.7	75.49
2	ALBU_BOVIN	Serum albumin OS=Bos taurus GN=ALB PE=1 SV=4	69.2	5.8	7	474.6 (M:474.6)	9	17.8	65.99
3	FETUA_BOVIN	Alpha-2-HS-glycoprotein OS=Bos taurus GN=AHSG PE=1 SV=2	38.4	5.2	4	395.6	6	24.0	45.55

						(M:395.6)			
4	IGHG2_HUMAN	Ig gamma-2 chain C region OS=Homo sapiens GN=IGHG2 PE=1 SV=2	35.9	8.8	2	393.2 (M:393.2)	3	23.9	76.63
5	TRY1_BOVIN	Cationic trypsin OS=Bos taurus PE=1 SV=3	25.8	9.5	1	332.4 (M:332.4)	12	20.7	52.53
6	CLC9A_MOUSE	C-type lectin domain family 9 member A OS=Mus musculus GN=Clec9a PE=1 SV=1	27.0	6.0	1	318.3 (M:318.3)	6	28.2	35.66
7	CALR_CRIGR	Calreticulin OS=Cricetulus griseus GN=CALR PE=2 SV=1	48.2	4.2	8	184.3 (M:184.3)	6	16.8	113.74
8	CO3_BOVIN	Complement C3 OS=Bos taurus GN=C3 PE=1 SV=2	187.1	6.4	1	48.5 (M:48.5)	1	0.6	19.62
9	CLUS_RAT	Clusterin OS=Rattus norvegicus GN=Clu PE=1 SV=2	51.3	5.4	2	48.0 (M:48.0)	1	1.8	48.71

Clec9a Lane 5

Row	Accession	Protein	MW [kDa]	pI	#Alt. Proteins	Scores	#Peptides	SC [%]	RMS90 [ppm]
1	IGHG1_HUMAN	Ig gamma-1 chain C region OS=Homo sapiens GN=IGHG1 PE=1 SV=1	36.1	9.4	2	630.2 (M:630.2)	17	37.3	184.18
2	A1AT_BOVIN	Alpha-1-antiproteinase OS=Bos taurus GN=SERPINA1 PE=1 SV=1	46.1	6.1	2	538.7 (M:538.7)	9	24.8	53.46
3	IGHG2_HUMAN	Ig gamma-2 chain C region OS=Homo sapiens GN=IGHG2 PE=1 SV=2	35.9	8.8	2	368.6 (M:368.6)	2	17.2	57.44
4	TRY1_BOVIN	Cationic trypsin OS=Bos taurus PE=1 SV=3	25.8	9.5	1	352.2 (M:352.2)	8	20.7	44.04
5	CH60_MOUSE	60 kDa heat shock protein, mitochondrial OS=Mus musculus GN=Hspd1 PE=1 SV=1	60.9	5.8	9	351.8 (M:351.8)	8	14.5	57.21
6	CLC9A_MOUSE	C-type lectin domain family 9 member A OS=Mus musculus GN=Clec9a PE=1 SV=1	27.0	6.0	1	302.4 (M:302.4)	6	26.1	35.22
7	FETUA_BOVIN	Alpha-2-HS-glycoprotein OS=Bos taurus GN=AHSG PE=1 SV=2	38.4	5.2	4	274.2 (M:274.2)	5	17.3	53.81
8	KPYM_HUMAN	Pyruvate kinase isozymes M1/M2 OS=Homo sapiens GN=PKM2 PE=1 SV=4	57.9	9.0	3	126.6 (M:126.6)	3	7.7	63.76
9	ALBU_MACMU	Serum albumin (Fragment) OS=Macaca mulatta GN=ALB PE=2 SV=1	67.8	5.8	6	72.5 (M:72.5)	1	2.5	31.85
10	SYA_PASMU	Alanyl-tRNA synthetase OS=Pasteurella multocida (strain Pm70) GN=alaS PE=3 SV=1	96.2	5.6	11	69.0 (M:69.0)	1	1.9	63.37
11	RL19_MYCA1	50S ribosomal protein L19 OS=Mycobacterium avium (strain 104) GN=rplS PE=3 SV=1	12.9	10.7	4	56.2 (M:56.2)	1	7.1	130.12

Clec9a-hFc band 6

Row	Accession	Protein	MW [kDa]	pI	#Alt. Proteins	Scores	#Peptides	SC [%]	RMS90 [ppm]
1	IGHG1_HUMAN	Ig gamma-1 chain C region OS=Homo sapiens GN=IGHG1 PE=1 SV=1	36.1	9.4	2	678.0 (M:678.0)	14	45.5	202.11
2	IGHG2_HUMAN	Ig gamma-2 chain C region OS=Homo sapiens GN=IGHG2 PE=1 SV=2	35.9	8.8	2	470.9 (M:470.9)	7	23.9	192.20
3	ANXA2_CANFA	Annexin A2 OS=Canis familiaris GN=ANXA2 PE=1 SV=1	38.6	7.6	8	395.0 (M:395.0)	6	21.2	35.84
4	TRY1_BOVIN	Cationic trypsin OS=Bos taurus PE=1 SV=3	25.8	9.5	1	342.6 (M:342.6)	9	20.7	135.15
5	CLC9A_MOUSE	C-type lectin domain family 9 member A OS=Mus musculus GN=Clec9a PE=1 SV=1	27.0	6.0	1	176.8 (M:176.8)	3	14.7	50.13
6	CLUS_RAT	Clusterin OS=Rattus norvegicus GN=Clu PE=1 SV=2	51.3	5.4	2	70.5 (M:70.5)	1	2.2	2.05
7	K1C9_HUMAN	Keratin, type I cytoskeletal 9 OS=Homo sapiens GN=KRT9 PE=1 SV=3	62.0	5.0	1	66.0 (M:66.0)	1	1.4	93.79
8	LIPL_RAT	Lipoprotein lipase OS=Rattus norvegicus GN=Lpl PE=1 SV=1	53.0	9.2	2	60.9 (M:60.9)	1	1.7	147.35
9	RL19_MYCA1	50S ribosomal protein L19 OS=Mycobacterium avium (strain 104) GN=rplS PE=3 SV=1	12.9	10.7	4	52.8 (M:52.8)	1	7.1	130.12